

University SAAD DAHLAB-Blida 1

Faculty of Technology



Renewable Energy Department

Major: Photovoltaics

Master Thesis

**OUT DOOR EXPERIMENTAL
CHARACTERIZATION OF A PV CELL UNDER
HIGH CONCENTRATED SOLAR FLUX**

Supervisor

Dr.N.Said

Board of lectures:

Dr.Nacer

Dr.O.Aitsahad

Mr.T.Domaz

Candidate

GHISANI Fairouz

ACADEMIC YEAR 2016-2017

Dedications and Acknowledgements

Dedications

This work reflects my respects:

Thank you Allah who helped me realize this work and acquire my goal.

To my family:

With their tender encouragement and great sacrifices, they could create the loving atmosphere that is conducive to the pursuit of my studies.

A big thank you especially my very dear mom, no dedication could express my respect, my consideration and my deep feelings toward them. I pray to God to bless them, to watch over them, hoping that they will always be proud of me.

*To all my teachers:
Their generosity and their support makes me express my deep my sincere respect and consideration.*

*To all my friends:
They will find here the witness of fidelity and boundless friendship.*

Thanks

Before beginning the presentation of this work, I take this opportunity to thank all those who contributed directly or indirectly to the realization of this project graduation.

I want to express my sincere thanks to my great and respectful teacher Mr.N.SAID, for agreeing to frame me for my graduation project, and for its support, its relevant remarks and encouragement.

I express my deep gratitude and all my thoughts gratitude to Mr.T.DOMAZ, Who accompanied me from near and far during any work or thing done in my life to availability, for the trust he has been able to give me valuable advice and he provided me throughout the realization of this project.

My thanks also go to all my professors, teachers and all people who supported me all the way, and have not stopped giving me very important tips in gratitude.

Table of Contents

Table of Contents	I
List of Figures	IV
List of Tables	VII
List of Symbols	VIII
List of Greek letters	VIII
List of Abbreviation	VIII
General introduction	IX
Chapter 1 Introduction	1
1.1 Project introduction	1
1.2 Document structure	2
Chapter 2 Research and literature review	3
2.1 Motivation of the research	3
2.2 PV cell research and review	4
2.2.1 Point-contact solar cells	5
2.2.2 Metal-Wrap-Through (MWT) and Emitter-Wrap-Through (EWT) solar cells	6
2.2.3 Sliver solar cells	7
2.3 PV cell under concentration research and review	8
Chapter 3 Concentration in Photovoltaics	12
3.1 Sun coordinates	12
3.1.1-Earth-Sundistance	13
3.1.2- Solar declination	13
3.1.3- Hour Angle	13
3.1.4- Geographical coordinates	14
3.1.5- Height of the Sun	14
3.1.6- Azimuth of the Sun	14
3.1.7- Day length	15

3.1.8- Sunshine duration	15
3.2 Solar radiation	16
3.3 CPV configuration	17
a) Concentration factor	17
b) Concentrator optics	18
• Refractive optics	18
• Reflective optics	19
• Solar cells for CPV	20
3.4 Tracking for CPV	21
3.4.1 Two-axis	21
• Roll-tilt structure	22
• Turntable	22
3.4.2 One-axis	23
• Horizontal axis	23
• Polar-axis	23
3.4.3 Arduino	24
3.4.4 Stepper motors	26
a) What are stepper motors good for?	26
b) What are stepper motors good for?	26
3.5 Cooling for CPV	27
3.6 Modelling analysis	28
3.6.1 <i>Ideal Solar Cell</i>	29
3.6.2 <i>Solar Cell with Series Resistance</i>	30
3.6.3 Simulation Results	32
Chapter 4 Experimental setup and testing	38
4.1 Description of the setup	38
4.2 Description of instruments used	39
4.2.1 Digital multimeter	39
4.2.2 Thermometer	40

4.2.3 Solar power meter	41
4.2.4 Light meter	42
4.2.5 Other tools	43
4.3 Cell testing under one sun	44
4.3.1 Current at short circuit	45
4.3.2 Voltage at open circuit	45
4.3.3 Maximum power	45
4.3.4 Fill factor	46
4.3.5 Efficiency	46
4.4 Cell testing under concentration	47
Chapter 5 Test results and analysis	49
5.1 One sun results and analysis	49
➤ Test 1	49
➤ Test 2	50
➤ Test 3	51
➤ Test 4	52
➤ Test 5	53
➤ Test 6	54
➤ Test 7	55
➤ Test 8	56
5.2 Results and analysis under concentration	59
➤ Test 1	59
➤ Test 2	60
➤ Test 3	61
➤ Test 4	62
➤ Test 5	63
➤ Test 6	64
➤ Test 7	65
5.3 Comparative study	68
Chapter 6 Conclusions and recommendations	70
6.1 Project conclusion	70

6.2 Recommendations for future works	71
Summary	72

List of Figures

Fig.2.1 : SunPower A-300 solar cell [4].	6
Fig.2.2 : MWT solar cell: a) structure of the cell and b) picture of a highly efficient industrially feasible MWT silicon solar cell [4].	6
Fig.2.3: Schematic drawing of an EWT solar cell of Advent Solar [4].	7
Fig.2.4: Schematic of sliver solar cells process and cell structure [4].	8
Figure.2.5: NREL chart for record efficiency solar cell [9].	11
Figure.3.1: The structure of the sun [10]	13
Figure.3.2: The equation of time E in minutes as a function of time of year [11]	14
Figure.3.3: Solar radiation spectrum [16].	16
Figure.3.4: A CPV fields & options [17].	17
Figure.3.5: basic Fresnel lens configuration: point focus and, linear Fresnel lens [18]	19
Fig.3.6: Example of a static concentrator configuration. A bifacial cell is mounted in a reflective CPC-like trough that is filled with liquid dielectric. [18]	20
Fig.3.7 (b,c): Roll-tilt structure two- axis tracking configurations [20].	22
Fig.3.7(d): Turntable tracking configurations [20]	23
Fig.3.7(a,b): One-axis tracking configurations: a) One-axis horizontal tracker with reflective trough; b) One-axis polar axis tracker with reflective trough [20].	23
Figure.3.8: Arduino board [25].	25

Figure.3.9: Stepper motor [28].	26
Figure.3.10: Schematics of passive and active cooling systems [29].	28
Figure.3.11 Ideal solar cell with single-diode [33].	29
Figure.3.12. Solar cell with single-diode and series resistance [34].	31
Figure. 3.13 I-V characteristics for various conditions of solar radiation [34].	33
Figure.3.14. I-V characteristics for a diode ideality variation between 1 and 2 [34].	33
Figure.3.15 I-V characteristics for the temperature variation between 0 and 75°C [34].	34
Figure.3.16. P-V characteristics for the temperature variation between 0 and 75°C [34]	34
Figure.3.17. I-V characteristics for various conditions of solar radiation (considering series resistance) [34].	35
Figure. 3.18. I-V characteristics for a diode ideality variation between 1 and 2 (considering series resistance) [34].	35
Figure. 3.19 I-V characteristics for the temperature variation between 0 and 75°C (considering series resistance) [34].	36
Figure. 3.20. P-V characteristics for $R_s = 20m\Omega$ [34].	36
Figure.3.21. P-V characteristics for the R_s variation [34].	37
Figure.4.1: The sun tracker and the solar cell employed in the tests.	39
Figure.4.2: Multimeter to measure the current and the voltage.	39
Figure.4.3: Thermometer.	40
Figure.4.4: Solar power meter.	41
Figure.4.5: light meter.	42

Figure.4.6: a) The resistance used in the work.	43
Figure.4.6: b) The Arduino board used in the experience.	43
Figure.4.6: c) Other tools used in the experience.	44
Figure.4.7: The sun tracker and the solar cell employed in the tests under one sun.	44
Figure.4.8: A normal behavior of a solar cell [34].	46
Figure.4.9: The sun tracker and the solar cell employed in the tests under concentration	47
Figure.5.1: <i>V-I</i> curve acquired during Test 1 under one sun.	49
Figure.5.2: <i>V-I</i> curve acquired during Test 2 under one sun.	50
Figure.5.3: <i>V-I</i> curve acquired during Test 3 under one sun.	51
Figure.5.4: <i>V-I</i> curve acquired during Test 4 under one sun.	52
Figure.5.5: <i>V-I</i> curve acquired during Test 5 under one sun.	53
Figure.5.6: <i>V-I</i> curve acquired during Test 6 under one sun.	54
Figure.5.7: <i>V-I</i> curve acquired during Test 7 under one sun.	55
Figure.5.8: <i>V-I</i> curve acquired during Test 8 under one sun.	56
Figure.5.9: I-V characteristics for various conditions of solar radiation (considering series resistance) under one sun.	58
Figure.5.10: <i>V-I</i> curve acquired during Test 1 under concentration.	59
Figure.5.11: <i>V-I</i> curve acquired during Test 2 under concentration.	60
Figure.5.12: <i>V-I</i> curve acquired during Test 3 under concentration.	61
Figure.5.13: <i>V-I</i> curve acquired during Test 4 under concentration.	62
Figure.5.14: <i>V-I</i> curve acquired during Test 5 under concentration.	63
Figure.5.15: <i>V-I</i> curve acquired during Test 6 under concentration.	64
Figure.5.16: <i>V-I</i> curve acquired during Test 7 under concentration.	65
Figure.5.17: <i>V-I</i> curves acquired during all the Tests under concentration.	67
Figure.5.18: Daily Average Power on fixed and tracking cell.	69

List of Tables

Table.5.1: Parameters characterizing of all Tests.	57
Table.5.2: Parameters characterizing of all Tests under concentration.	66
Table.5.3: The average power of the solar cell.	69

List of Symbols

A_{cell}	: Cell Area
A_{lens}	: Lens Area
C_{goc}	: Ratio of the cell area and the lens area
EQT	: Equation of time
FF	: Fill Factor
G	: Global irradiation
G_n	: Experimental Global irradiation
T	: Normalised temperature
T_n	: temperature of the cell
N_s	: cell number
I_{cc}	: Short-circuit current
V_{co}	: Open-current voltage
k	: Boltzmann constant
q	: Elementary charge
P	: Power
P_m	: Maximum power
P_{in}	: Incident power

List of Greek letters

η	: Efficiency
η_{opt}	: Optical Efficiency
a	: Quality factor for the diode, $n=2$ for crystalline

List of Abbreviations

AC	: Alternative current
CdTe	: Cadmium Telluride
CIS	: Copper indium Selenium
CPV	: Concentrated Photovoltaic
DC	: Direct current
MPPT	: Maximum power point tracking
NERC	: National energy research center
NOCT	: Normal Operating cell temperature
NREL	: National Renewable Energy Laboratory
Poly-cr	: Polycrystalline Photovoltaic
PV	: Photovoltaics
STC	: Standard Test Condition
SOPHIA	: Solar Photovoltaic European Research Infrastructure
WEO 2009	: World Energy Outlook, 2009

General introduction

One of the major concerns in the power sector is the day-to-day increasing power demand but the unavailability of enough resources to meet the power demand using the conventional energy sources. Demand has increased for renewable sources of energy to be utilized along with conventional systems to meet the energy demand. Renewable sources like wind energy and solar energy are the prime energy sources which are being utilized in this regard. The continuous use of fossil fuels has caused the fossil fuel deposit to be reduced and has drastically affected the environment depleting the biosphere and cumulatively adding to global warming.

Solar energy is abundantly available that has made it possible to harvest it and utilize it properly. Solar energy can be a standalone generating unit or can be a grid connected generating unit depending on the availability of a grid nearby. Thus it can be used to power rural areas where the availability of grids is very low. Another advantage of using solar energy is the portable operation whenever wherever necessary. In order to tackle the present energy crisis one has to develop an efficient manner in which power has to be extracted from the incoming solar radiation. The power conversion mechanisms have been greatly reduced in size in the past few years. The development in power electronics and material science has helped engineers to come up very small but powerful systems to withstand the high power demand. But the disadvantage of these systems is the increased power density.

As a result, the demand for solar cells, which convert sunlight directly into electricity, is growing. Solar or photovoltaic (PV) cells are made up of semiconductor materials that absorb photons from sunlight and then release electrons, causing an electric current to flow when the cell is connected to a load. A variety of measurements are used to characterize a solar cell's performance, including its output and its efficiency. This electrical characterization is performed as part of research and development of photovoltaic cells and materials, as well as during the manufacturing process. The research investigates electrical power extracted, efficiency, temperatures reached, and possible damages of the photovoltaic cell. In the past several years there has been a growing commercial interest in Concentration PhotoVoltaics (CPV) thanks to its promise of low cost electrical power generation. While the technology of CPV using point-focus Fresnel-like optical elements is reaching maturity, the systems based on dense array receivers still need further scientific progress. This thesis explores the field of characterization of the solar cell under one sun and under concentration. Outdoor experimentation of solar cells is essential to maximize their performance and to assess utilization requirements and limits. More generally tests with direct exposure to the sun are useful to understand the behavior of components and new materials for solar applications in real working conditions. Insolation and ambient factors are uncontrollable but can be monitored to know the environmental situation of the solar exposure experiment.

Chapter 1

Introduction

1.1 Project introduction

The increasing demand for clean energy and the largely untapped potential of the sun as an energy source is making solar energy conversion technology increasingly important. As a result, the demand for solar cells, which convert sunlight directly into electricity, is growing. Solar or photovoltaic (PV) cells are made up of semiconductor materials that absorb photons from sunlight and then release electrons, causing an electric current to flow when the cell is connected to a load. A variety of measurements are used to characterize a solar cell's performance, including its output and its efficiency. This electrical characterization is performed as part of research and development of photovoltaic cells and materials, as well as during the manufacturing process. Several parameters are used to characterize the efficiency of the solar cell, including the maximum power point (P_{max}), the energy conversion efficiency (η), and the fill factor (FF). Electrical characterization is important in determining how to make the cells as efficient as possible with minimal losses. Outdoor experimentation of solar cells is essential to maximize their performance and to assess utilization requirements and limits. More generally tests with direct exposure to the sun are useful to understand the behavior of components and new materials for solar applications in real working conditions. Insolation and ambient factors are uncontrollable but can be monitored to know the environmental situation of the solar exposure experiment. Outdoor measurements monitor the effects of the exposure of a monocrystalline photovoltaic cell made of silicon, to exposure it under one sun then to focused sunlight on it. The main result is the continuous acquisition of the $V-I$ (voltage-current) curve for the cells in different conditions of solar concentration and temperature of exercise to assess their behavior. The research investigates electrical power extracted, efficiency, temperatures reached, and possible damages of the photovoltaic cell in the case if the environment does not fit the solar cell.

The test methodology proposed in this paper uses solar light and a Fresnel lens to concentrate light on the silicon PV cell. The device is equipped with a solar tracking. Hence, the main advantage of solar outdoor experimentation is to work in the real operating conditions of a solar installation. Insolation (solar irradiance) and ambient factors are not controllable but the outdoor test conditions can be surveyed and recorded by measuring proper physical quantities with appropriate instruments. Another benefit of using direct sunlight is to avoid the employment of artificial sources, lamps, or solar simulators, which can only try to reproduce spectral distribution, divergence and intensity of sunlight.

1.2 Document structure

Chapter 2

The primary types of PV cell and concentrators and the main features to consider for the design of a CPV system are discussed. These characteristics include the type of optic, the concentration level, the solar cell materials and the type of sun-tracking.

Chapter 3

In this part, we discuss the sun energy and some characterization methods that have been used for CPV concentrators as its configuration, tracking cooling for CPV are also presented.

Chapter 4

The prototype and the process to realize the device are described in this present chapter, which treats the experimental setup of the project and its testing that shows the different solar cell's features, current in short circuit, the voltage at open circuit the maximum power, the fill factor and the efficiency that helps us to evaluate the performance of the solar cell used.

Chapter 5

The subject of this chapter is the experimental proof that was already predicted in Chapter 4. The first experiment here presented has been performed outdoor and made use of devices that have PV cell under one sun. The second experiment has been performed with PV cell under a high concentrated solar light. The comparison of these two studies shows the range of current and the temperature we attend. After that, the characteristics of solar cell we have used are described. The current-voltage curves at different illumination levels for the cell have been measured in the concentrator system.

Chapter 6

Experimentation with direct exposure to sunlight is essential to evaluate the behavior of solar components in situations very similar to operative solar plants. The proposed methodology has the advantage of reproducing the real working conditions. According to this experimentation, we are able to recommend that kind of work by avoiding the obstacles we coped for a better result. This part concludes our work and some valuable recommendations are outlined.

Chapter 2

Research and literature review

2.1 Motivation of the research

Several technical challenges such as optical efficiency, sun tracking, thermal management, light homogeneity, and packaging are still the main discussions in the field of renewable energies. These challenges led to the objective of this project, which is to evaluate the performance of a solar cell under a high solar flux with a two axis tracking mechanism.

The project based on the idea of implementing a solar tracker to characterize a solar cell under a high solar flux. This study is required in order to properly design a PV receiver and which serves for other solar energy projects. In fact, regardless of the kind of solar energy application, the receiver has to consider the main parameters that define the illumination spot at the focal plane, i.e. the total solar flux, the peak and average power densities, the distribution of the concentrated light. These spot properties allow assessing the optical efficiency of the concentrator and give an insight into the quality of the optical components. It follows that work of characterization is also needed to have an evaluation of the solar cell manufacturing process.

As long as optical elements are well aligned and all produce the same incident power on the cells. In dense array CPV systems, the power on the cells can be very different and this is the main reason why most of CPV companies have forsaken the development of dense-arrays in favor of Fresnel-like systems. In fact, the current mismatch among the cells in the array can lead to severe degradation in system performance, as well as danger of cell damage due to reverse-bias operation and overheating. A possible solution is to use a secondary optical element (SOE), which can improve the light homogeneity but which also inflict optical losses. The common method to protect cell from reverse bias damage is to install bypass diodes parallel to each cell. This measure protects cells against damage but does not fully recover the power loss due to current mismatch.

All these issues must to be dealt since they seriously affect the reliability and the performance of a CPV dense array. In the current state of development we are not interested in building an optimal receiver in terms of light collection efficiency (spacing between cells and between connections), but we want to realize a device that allows performing consistent test operations for an array of the cell under a high concentration. This way the goal is to build a quite robust receiver that will stand several working cycles under outdoor operation and that will prevent cell heating.

This device will be used as a practical work for the students of Renewable Energy Department, in order to be more familiar to this new field.

2.2 PV cell research and review

The early dominance of silicon in the laboratory has extended to the market for commercial modules. Crystalline silicon designs have never accounted for less than 80% of the market for commercial modules and nearly 15–18% of the market was not crystalline silicon. It was based on amorphous silicon—a PV technology that is almost exclusively used for consumer electronics such as watches and calculators. If we were to exclude electronics and define the market as electricity delivery system of 1 kW or more, current production is dominated by single-crystal and polycrystalline silicon modules, which represent 94% of the market [1]. There are a wide range of PV cell technologies on the market today, using different types of materials, and an even larger number will be available in the future. PV cell technologies are usually classified into three generations, depending on the basic material used and the level of commercial maturity [2].

(i) First-generation PV systems (fully commercial) use the wafer-based crystalline silicon (c-Si) technology, either single crystalline (sc-Si) or multicrystalline (mc-Si).

(ii) Second-generation PV systems (early market deployment) are based on thin-film PV technologies and generally include three main families: (1) amorphous (a-Si) and micromorph silicon (a-Si/ c-Si); (2) cadmium telluride (CdTe); and (3) copper indium selenide (CIS) and copper indium-gallium diselenide (CIGS).

(iii) Third-generation PV systems include technologies, such as concentrating PV (CPV) and organic PV cells that are still under demonstration or have not yet been widely commercialized, as well as novel concepts under development.

Commercial production of c-Si modules **began in 1963** when Sharp Corporation of Japan started producing commercial PV modules and installed a 242 Watt (W) PV module on a lighthouse, the world's largest commercial PV installation at the time. Total PV cells/modules production by region 2007–2011. It has been observed that Japan attributed to increase their PV cells/modules production capacity from 1997 to 2004 and then drastically reduced their production capacity after 2004. Same trend was observed in PV cells/module production in Europe also but up to year 2008, and then they reduced their production capacity [2]. On the other hand in year 1997, PV cells/module production capacity of US was the highest, and after then they reduced their production capacity every year. Whereas PV cells/modules production scenarios of China were just the reverse compared to US. Given the vast potential of photovoltaic technology, worldwide production of terrestrial solar cell modules has been rapid over last several years, with China recently taking the lead in total production volume [2]. Another interesting picture related to the global cumulative PV installation until 2011 was noticed [3]. It was observed that still Germany including other European country contributed to major role towards the global cumulative PV installation until 2011, that

is, 70% of global PV installation. So PV installation market in Europe is too much promising till now compared to other countries.

Photovoltaic (PV) technology is a clean and inexhaustible solution to convert sunlight energy into electrical energy. The growing interest on this technology has significantly increased in the 1970s with the oil crisis. Since the early days of terrestrial PV application, and given that the available solar cells (basic converter unit of a PV system) were perceived to be too expensive, the use of concentrating sunlight has arisen as a possible shortcut to significantly reduce the cost of PV electricity. This concept is known as concentrator photovoltaic technology and consists in redirecting the sunlight onto a small solar cell area through optical devices. Thus, the area of the PV cell is reduced while, at the same time, the light intensity on the device increases by the same ratio. Of course, the expectation is that the replacement of the expensive PV solar cells by less expensive optical material (lenses and/or mirrors) may lead to some savings in system costs [4].

Nowadays, we may find MJ solar cells that feature very high efficiency but these cells are mainly produced in small quantities by dedicated manufacturers thus having very high cost which has inhibited their integration in low and some medium concentration systems. One should notice, however, that silicon solar cells may be particularly competitive for these classes of concentration systems due two main reasons [4]:

- Silicon solar cells technology has a track recorded field demonstration on terrestrial applications;
- Introducing high efficiency features on standard silicon solar cell processing will increase the cost but it will most likely still be affordable when integrated in CPV systems. Benefiting from economies of scale this may lead to spill over to standard PV modules technologies, which will decrease the price and increase its competitiveness for CPV application.

2.2.1 Point-contact solar cells

This solar cell structure was firstly developed by Swanson and co-workers at Stanford University. It can operate at higher concentration and has reached efficiencies of more than 26% under concentrated light. The absence of grid on the front face allows a better efficiency and all the electric contacts are made on the rear face through interdigitated dense grids (Fig.2.1).

Thus, series resistance is no longer a limit for high concentration efficiency. Instead, the high concentration efficiency is affected by the Auger recombination. From 2003, SunPower manufactures a simplified version of this Point-Contact (PC)cell, A-300, with one-sun efficiencies of about 20% and relatively low cost.

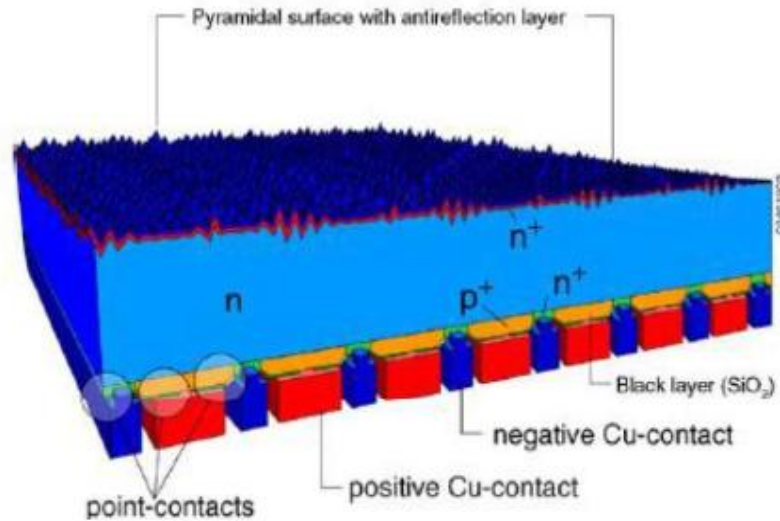


Fig.2.1 : SunPower A-300 solar cell [4].

2.2.2 Metal-Wrap-Through (MWT) and Emitter-Wrap-Through (EWT) solar cells

Lower-quality silicon material cannot make use of a back junction cell structure, as in A-300. Thus, it is necessary to implement a collecting emitter on the front side of the cell to make the cell structure less sensitive to low-diffusion lengths. To keep both contacts in the rear of the cell, to reduce front surface shading and facilitate cells interconnection, the emitter can be connected to the rear electrode of the cell by either metalized vias connecting the front fingers with the rear bus bar in the Metal-Wrap-Through (MWT) structure or by emitter-diffused holes in the Emitter-Wrap-Through (EWT) structure. The MWT design is relatively easy to be adapted to existing cell production lines.

The major difference with respect to standard cells is the busbar transference to the rear side (see Fig.2.2), while the fingers remain on the front side. This technology is commercialized by Photovolttech and a similar cell structure, PUM cell, is developed by ECN. Recently, Fraunhofer ISE has achieved the maximum efficiency of 18.6% for MWT solar cell, which according to the authors is industrially feasible [4].

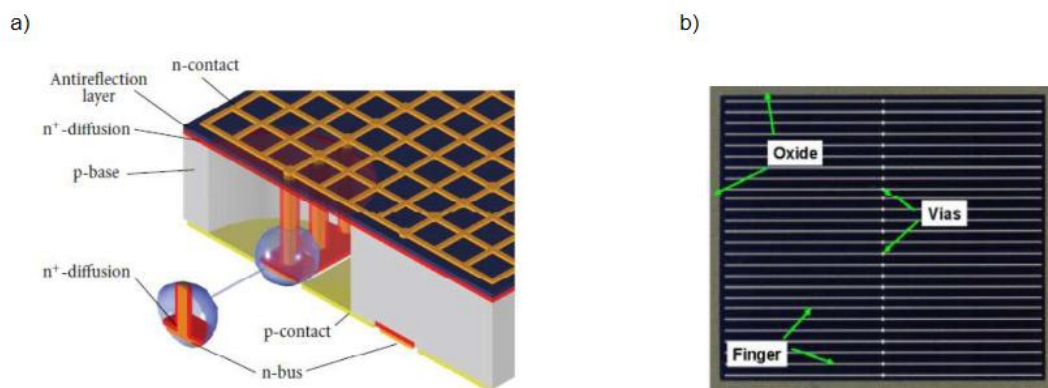


Fig.2.2 : MWT solar cell: a) structure of the cell and b) picture of a highly efficient industrially feasible MWT silicon solar cell [4].

In the EWT concept (see Fig.2.3), all the metal structure is on the rear side. It uses laser-drilled vias to wrap the emitter on the front surface to contacts on the rear surface and uses a potentially low-cost process sequence. This technology has demonstrated 21.4% of efficiency and it is suitable for industrial production as established by Advent Solar, resulting in cells efficiencies above 15%.

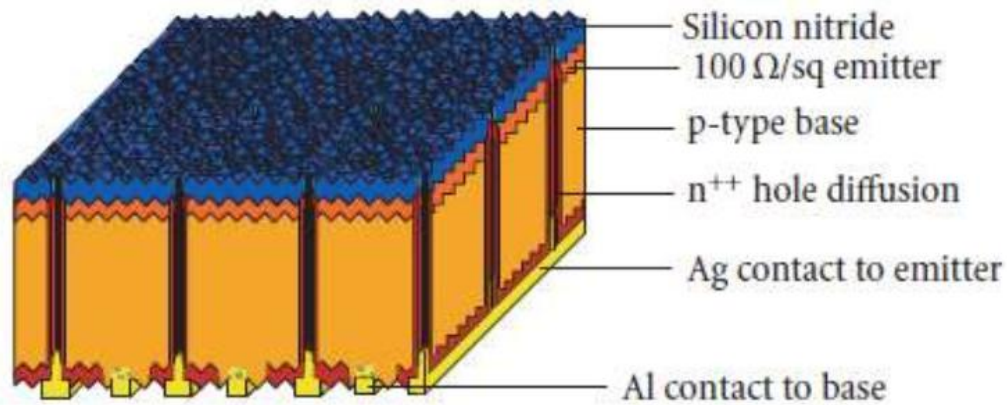


Fig.2.3: Schematic drawing of an EWT solar cell of Advent Solar [4].

2.2.2 3 Sliver solar cells

Sliver technology was conceived and developed at the Centre for Sustainable Energy Systems at the Australian National University (ANU), supported by the Australian Company, Origin Energy. Instead of manufacturing a single solar cell on the surface of a wafer, Sliver cells are produced by etching a thousand grooves in the wafer volume which leads to many very thin strips, each becoming a Sliver solar cell (Fig.2.4). Once again, and according to the authors, all the manufacturing steps use standard techniques from the semiconductor industry. The resulting Sliver monocrystalline solar cells are long, narrow and thin. The size of each cell depends on the starting wafer dimensions and groove patterning details; typical length is within 512 cm, the width varies in the range of 0.52 mm, and the thickness is between 20100 m. Moreover, the cells are flexible, because they are thin, and bifacial because the positive and negative contacts of each cell are located on the two edges (Fig.2.4), rather than on the cells surface as in standard solar cells [4].

This eliminates the losses that metal fingers originate on the cells due to shading, and allows easy series interconnection of the cells but requires the use of very good quality crystalline silicon. The best cells achieved efficiencies above 20% at 1 sun, 18.8% at 9 suns and 18.4% at 37 suns, being suitable for illumination intensities up to 50 suns with emitter resistance limiting the performance for higher intensities. For CPV, these cells are convenient due to their narrowness, which matches with the reduced width of the concentrator optics, and their flexibility, which allows them to be bonded directly into a pipe for cooling.

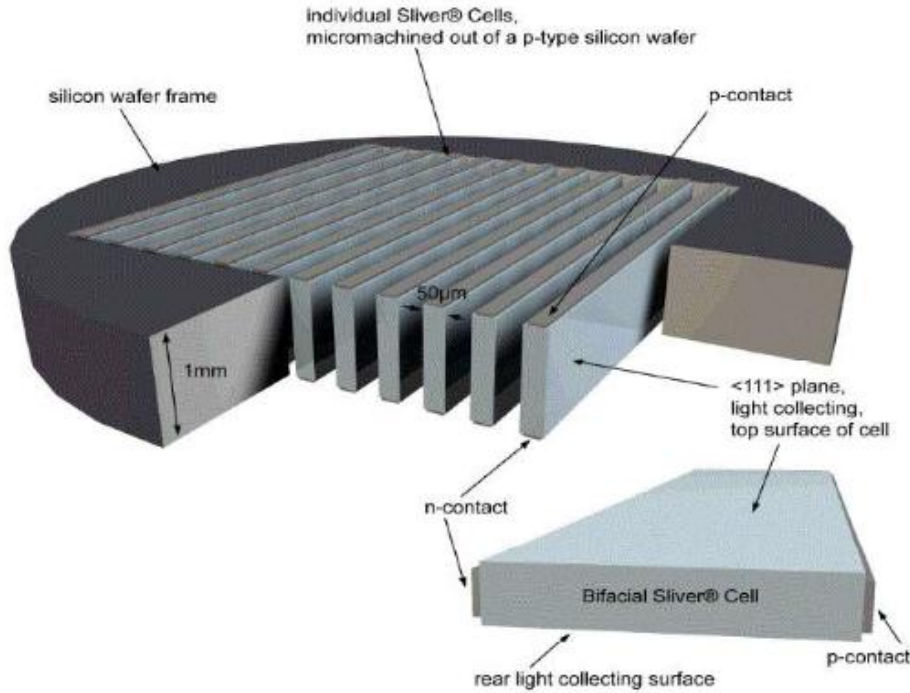


Fig.2.4: Schematic of sliver solar cells process and cell structure [4].

2.3 PV cell under concentration research and review

Today, the world is in great need of a change in the way that energy is generated. On one hand, most governments have in their agenda the concerns about greenhouse gas emissions and climate change while, on the other hand, the rising prices of energy and fossil fuels and the Fukushima nuclear disaster have led to increasing interest in renewable energy sources in general, and solar in particular [7]. Photovoltaic (PV) technology is a clean and inexhaustible solution to convert sunlight energy into electrical energy. The growing interest on this technology has significantly increased in the 1970s with the oil crisis [5].

Since the early days of terrestrial PV application, and given that the available solar cells (basic converter unit of a PV system) were perceived to be too expensive, the use of concentrating sunlight has arisen as a possible shortcut to significantly reduce the cost of PV electricity. This concept is known as concentrator photovoltaic technology and consists in redirecting the sunlight onto a small solar cell area through optical devices. Thus, the area of the PV cell is reduced while, at the same time, the light intensity on the device increases by the same ratio [7]. Of course, the expectation is that the replacement of the expensive PV solar cells by less expensive optical material (lenses and/or mirrors) may lead to some savings in system costs. Research on CPV systems began in 1975 and its development was encouraged by the US **“Concentrator Program”** which arose due to the prediction of the increased costs of fossil fuels in the aftermath of the 70’s oil crises [8].

CPV was mainly conceived for large power plants, aiming to produce large amounts of renewable energy and compete with conventional fossil fuel plants. Within this program, the first concentrator prototype was developed at Sandia National Laboratories of Albuquerque in the mid 1976 [7]. This prototype was a 40x concentrator, making use of

silicon solar cells and Fresnel lenses mounted on a two-axis tracking system. Shortly afterwards, several prototypes were developed in Europe. They were all similar to the one made by Sandia Labs.

However, the electricity market changed in a somewhat unexpected direction. Global politics and the discovery of new oil sources kept electricity prices of the mature fossil fuel plants at a very low level. Since the concentrator programs were initially conceived to construct CPV for large power plants, i.e. to compete with fossil fuel generators, most of them were suspended in the face of the unexpected abundant fossil fuel supply. This situation has slowed down the development of CPV systems. In the mid of 1980s, R&D on concentrators faded although some groups maintained activity. In the niche market of small remote loads used for grid extension applications (e.g. small amount of electricity to telecommunication stations) flat-plate PV emerged as an important and viable power source [8]. CPV however, due to the need to be mounted on movable structures to track the sun, is particularly unsuitable for these applications and has never gained a significant market share. In the meantime, the new paradigm of sustainability, the need to confront global warming and the external costs associated with pollution became the driving force for PV development. Subsidized grid-connected market of a few kWp has emerged more recently in many developed countries. In these applications CPV also played a minor role in PV market for more than 25 years. The PV systems in the subsidized grid connected market were often mounted on the roof or integrated in facades (reducing some of the installation cost) which again are less suitable for CPV. However, we may find some CPV systems installed under feed-in tariff schemes in places where extensive grounds are available [7] and [8].

This brief historic overview emphasises the main barriers that CPV has faced when trying to gain market acceptance. In spite of all these challenges, it should also be noticed that the development of CPV technology has contributed to some advances in other areas. One example of such contribution is the improvement of the efficiency of solar cells. The high power density of CPV allows the use of cells with higher cost per unit area. Thus, many designs were developed specifically for concentration applications. Some of these concepts have been successfully applied to one-sun solar cells. Another technological development which has spill over from CPV to conventional PV is tracker technology. Standard modules mounted on tracking structures may lead to higher yields that overcome the extra cost of the trackers, in particular in locations with high direct insolation. An additional side effect of the development of CPV was the knowledge acquired about the availability of direct normal irradiation (DNI) [8].

The boost of energy yield on CPV systems is mostly related with the amount of direct sunlight (radiation that falls on Earth without being scattered by haze, clouds, etc). In the early days of the Concentrator Program it was feared that the percentage of such radiation was considerably less than the solar resource available for flat-plate systems, which make use of global radiation. However, it was found that in many regions of good solar resource, the annual energy available to a two-axis tracking concentrator is actually greater than the global radiation resource available to flat-plate systems. During the mid 2000s, and in spite of very significant political and economic support, the cost reduction

of conventional flat plate PV was perceived to be too slow and therefore a lot of effort, and research funding, both public and private, was re-directed to CPV, which offered the promise of a faster learning curve. Examples are large scale CPV demonstration program in the region of Castilla La Mancha, Spain, and in Portugal, as well as numerous start-ups dedicated to CPV that emerged in the past 5-10 years [8].

Best Research-Cell Efficiencies

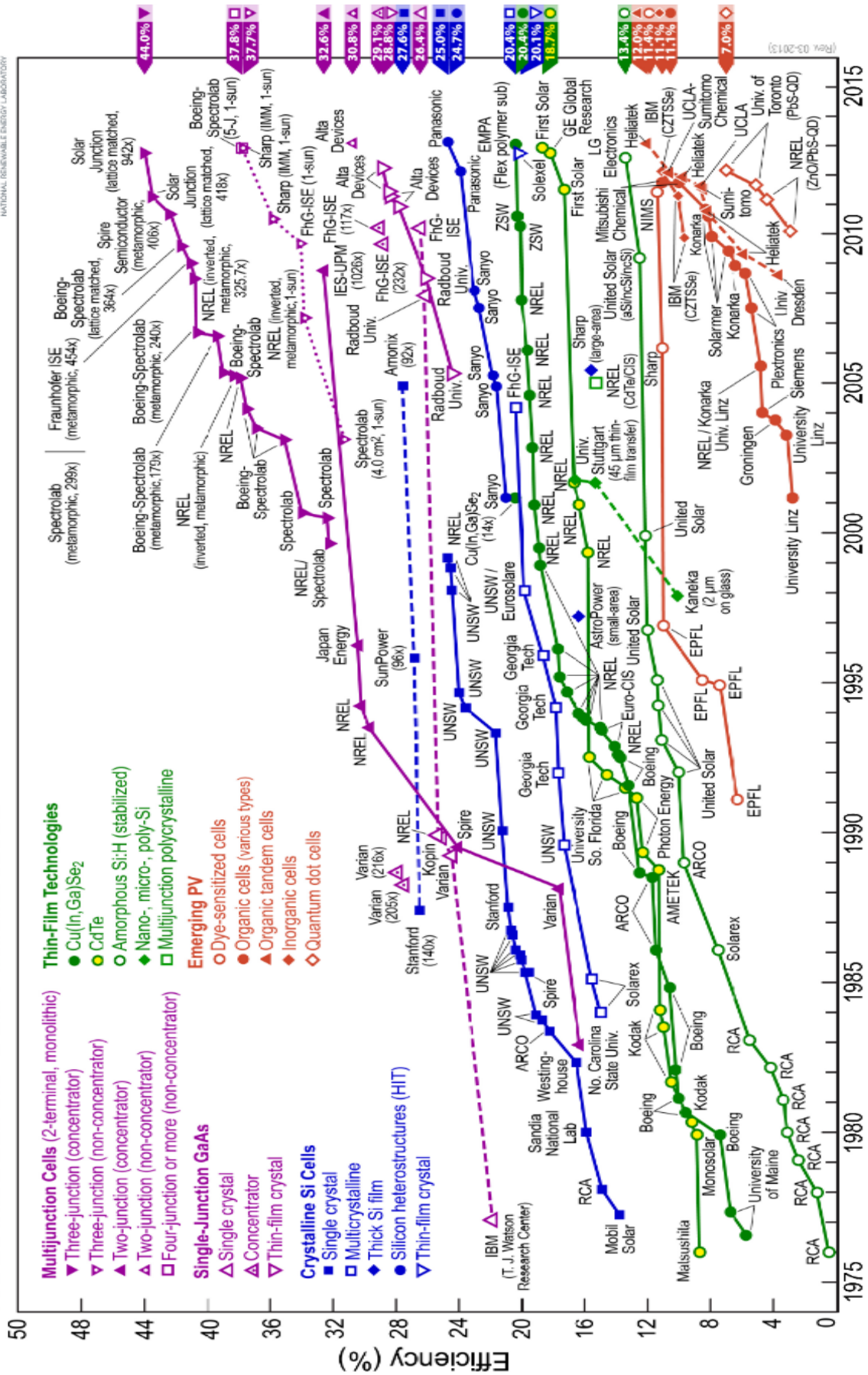


Figure.2.5: NREL chart for record efficiency solar cell [9].

Chapter 3

Concentration in Photovoltaics

3.1 Sun coordinates

The sun is a sphere of intensely hot gaseous matter with a diameter of 1.39×10^9 m and is, on the average, 1.5×10^{11} m from the earth. As seen from the earth, the sun rotates on its axis about once every 4 weeks. However, it does not rotate as a solid body; the equator takes about 27 days and the Polar Regions take about 30 days for each rotation. The sun has an effective blackbody temperature of 5777 K° . The temperature in the central interior regions is variously estimated at 8×10^6 to $40 \times 10^6 \text{ K}^\circ$ and the density is estimated to be about 100 times that of water. The sun is, in effect, a continuous fusion reactor with its constituent gases as the “containing vessel” retained by gravitational forces. Several fusion reactions have been suggested to supply the energy radiated by the sun. The one considered the most important is a process in which hydrogen (i.e., four protons) combines to form helium (i.e., one helium nucleus); the mass of the helium nucleus is less than that of the four protons, mass having been lost in the reaction and converted to energy. The energy produced in the interior of the solar sphere at temperatures of many millions of degrees must be transferred out to the surface and then be radiated into space [10] and [13]. A succession of radiative and convective processes occur with successive emission, absorption, and reradiation; the radiation in the sun’s core is in the x-ray and gamma-ray parts of the spectrum, with the wavelengths of the radiation increasing as the temperature drops at larger radial distances [10] and [12].

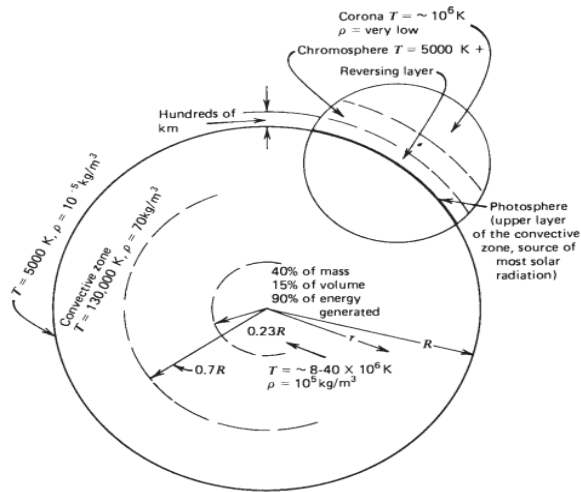


Figure.3.1: The structure of the sun [10].

3.1.1-Earth-Sun distance:

The trajectory of the Earth around the Sun is an ellipse with Sun at one of the foci. The mean Earth-Sun distance varies from 144 (21 December) to 154 million km (21 June). The correction coefficient of the Earth-Sun distance (dimensionless) can be calculated by the equation :

$$c_t = 1 + 0.034. \cos(j - 2) \quad (1)$$

Where J is the day number of the year, ranging from 1 on 1 January to 365 on 31December.

3.1.2- Solar declination:

the solar declination δ (degrees) is the angle between the direction of the Sun with the equatorial plane of the Earth. The declination varies from $-23^\circ 27'$ at the winter solstice to $+23^\circ 27'$ at the summer solstice, while at the equinoxes is zero. The solar declination can be calculated by the equation given by Copeer (1967) :

$$\delta = 23.25. \sin(0.986. (j + 284)) \quad (2)$$

3.1.3- Hour Angle:

The hour angle ω (degrees) is the angle between the meridian plane passing through

the center of the Sun and the vertical plane of the place (meridian) and defines the true solar time T_{sv} (hours). The hour angle can be calculated by the next equation :

$$\omega = 15. (12 - T_{sv}) \quad (3)$$

With T_{sv} (hours) is the true solar time of the local studied and it is determined by the relationship:

$$T_{sv} = T_l - DT_l + (D_{hg} + E/60)/60 \quad (4)$$

- T_l : local time (hours).
- DT_l : Difference of local and standard time (hours).
- D_{hg} : the time difference (advance of 4 minutes per degree).
- E : equation of time, which is calculated by the equation (second):

$$E = 45.8. \sin\left(\frac{2. \pi. j}{365} - 0.026903\right) + 595.4. \sin\left(\frac{4. \pi. j}{365} + 0.352835\right) \quad (5)$$

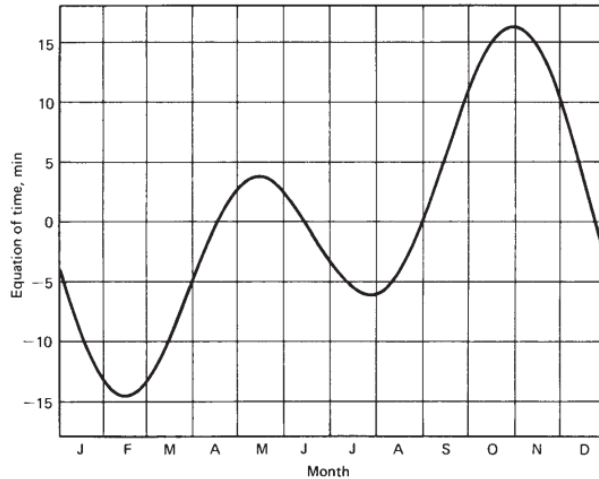


Figure.3.2: The equation of time E in minutes as a function of time of year [11].

3.1.4- Geographical coordinates:

The geographical coordinates of the studied location are represented by the latitude

φ (degrees), longitude (degrees) and altitude z (m), where the latitude is the angle between the position study with the equator and longitude is the angle between the meridian of the study with the meridian position.

3.1.5- Height of the Sun:

The height of the Sun h (degrees) is the angle between the horizontal planes with the direction of the Sun. The value $h=0$ is at sunrise and sunset, The Height of the Sun varies between 90° (zenith) and -90° (nadir) and is calculated by the following formula:

$$h = \sin^{-1}(\sin(\varphi) \cdot \sin(\delta) + \cos(\varphi) \cdot \cos(\delta) \cdot \cos(\omega)) \quad (6)$$

3.1.6- Azimuth of the Sun:

The azimuth of the sun ψ (degrees) is the angle on the horizontal plane, being the projection of the direction of the Sun with the direction to the south. The azimuth is between $-180^\circ \leq \psi \leq 180^\circ$, and it is a function of the solar declination δ , Height of the Sun h and hour angle ω , can be calculated by the next formula:

$$\psi = \sin^{-1}(\cos(\delta) \cdot \frac{\sin(\omega)}{\cos(h)}) \quad (7)$$

3.1.7- Day length:

it is calculated by the following formula:

$$S_j = 24 \left(1 - \frac{\cos^{-1}(\tan(\delta) \cdot \tan(\lambda))}{\pi}\right) \quad (8)$$

It is expressed in hours .

3.1.8- Sunshine duration:

It is calculated by the following formula:

$$S_g = \frac{2}{15} \cdot \cos^{-1}(-\tan(\varphi) \cdot \tan(\delta)) \quad (9)$$

It is expressed in hours.

3.2 Solar radiation

Solar irradiance is the power per unit area received from the Sun in the form of electromagnetic radiation in the wavelength range of the measuring instrument. Irradiance may be measured in space or at the Earth's surface after atmospheric absorption and scattering. It is measured perpendicular to the incoming sunlight. Total solar irradiance (TSI), is a measure of the solar power over all wavelengths per unit area incident on the Earth's upper atmosphere [14].

Irradiance is a function of distance from the Sun, the solar cycle, and cross-cycle changes. Irradiance on Earth is also measured perpendicular to the incoming sunlight. Insolation is the power received on Earth per unit area on a horizontal surface. It depends on the height of the Sun above the horizon [14] and [15].

Part of the radiation reaching an object is absorbed and the remainder reflected. Usually the absorbed radiation is converted to thermal energy, increasing the object's temperature. Manmade or natural systems, however, can convert part of the absorbed radiation into another form such as electricity or chemical bonds, as in the case of photovoltaic cells or plants. The proportion of reflected radiation is the object's reflectivity or albedo [16].

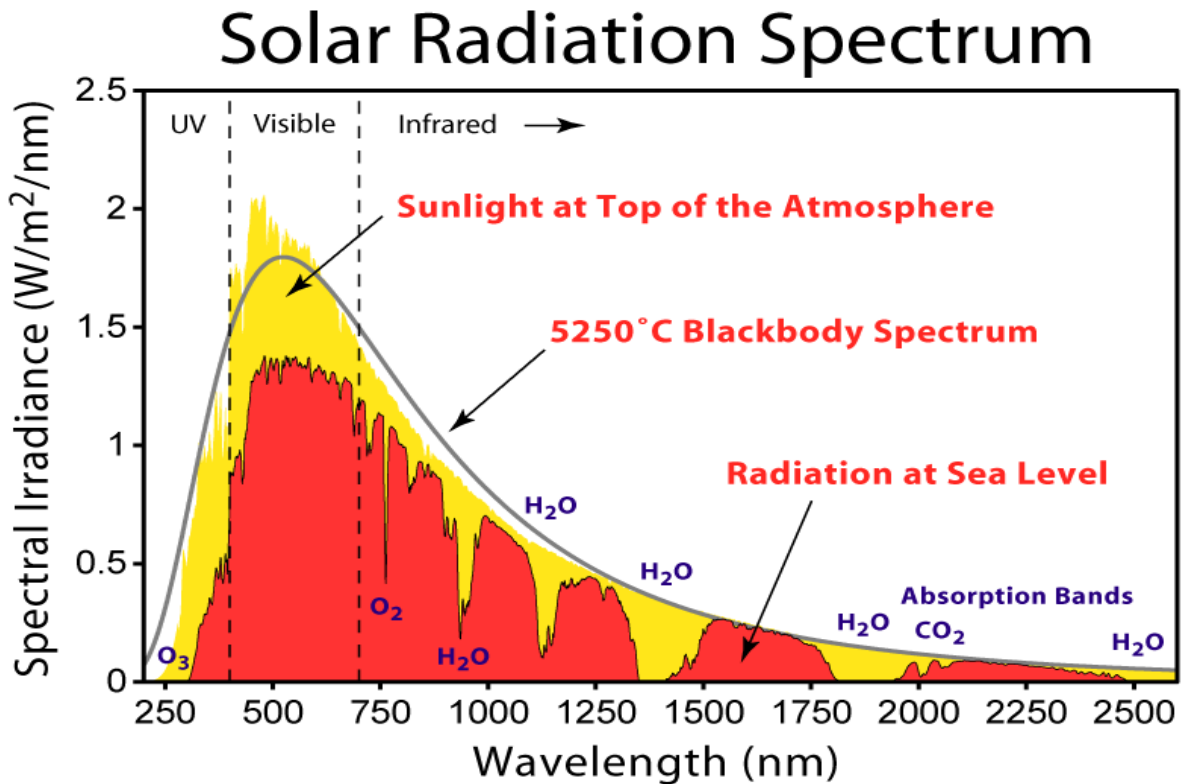


Figure.3.3: Solar radiation spectrum [16].

3.3 CPV configuration

There are many different CPV systems configurations. The technical solutions taken for each component may vary significantly and in the following lines we present and discuss some of the most common configurations for each component, as summarized in Fig.3.4. Some of the most noticeable examples are also presented in the next section [17].

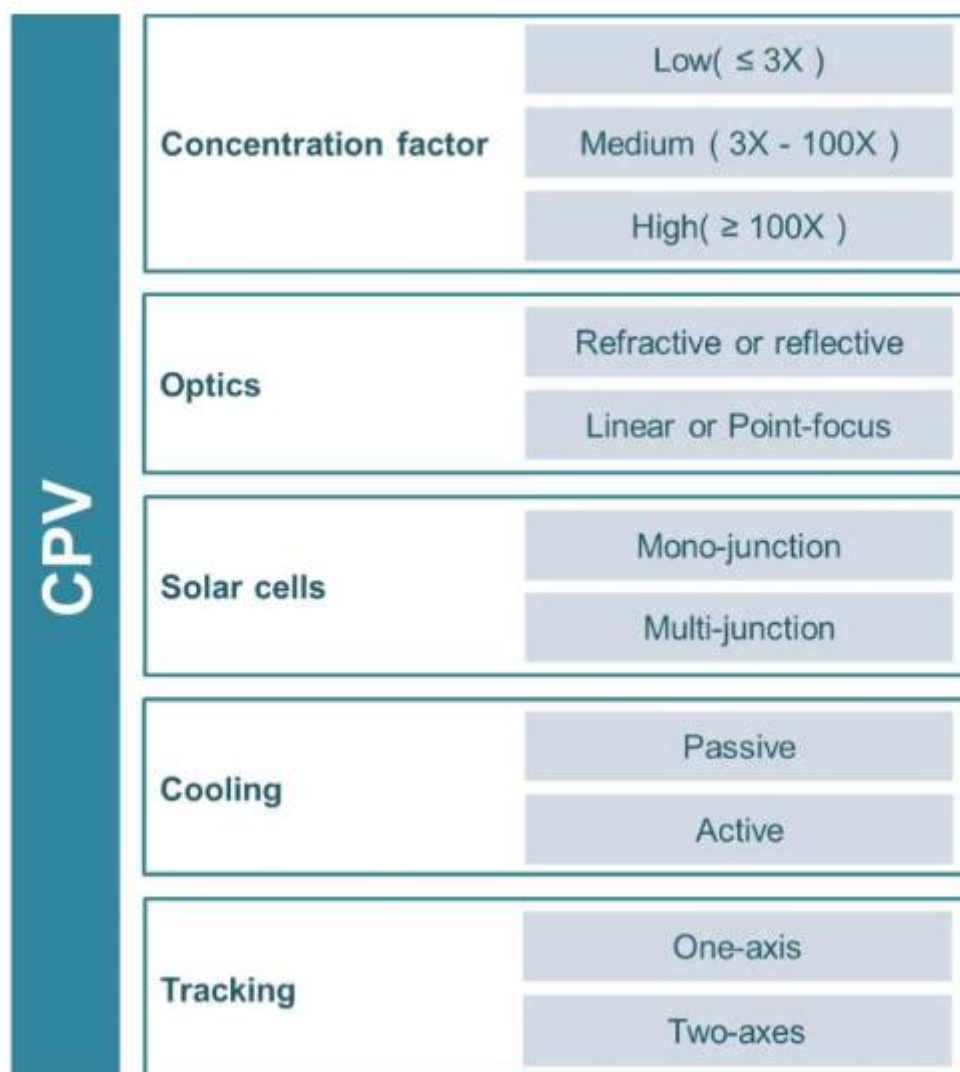


Figure.3.4: A CPV fields & options [17].

a) Concentration factor

The PV concentrators have many more characteristic parameters than the flat modules, and they can be classified under many more possible criteria. For example they

can be roughly divided in two main categories with respect to the concentration level they achieve [18]:

- i. High concentration (>300 X, HCPV) point point-focus systems with highly efficient III–V cells ($>35\%$) and with a high specific cost.
- ii. Low or medium concentration (2–60 X) with silicon cells of up to 20–22% efficiency and at low cost.

Beyond this, concentrators may be classified depending on the optical means used to concentrate the light, the number of axes of the tracking of the sun, the mechanical mechanism that affects the tracking, and so on.

b) Concentrator optics

The concentrator optics must be designed in such a way that its acceptance angle, i.e. the maximum angle at which the rays entering the optics reach the cell, admits the misalignments and tolerances that the manufacturing processes or tracking might introduce. The optics must be designed in order to accept 90% of the rays coming from a cone of semi-angle which is defined as the angular -diameter, of 0.26° .

Concentrator optics can be designed in a number of ways; however, most concentrator optics found on literature can be grouped in two main categories: refractive lenses or reflective dishes and troughs (Antonio Luque & Hegedus 2003) as explained in the following lines [18].

- **Refractive optics**

Fresnel lenses are the most common option due to its low thickness and low cost. A Fresnel lens may be thought as a standard plan convex lens that has been collapsed at a number of locations into a thinner profile. Fresnel lenses may be divided into: a) point-focus if the lenses have circular symmetry about their axis and this configuration usually uses one cell behind each lens; or b) linear focus, when the lenses have a constant cross section along transverse axis and focus the light into a line (Fig.3.5).

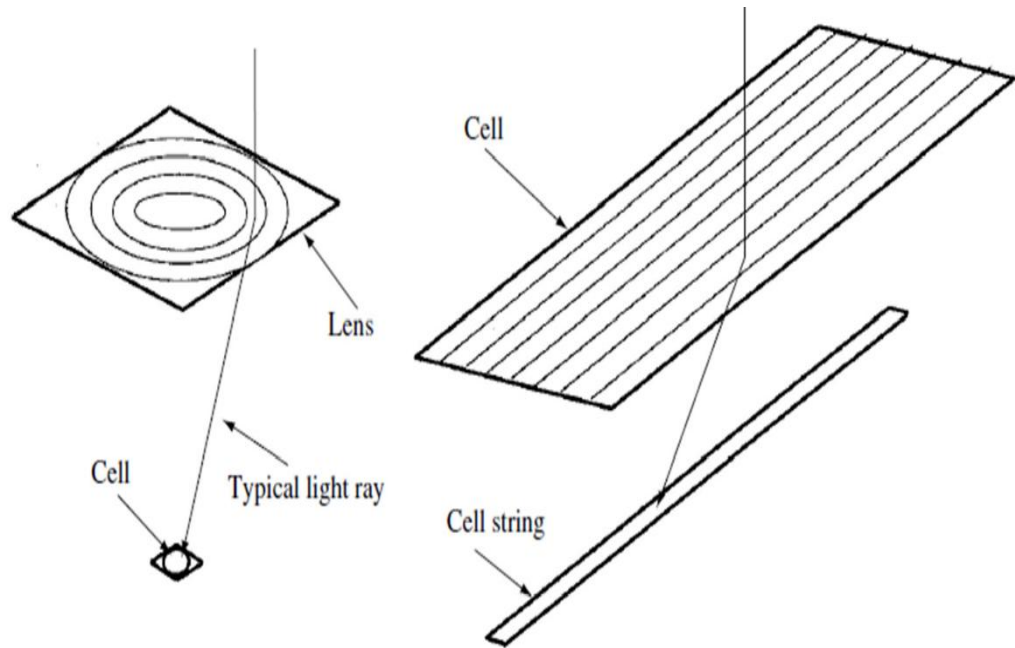


Figure.3.5: basic Fresnel lens configuration: point focus and, linear Fresnel lens [18].

- **Reflective optics**

A reflective surface with the shape of a parabola will focus all the light parallel to the parabola's axis to a point located at a parabola's focus. Like lenses, parabolas could be grouped as:

- i) point-focus, which is formed by rotating the parabola around its axis and creating a paraboloid;
- ii) or line focus: which is formed by translating the parabola perpendicular to its axis. Another design option is the compound parabolic concentrator (CPC) (Oliveira et al. 1995), which typical configuration is sketched in Fig.3.6

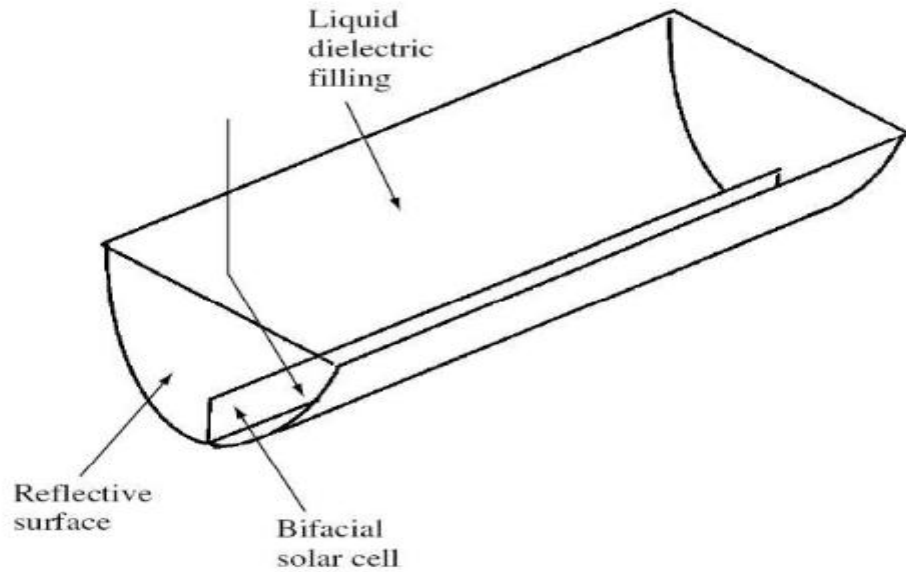


Fig.3.6: Example of a static concentrator configuration. A bifacial cell is mounted in a reflective CPC-like trough that is filled with liquid dielectric [18].

Regarding line focus systems, they typically produce Gaussian illumination profiles, i.e. the center of the solar cells is more illuminated than its edges. The impact of this effect on the performance of the receiver will be discussed below in detail in this thesis [19]. Another challenge in line focus configuration arises when using single-axis tracking systems: the end of the receiver is less illuminated than the central region and since the solar cells in the receiver are typically connected in series, placement of bypass diodes is mandatory to avoid shaded cells to be harmful for receiver performance.

- **Solar cells for CPV**

In early designs, the solar cells integrated in CPV systems consisted of conventional silicon solar cells or modified silicon cells for better performance under higher (more than 1 sun) irradiation levels. At that time, multi-junction (MJ) solar cells based on III-V semiconductors, which are more efficient, were only used in space applications since they were too expensive. However, this perspective has changed as high and very high concentration CPV systems were developed, which can afford these high efficiency cells without significant weight on the CPV system total cost due to the very small cell area required [18].

Regarding solar cells efficiency, we must bear in mind that, when comparing with flat-plate PV: CPV systems are only able to correctly collect direct radiation (which is about

80% of global radiation in sunny regions) and CPV optical efficiency (typically about 80%) will further decrease the efficiency of the system. Nowadays, we may find MJ solar cells that feature very high efficiency but these cells are mainly produced in small quantities by dedicated manufacturers thus having very high cost which has inhibited their integration in low and some medium concentration systems. One should notice, however, that silicon solar cells may be particularly competitive for these classes of concentration systems due two main reasons [19]:

- Silicon solar cells technology has a track recorded field demonstration on terrestrial applications;
- Introducing high efficiency features on standard silicon solar cell processing will increase the cost but it will most likely still be affordable when integrated in CPV systems. Benefiting from economies of scale this may lead to spill over to standard PV modules technologies, which will decrease the price and increase its competitiveness for CPV application.

3.4 Tracking for CPV

Trackers are used to enable the optical components in the CPV and CSP systems. The optics in concentrated solar applications accept the direct component of sunlight light and therefore must be oriented appropriately to collect energy. Tracking systems are found in all concentrator applications because such systems do not produce energy unless pointed at the Sun [20].

The tracking structures have movable parts, which are subjected to fatigue. Thus, regular maintenance is advised, carrying additional costs to the system. These systems also require additional devices such as drive motors, computers and sensors. They usually require larger deployment areas, to avoid shadows on one another and there are also some challenges associated with system's foundation and maximum operative wind speed [21]. The foundation and motor have to withstand considerable force, even when the wind is calm. Most trackers today have wind sensors that tell the unit to move into a safe horizontal position in the event of wind loads threatening to damage the system. There is no general accepted list of criteria for the stability of PV tracking systems [21].

3.4.1 Two-axis Tracking systems with two axes means that the system is pointed exactly towards the sun position during all day and year. Depending on location, this kind of trackers may lead to an increase of about 35% in the yearly energy yield. There are three types of common two-axis systems (Fig.3.7) [20]:

- Roll-tilt structure:** wind loads on drive components are considerably reduced; however more rotating bearings and linkages are required. The design consists on a roll axis, usually placed in a north-south direction (as it minimizes shadowing by adjacent modules) and supported by multiple foundations that must be aligned, complicating installation. It is also necessary to have a tilt axes which moves according to the height of the sun (Fig.3.7 b) and c)).

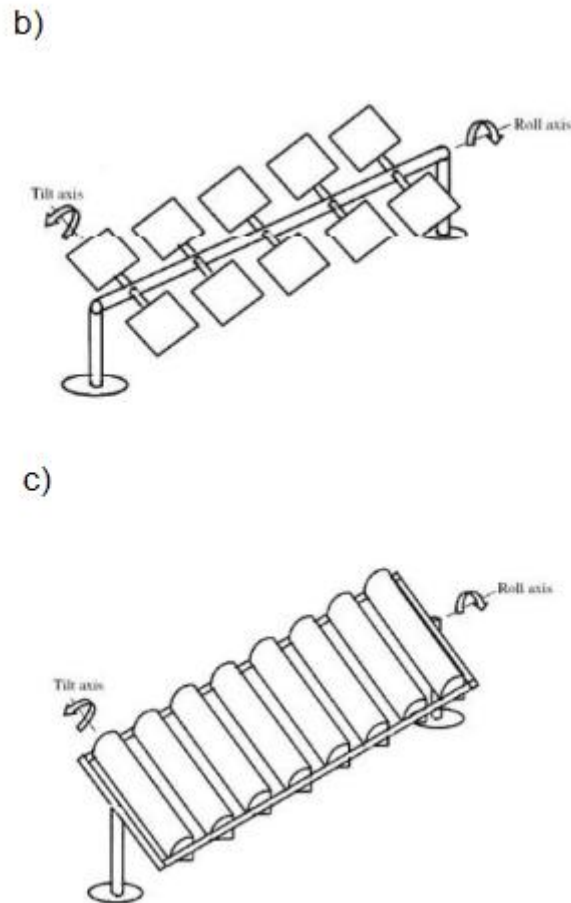


Fig.3.7 (b,c): Roll-tilt structure two- axis tracking configurations [20].

- Turntable:** provides for the lowest profile and lowest wind loading, and can use rather small drive components and support members (Fig.3.7 d)). However, this design structure presents the most complex installation scenario.

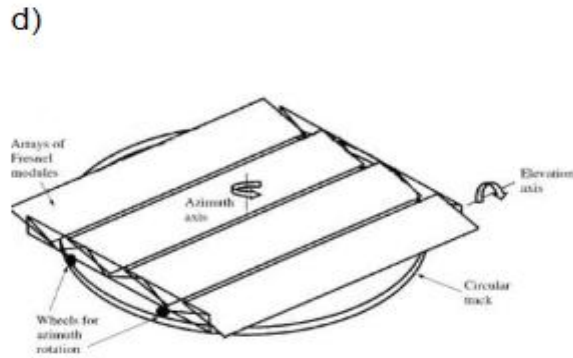


Fig.3.7(d): Turntable tracking configurations [20].

The azimuth elevation pedestal structure is the most common; this was the structure adopted in the first Sandia prototype.

3.4.2 One-axis The one-axis tracking system provide lower yields than dual-axis but are considerably less expensive to produce and less susceptible to problems. One of its main advantages is a lower installation height, and therefore lower wind sensitivity and space requirements. Thus, these solutions are sometimes the system of choice for roof top systems [20].

The most common one-axis structure designs are :

- **Horizontal axis:** provides lower profile and larger area per tracking structure, as compared to the polar axis approach.
- **Polar-axis:** gives higher intercepted annual energy and limits the incoming sun angle to a maximum of 23° from the plane of the concentrator (Fig.3.7 b)).



Fig.3.7(a,b): One-axis tracking configurations: a) One-axis horizontal tracker with reflective trough; b) One-axis polar axis tracker with reflective trough [20].

The simplicity and low profile of the horizontal-axis configuration makes it the more common choice over the polar-axis approach [20]. One-axis tracking is possible in linear systems using parabolic troughs or line focus reflective troughs.

One simple way of designing a solar tracker is the use of a microcontroller to driver position motors. An attractive solution is to combine an arduino to stepper moteurs:

3.4.2 Arduino

The Arduino Uno is a microcontroller board based on the ATmega328. It has 14 digital input/output pins (of which 6 can be used as PWM outputs), 6 analog inputs, a 16 MHz crystal oscillator, a USB connection, a power jack, an ICSP header, and a reset button. It contains everything needed to support the microcontroller; simply connect it to a computer with a USB cable or power it with a AC-to-DC adapter or battery to get started.

The Uno differs from all preceding boards in that it does not use the FTDI USB-to-serial driver chip. Instead, it features the Atmega8U2 programmed as a USB-to-serial converter. "Uno" means one in Italian and is named to mark the upcoming release of Arduino 1.0. The Uno and version 1.0 will be the reference versions of Arduino, moving forward. The Uno is the latest in a series of USB Arduino boards, and the reference model for the Arduino platform; for a comparison with previous versions, see the index of Arduino boards [24], [25].

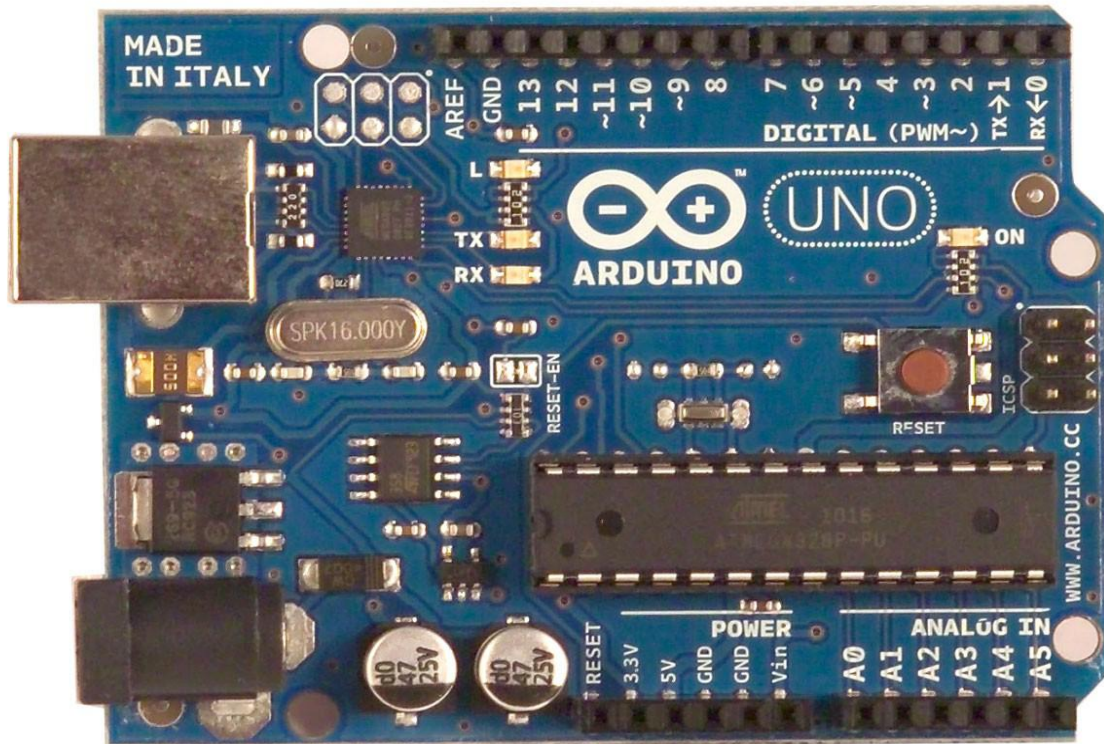


Figure.3.8: Arduino board [25].

Technical specification [26]:

- Microcontroller ATmega328
- Operating Voltage 5V
- Input Voltage (recommended) 7-12V
- Input Voltage (limits) 6-20V
- Digital I/O Pins 14 (of which 6 provide PWM output)
- Analog Input Pins 6
- DC Current per I/O Pin 40 mA
- DC Current for 3.3V Pin 50 mA
- Flash Memory 32 KB of which 0.5 KB used by Bootloader

- SRAM 2 KB
- EEPROM 1 KB
- Clock Speed 16 MHz

3.4.4 Stepper motors

Stepper motors are DC motors that move in discrete steps. They have multiple coils that are organized in groups called "phases". By energizing each phase in sequence, the motor will rotate, one step at a time [27].

With a computer controlled stepping you can achieve very precise positioning and/or speed control. For this reason, stepper motors are the motor of choice for many precision motion control applications. Stepper motors come in many different sizes and styles and electrical characteristics [28].

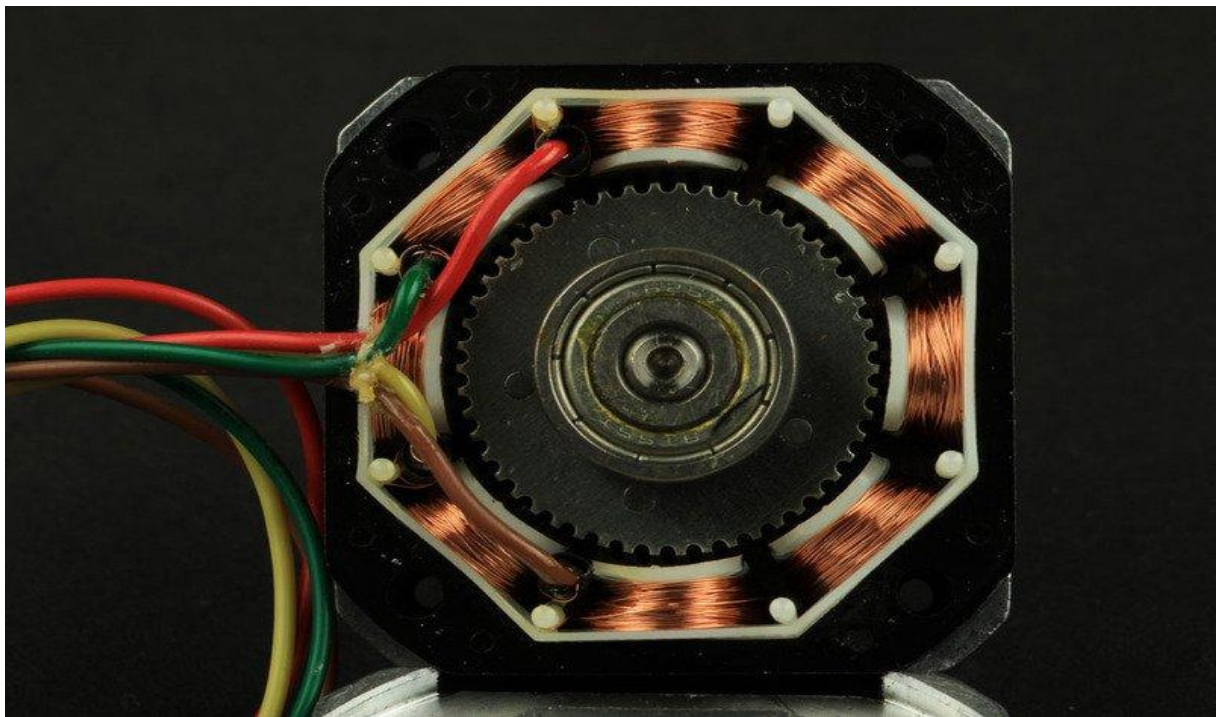


Figure.3.9: Stepper motor [28].

a) What are stepper motors good for?

- **Positioning** – Since steppers move in precise repeatable steps, they excel in applications requiring precise positioning such as 3D printers, CNC, Camera

platforms and X,Y Plotters. Some disk drives also use stepper motors to position the read/write head.

- **Speed Control** – Precise increments of movement also allow for excellent control of rotational speed for process automation and robotics.
- **Low Speed Torque** - Normal DC motors do not have very much torque at low speeds. A Stepper motor has maximum torque at low speeds, so they are a good choice for applications requiring low speed with high precision.

b) What are their limitations?

- **Low Efficiency** – Unlike DC motors, stepper motor current consumption is independent of load. They draw the most current when they are doing no work at all. Because of this, they tend to run hot.
- **Limited High Speed Torque** - In general, stepper motors have less torque at high speeds than at low speeds. Some steppers are optimized for better high-speed performance, but they need to be paired with an appropriate driver to achieve that performance.
- **No Feedback** – Unlike servo motors, most steppers do not have integral feedback for position. Although great precision can be achieved running ‘open loop’. Limit switches or ‘home’ detectors are typically required for safety and/or to establish a reference position [28].

3.5 Cooling for CPV

In photovoltaic systems, the sunlight energy striking the cell is only partially converted into electricity; the remaining energy is converted into thermal energy. In CPV systems, due to the very high amount of incident light on the cells, they would reach very high temperatures [29]. Moreover, resistive losses on the cell may also contribute to its temperature increase [29]. An increase in cell temperature decreases the band gap leading to a decrease of the cell open-circuit voltage (V_{oc}) and efficiency, on the short-term, or even long-term irreversible damage[30]. Thus, the cell ought to be kept at relatively low temperatures, i.e. the generated heat must be extracted from the cell. For such purpose CPV systems may integrate a cooling mechanism whose design considerations should follow some important criteria [29]:

Low temperatures: solar cells have a maximum operating temperature, a value above which the devices operation may show long term degradation; moreover, as mentioned above, the photovoltaic efficiency decreases with increasing temperature so, solar cells should operate at low temperatures.

Temperature uniformity: in this point two situations must be taken into account: a) the solar cell efficiency decreases with the spatial non-uniformity of the temperature on the cell; and b) in a CPV receiver the solar cells are usually connected in series and some of these series connections may be connected in parallel. Therefore, the receiver's V_{oc} is limited by the lowest V_{oc} , which usually is dictated by the group in series connection at highest temperature, which means that all the cells in the string should be in operation under the same temperature in order to achieve highest efficiency [30].

Minimal requirements: the cooling system should have minimal maintenance and power consumption in order to keep total CPV system costs at the lowest level possible. Ability to deal with 'worst case scenarios': the cooling system must be robust in order to withstand situations such as;

- a) power outages
- b) tracking anomalies
- c) electrical faults.

Cooling systems may be divided into passive or active (Fig.3.7). The passive cooling relies on solutions such as the integration of heat sinks (multi-fined structure) or can simply consist on the back of the module surface spreading the heat across it to interchange heat with the surrounding air. Regarding active cooling, typically a fluid is used to extract the heat from the cells. The passive cooling option is generally preferred since it usually is simpler, cheaper, maintenance free and avoids the use of water [29].

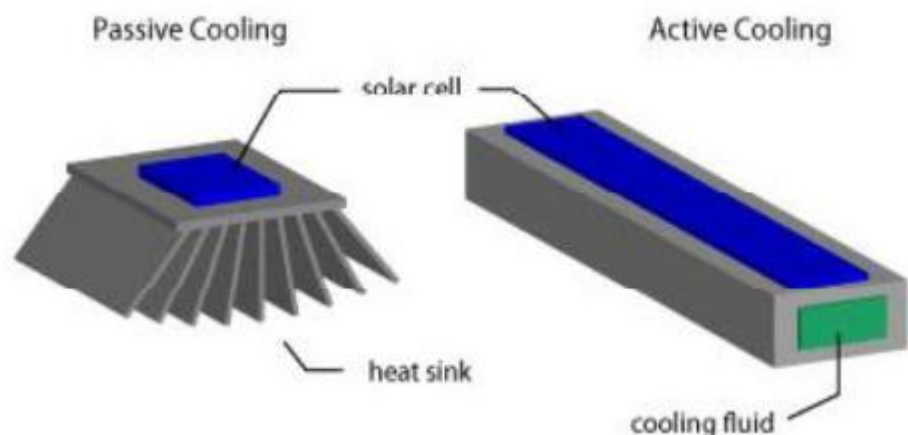


Figure.3.10: Schematics of passive and active cooling systems [29].

3.6 Modelling analysis

A PV system directly converts sunlight into electricity. The main device of a PV system is a solar cell. Cells may be grouped to form panels or arrays. Power electronic converters are usually required to process the electricity from the PV device. These converters may be used to regulate the voltage and current at the load, to control the power flow in grid-connected systems, and for the maximum power point tracking (MPPT) of the device (Practical Solar - Technology- février 2008) [31].

The solar cell is basically a semiconductor diode exposed to light. Solar cells are made of several types of semiconductors using different manufacturing processes.

The electrical energy produced by a solar cell at any time instant depends on its intrinsic properties and the incoming solar radiation. The solar radiation is composed of photons of different energies, and some are absorbed at the $p-n$ junction.

Photons with energies lower than the bandgap of the solar cell are useless and generate no voltage or electric current. Photons with energy superior to the bandgap generate electricity, but only the energy corresponding to the bandgap is used. The remainder of energy is dissipated as heat in the body of the solar cell [32]. A single-diode PV cell model is considered in this paper, including the effect of the series resistance. The paper uses the equivalent circuit of a solar cell with its parameters as a tool to simulate in order to consider the irradiance and temperature change, the I-V characteristics of PV cell.

3.6.1 Ideal Solar Cell

As mentioned previously, the solar cells are semiconductor with a $p-n$ junction fabricated in a thin wafer or layer of semiconductors. When exposed to light a photo current proportional to the solar radiation is generated, if the photon energy is greater than the band gap. In the dark, the I-V characteristics of a solar cell have an exponential characteristic similar to that of a diode. In order to maximize the extracted output power from a PV power plant with the help of MPPT control, the understanding and modelling of PV cell is necessary [33].

The ideal equivalent circuit of a solar cell is a current source in parallel with a single-diode. The configuration of the simulated ideal solar cell with single-diode is shown in Figure.3.11.

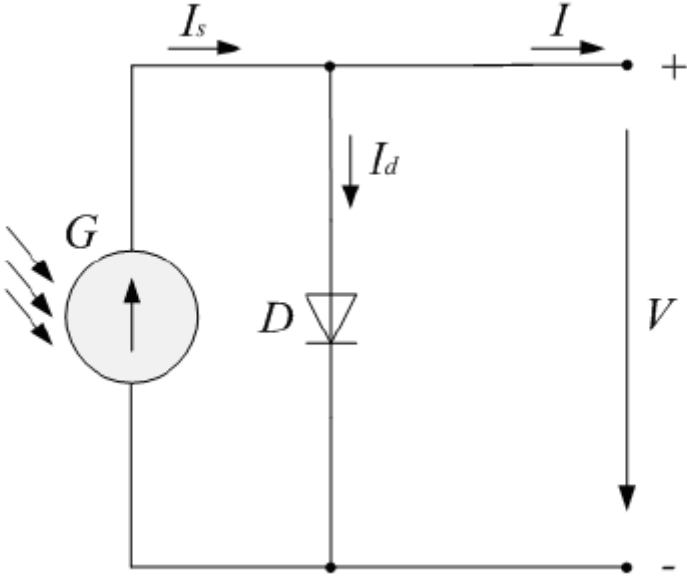


Figure.3.11 Ideal solar cell with single-diode [33].

The I-V characteristics of the ideal solar cell with single diode are given by:

$$I = I_s - I_0 \left(e^{\frac{qV}{mkT}} - 1 \right) \quad (10)$$

Where I_0 is the diode reverse bias saturation current, q is the electron charge, m is the diode ideality factor, k is the Boltzman's constant, and T is the cell temperature. A solar cell can at least be characterised by the short circuit current I_{sc} , the open circuit voltage V_{oc} , and the diode ideality factor m [33].

$$I_{sc} = I = I_s \quad \text{for} \quad V = 0 \quad (11)$$

For the same irradiance and $p-n$ junction temperature conditions, the short circuit current I_{sc} it is the greatest value of the current generated by the cell. The short circuit current I_{sc} is given by:

$$V = V_{oc} = \frac{mkT}{q} \ln \left(1 + \frac{I_{sc}}{I_0} \right) \quad \text{for} \quad I = 0 \quad (12)$$

The output power is given by:

$$P = V \left[I_{sc} - I_0 \left(e^{\frac{qV}{mkT}} - 1 \right) \right] \quad (13)$$

3.6.2 Solar Cell with Series Resistance

More accuracy can be introduced to the model by adding a series resistance. The configuration of the simulated solar cell with single-diode and series resistance is shown in Figure.3.12 [33] and [34].

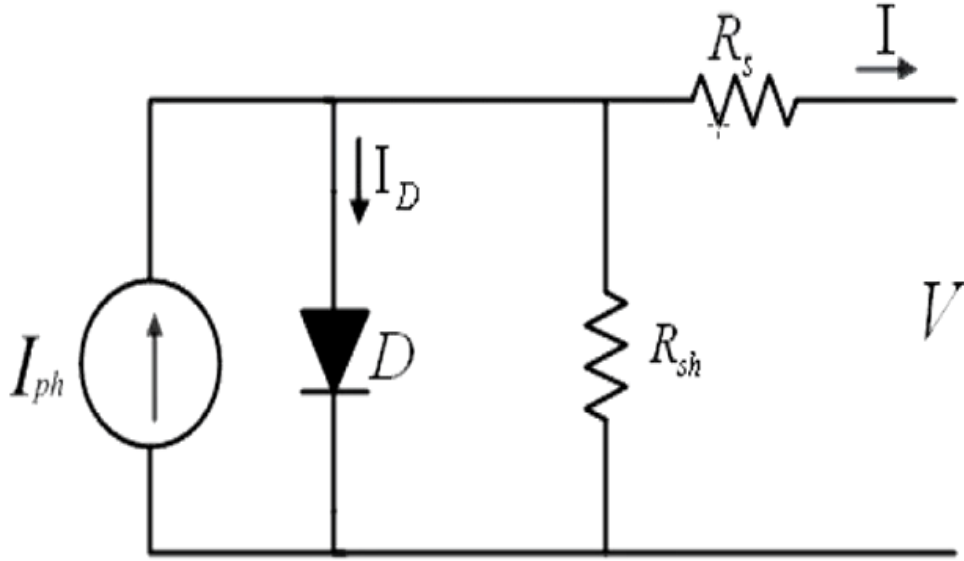


Figure.3.12. Solar cell with single-diode and series resistance [34].

The I-V characteristics of the solar cell with single-diode and series resistance are given by these equations:

$$I = I_{pv} - I_0 \left[\exp \left(\frac{V + IR_s}{aV_T} \right) - 1 \right] - \frac{V + IR_s}{R_{sh}} \quad (14)$$

$$V_T = \frac{N_s k T}{q} \quad (15)$$

$$I_{pv} = \frac{G}{G_n} [I_{pvn} + K_I (T - T_n)] \quad (16)$$

$$I_0 = I_{0n} \left(\frac{T}{T_n} \right)^3 \exp \left[\frac{qE_g}{ak} \left(\frac{1}{T_n} - \frac{1}{T} \right) \right] \quad (17)$$

$$I_{0n} = \frac{I_{scn}}{\exp(V_{0cn}/aV_{Tn}) - 1} \quad (18)$$

3.6.3 Simulation Results

The mathematical models for the ideal solar cell and the solar cell with series resistance were implemented in Matlab/Simulink. The I-V characteristics for various conditions of solar radiation and $m = 1.66$, considering the ideal solar cell, are shown in Figures [34].

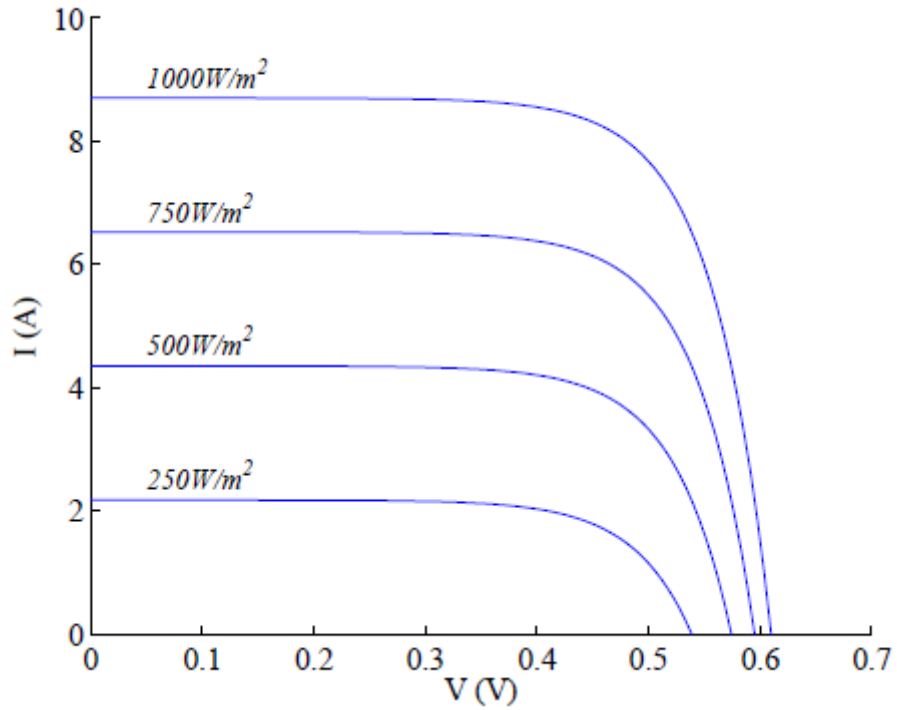


Figure. 3.13 I-V characteristics for various conditions of solar Radiation [34].

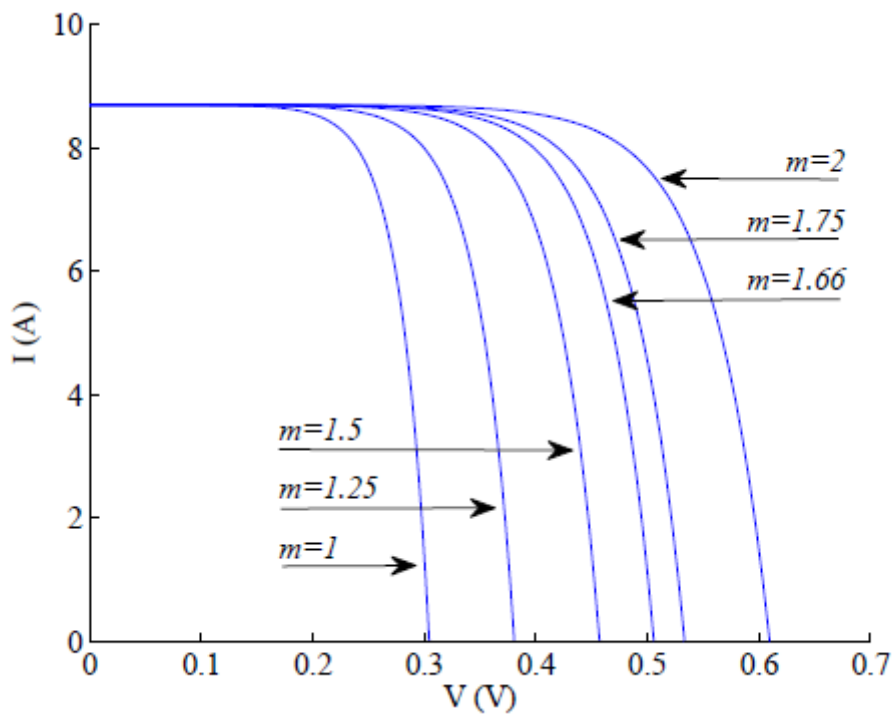


Figure.3.14. I-V characteristics for a diode ideality variation between 1 and 2 [34].

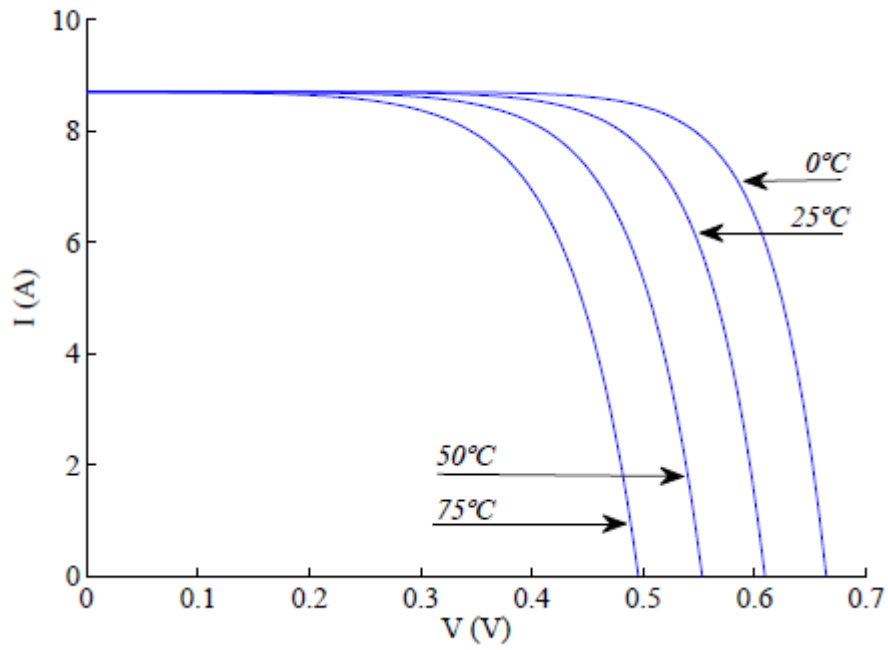


Figure.3.15 I-V characteristics for the temperature variation between 0 and 75°C [34].

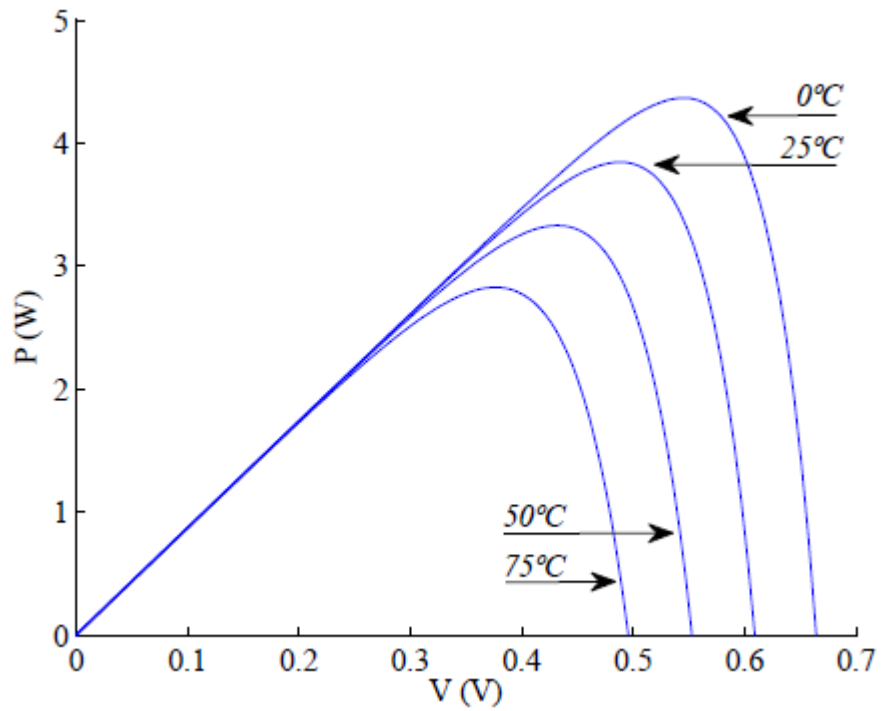


Figure.3.16. P-V characteristics for the temperature variation between 0 and 75°C [34].

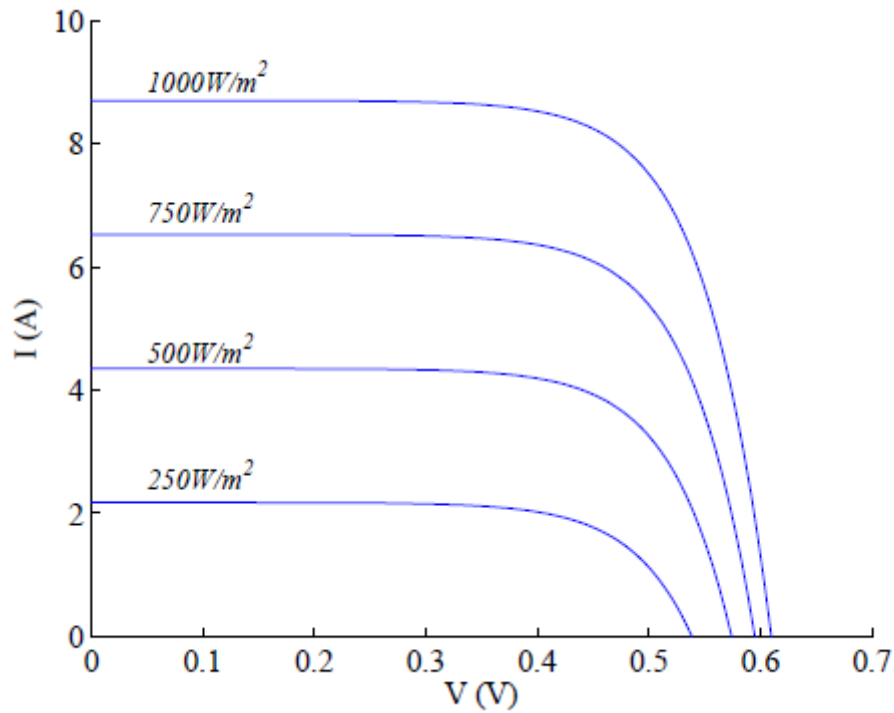


Figure.3.17. I-V characteristics for various conditions of solar radiation (considering series resistance) [34].

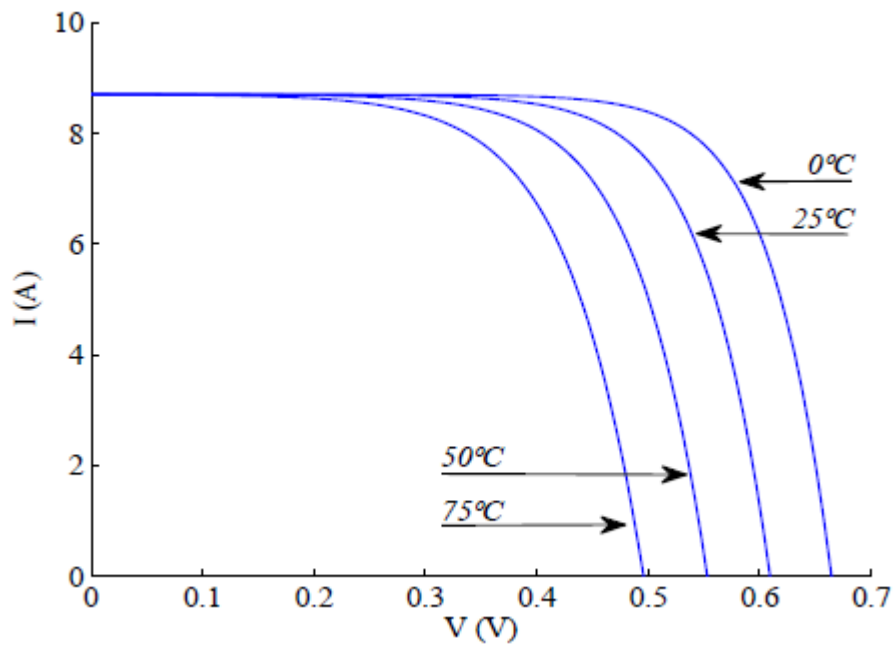


Figure. 3.18. I-V characteristics for a diode ideality variation between 1 and 2 (considering series resistance) [34].

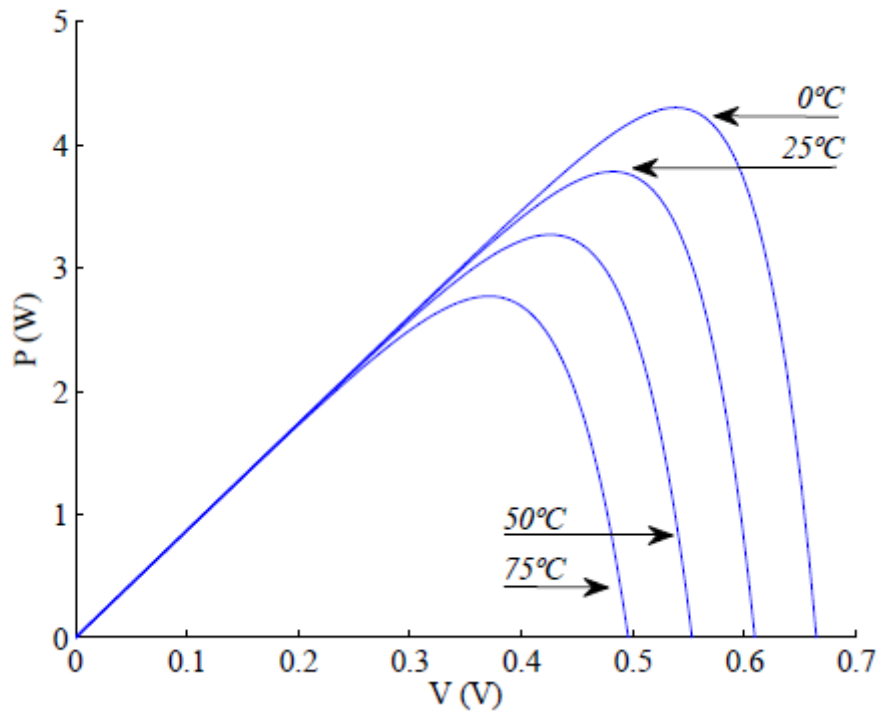


Figure. 3.19 I-V characteristics for the temperature variation between 0 and 75°C (considering series resistance) [34].

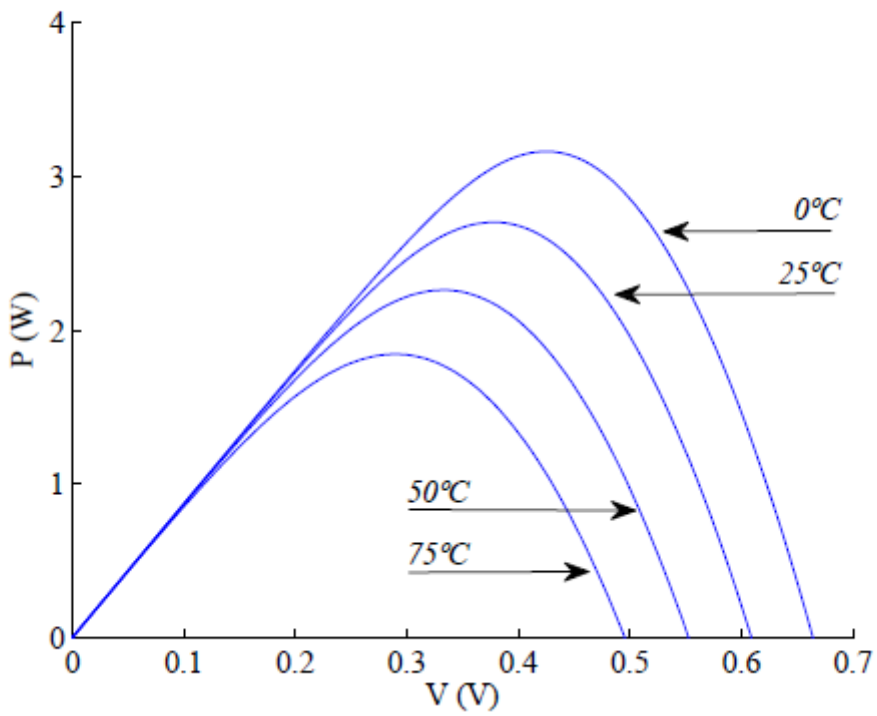


Figure. 3.20. P-V characteristics for $R_s = 20m\Omega$ [34].

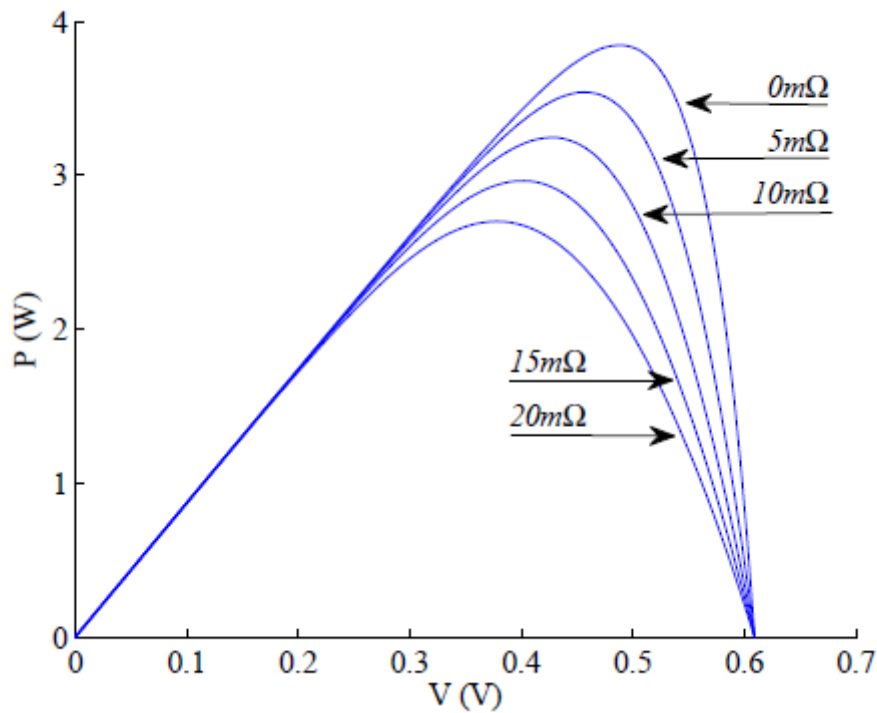


Figure.3.21. P-V characteristics for the R_s variation [34].

With the change of the temperature, the solar radiation, and the diode ideality factor, the I-V and P-V will change accordingly.

The behaviour of ideal solar cell model and the behavior of the solar cell with series resistance model are studied in this paper. Included effects are: temperature dependence, solar radiation change, diode ideality factor and series resistance influence [32]. The solar cell with series resistance model offers a more realistic behaviour for the photovoltaic systems. Particularly, this model is to be considered in panels with series cells, because the series resistance is proportional to the number of solar cells in the panel.

Chapter 4

Experimental setup and testing

4.1 Description of the setup

Several technologies such as mechanics, electronics, optics, and thermal are used in the field of renewable energies. The experimental investigation is carried out on a double axis solar tracker that has a photovoltaic solar cell made from highly pure silicon and has an area of 2 cm x 2 cm.

The fully metallized backside of the solar cell is put on cooling system just to decrease the temperature. When the solar cell is operating under the outdoor condition, the variation in the temperature for a given operating voltage will vary the cell operating condition where the front metal busbar is electrically connected with a spring contact. A thermometer is used to measure the temperature of the cell. The goal of achieving ever increasing solar cell efficiency and reduced cost, demands: accurate, repeatable, fast, and reliable test results. The research, design, and development work necessary to achieve superior performance requires accurate test equipment.

For the mechanic part, the device in Figure.4.1 is a two-axis solar tracker, equipped with two stepper motors. Using the Arduino board helps us to set up the rotation step of the motors. In the other hand, a Fresnel lens of an area of $15 \times 15 \text{ cm}^2$ is used to concentrate the solar direct incident irradiance on the cell.

Our experimental work is divided in two parts:

1st part: consists on the characterization of the solar cell by testing it under one sun.

2nd part: is to test the cell under concentration.

A variety of measurements is used to characterize a solar cell's performance, including its output and its efficiency. This electrical characterization is performed as part of research and development of photovoltaic cells and materials, as well as during the manufacturing process. Several parameters are used to characterize the efficiency of the solar cell, including the maximum power point (P_{max}), the energy conversion efficiency (η), and the fill factor (FF). To take these measures we need two digital multimeters for the current and voltage and one thermometer for temperature. For more precision, we use a light meter and a solar power meter.

These measurements are usually performed at different light intensities and under different temperature conditions. Instrumentation such as the multimeter, which can measure both current and voltage, is to simplify testing photovoltaic materials, these tests, which include I- V, and temperature.



Figure.4.1: The sun tracker and the solar cell employed in the tests.

4.2 Description of instruments used

4.2.1 Digital multimeter

A **digital multimeter (DMM)** is a test tool used to measure two or more electrical values—principally voltage (volts), current (amps) and resistance (ohms).



Figure.4.2: Multimeter to measure the current and the voltage.

4.2.2 Thermometer

A thermocouple is an electrical device consisting of two dissimilar conductors forming electrical junctions at differing temperatures. A thermocouple produces a temperature-dependent voltage as a result of the thermoelectric effect, and this voltage can be interpreted to measure temperature.



Figure.4.3: Thermometer.

4.2.3 Solar power meter

A solar power meter is a device that used for measuring solar irradiance on a planar surface and it is designed to measure the solar radiation flux density (W/m^2) from the hemisphere above within a wavelength range $0.3 \mu\text{m}$ to $3 \mu\text{m}$.



Figure.4.4: Solar power meter.

4.2.4 Light meter

A light meter is a device used to measure the amount of light. It is used in the general field of lighting, where it can help to reduce the amount of waste light used in the home, light pollution outdoors, and plant growing to ensure proper light levels.



Figure.4.5: light meter.

4.2.5 Other tools

To reach the goal of measuring the tests, we needed in the project some other items to connect each part of it: instruments used, the solar cell the Arduino board to have one piece that functions.

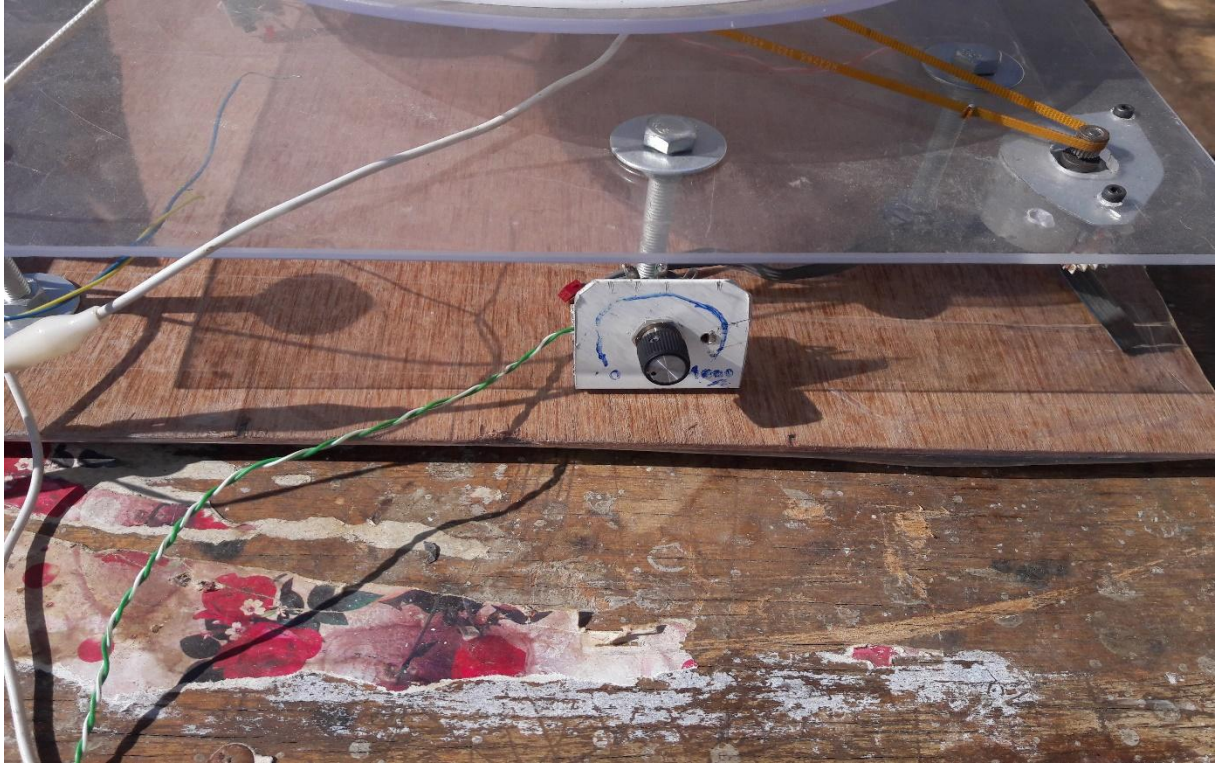


Figure.4.6: a) The resistance used in the work.

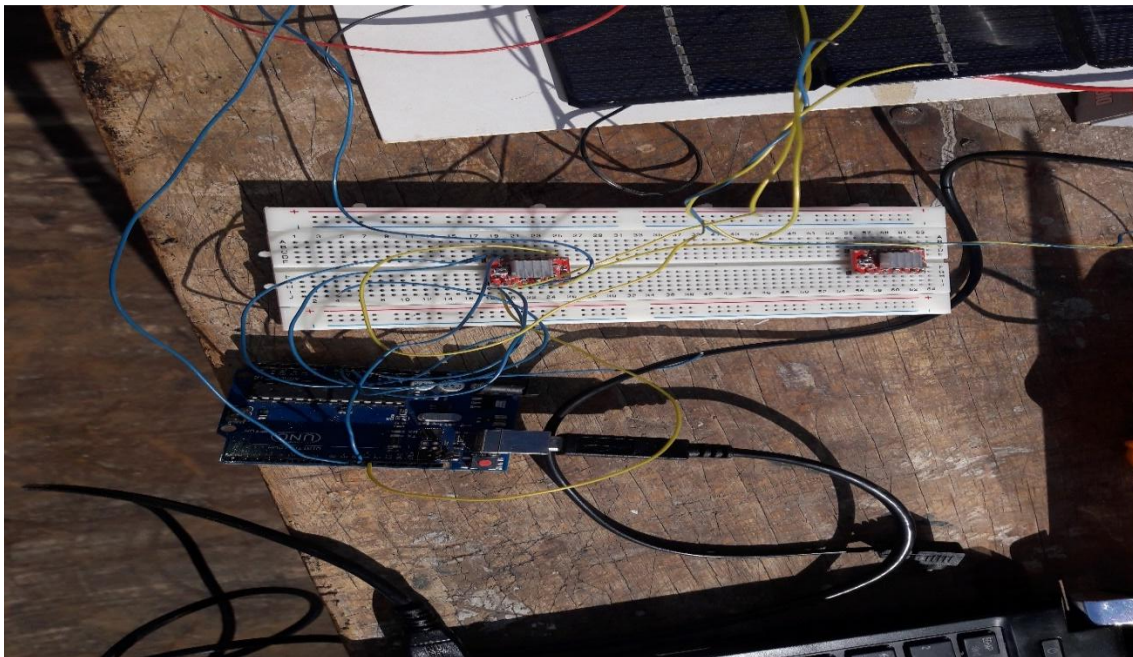


Figure.4.6: b) The Arduino board used in the experience.

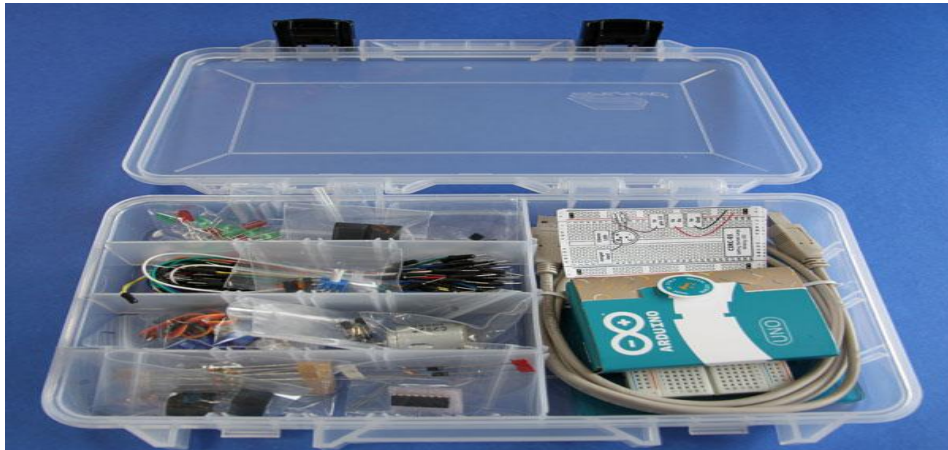


Figure.4.6: c) Other tools used in the experience.

4.3 Cell testing under one sun

The cells is carried out utilizing the sun tracker as shown in Figure.4.7. A variety of measurements are used to characterize the solar cell's performance, at different light intensities.

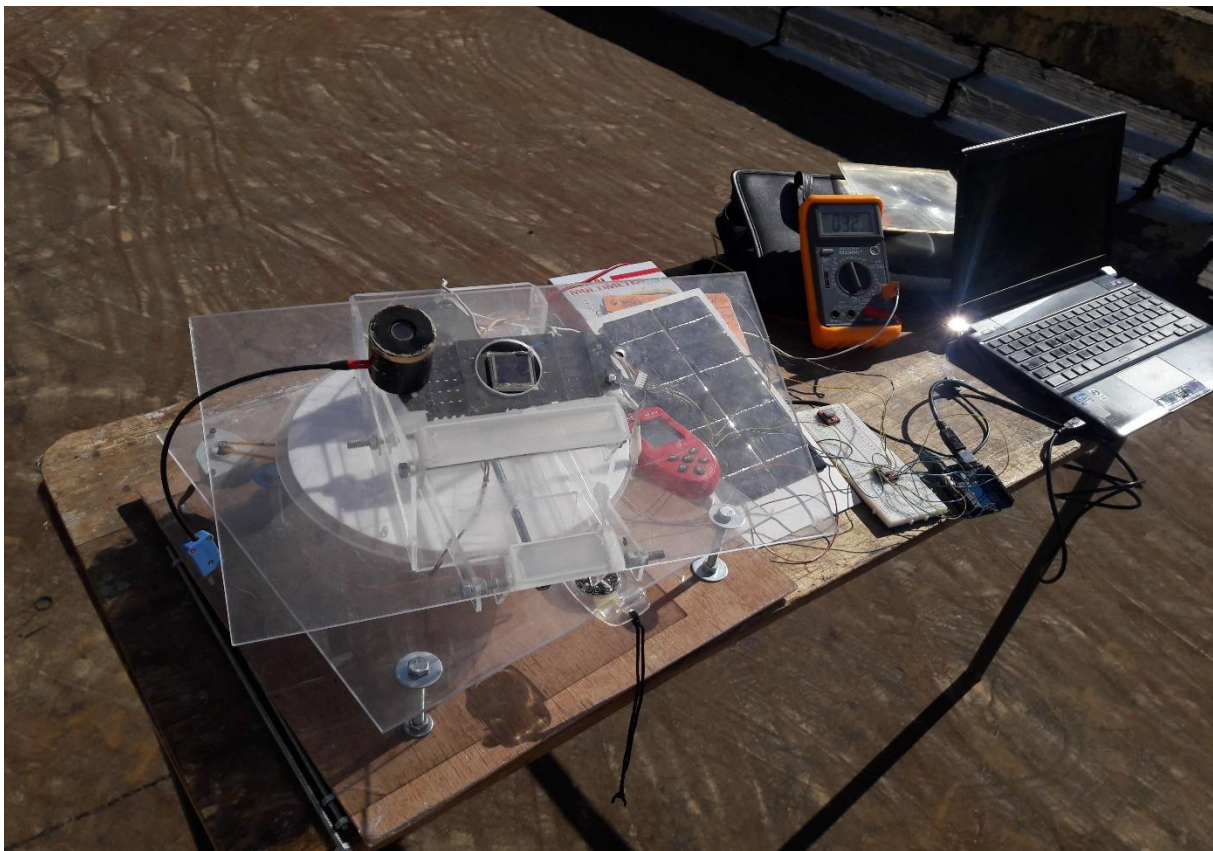


Figure.4.7: The sun tracker and the solar cell employed in the tests under one sun.

4.3.1 Current at short circuit

The maximum current that a solar cell can deliver without harming its own constriction. It is measured by short circuiting the terminals of the cell at most optimized condition of the cell for producing maximum output. The term optimized condition is used because for fixed exposed cell surface the rate of production of current in a solar cell also depends upon the intensity of light and the angle at which the light falls on the cell. As the current production also depends upon the surface area of the cell exposed to light, it is better to express maximum current density instead maximum current. Maximum current density or short circuit current density rating is nothing but the ration of maximum or short circuit current to exposed surface area of the cell [34].

$$J_{sc} = \frac{I_{sc}}{A} \quad (19)$$

Where, I_{sc} is short circuit current, J_{sc} maximum current density and A is the area of solar cell.

4.3.2 Voltage at open circuit

It is measured by measuring voltage across the terminals of the cell when no load is connected to the cell. This voltage depends upon the techniques of manufacturing and temperature but not fairly on the intensity of light and area of exposed surface. Normally open circuit voltage of solar cell is nearly equal to 0.5 to 0.6 volt. It is normally denoted by V_{oc} [34].

4.3.3 Maximum power

The maximum electrical power one solar cell can deliver at its standard test condition. If we draw the I (V) characteristics of a solar cell maximum power will occur at the bend point of the characteristic curve. It is shown in the I (V) characteristics of solar cell by P_m [34].

Current at Maximum Power Point

The current at which the maximum power occurs is called the “Current at Maximum Power Point” and is shown in the I (V) characteristics curve of solar cell by I_m .

Voltage at Maximum Power Point

The voltage at which maximum power occurs is called the “Voltage at Maximum Power Point” and is shown in the I (V) characteristics of solar curve cell by V_m .

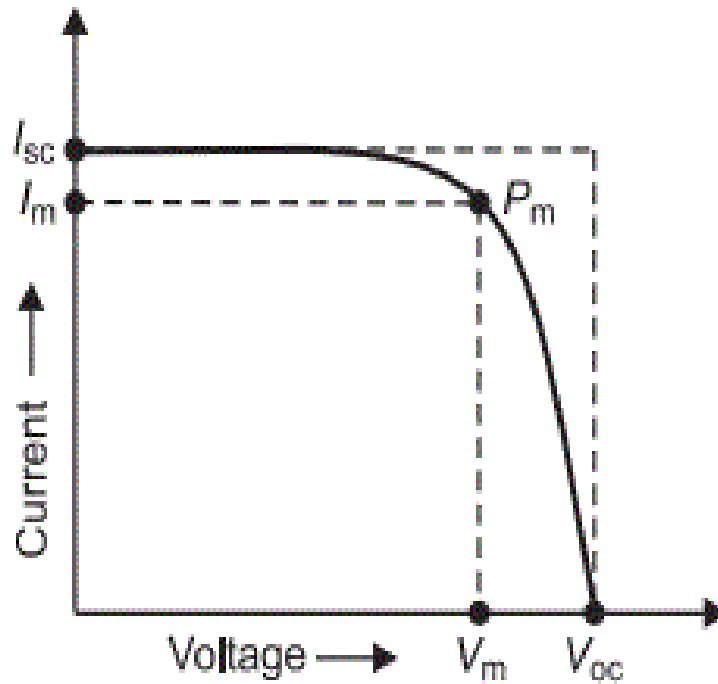


Figure.4.8: A normal behavior of a solar cell [34].

4.3.4 Fill factor

The fill factor is the ratio of the product of current and voltage at maximum power point to the product of short circuit current and open circuit voltage of the solar cell [34].

(20)

$$\text{Fill Factor} = \frac{P_m}{I_{sc} \times V_{oc}}$$

4.3.5 Efficiency

It is defined as the ratio of maximum electrical power output to the radiation power input to the cell.

(21)

$$\text{Efficiency}(\eta) = P_m / P_{in}$$

4.4 Cell testing under concentration

The optical experimentation consists in exposing the solar cell to solar light concentrated by the Fresnel lens which is installed on the solar tracking system as shown in Figure.4.8. The lens is constrained to the grid by means of four small columns, which hold it fixed at a certain distance (7cm and 8cm) and parallel to the grid plane.

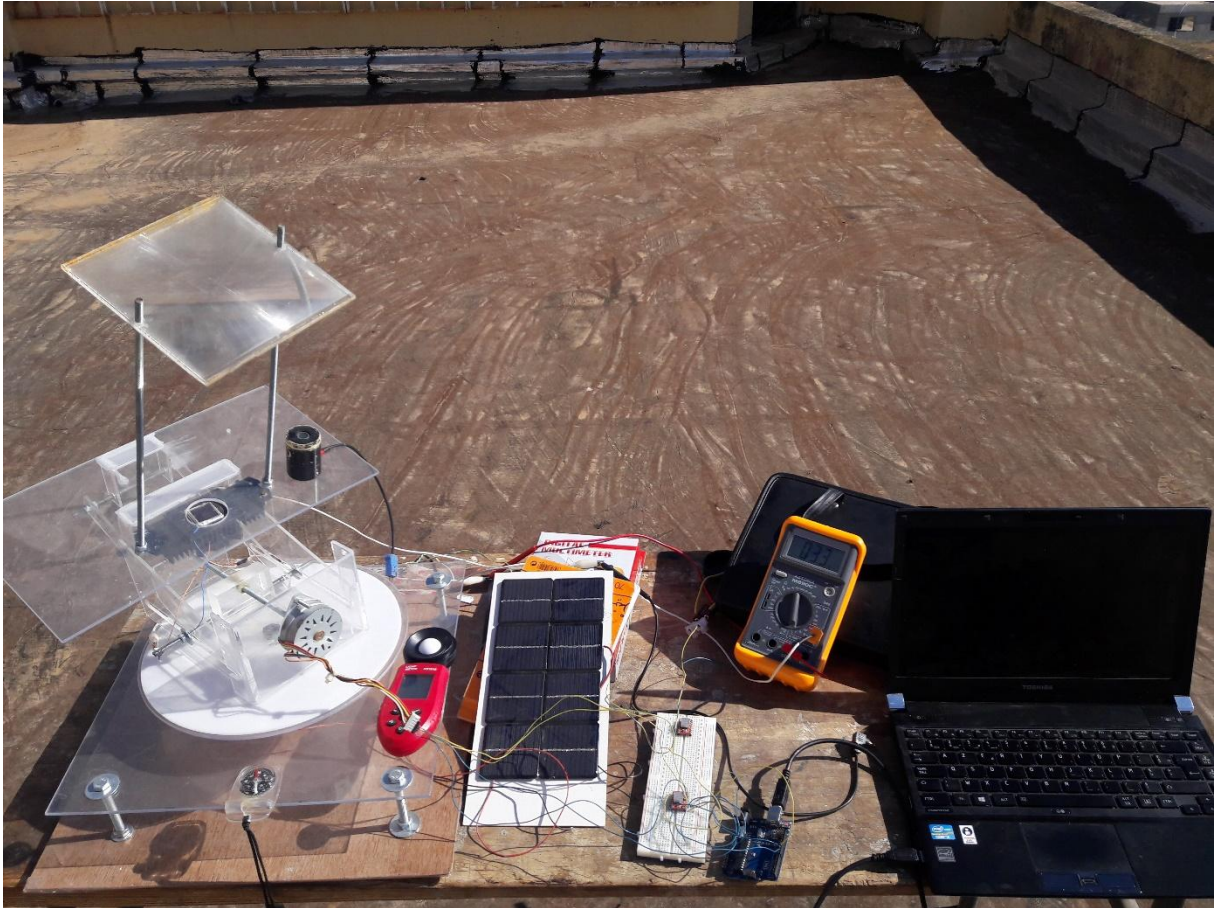


Figure.4.9: The sun tracker and the solar cell employed in the tests under concentration.

The same characterization for the cell under one sun is used for the one under concentration, with the same way to measure, except the incident power changes seen tracking effect aging and alignment we add another factor.

$$P_{(\text{under concentration})} = \text{DNI} * X * A_{\text{cell}} * \eta_{\text{cell}} \quad (21)$$

$$X = C_{\text{goc}} * \eta_{\text{opt}} \quad (22)$$

$$C_{\text{goc}} = A_{\text{lens}}/A_{\text{cell}} \quad (23)$$

Many factors influence in a experiment work, that is why the optical efficiency(η_{opt}) is about 0.75 for more precision [35].

$$\eta_{\text{opt}} = 0.75 \quad (24)$$

Where the efficiency becomes:

$$\textit{Efficiency}(\eta_{\text{cell}}) = P_{\text{(under concentration)}}/ \text{DNI} * X * A_{\text{lens}} \quad (25)$$

Chapter 5

Test results and analysis

5.1 One sun results and analysis

Test 1

The working conditions measured in correspondence with the $V-I$ curve plotted in Figure.5.1; with an exposure duration of almost 3 hours, under light intensity of 143W/m^2 , where the ambient temperature is 33°C , the cell temperature at the beginning of the experiment work is 27°C then it reaches 41°C by the third hour.

The principal characterization of the behavior of the solar cell is illustrated by the $V-I$ curve as shown in Figures.5.1.

The voltage is almost stable where the current decreases from 19.82mA , and the voltage takes a range between 0.260V and 0.276V . The cell temperature is increasing. The chart represents a correct behavior for a photovoltaic cell.

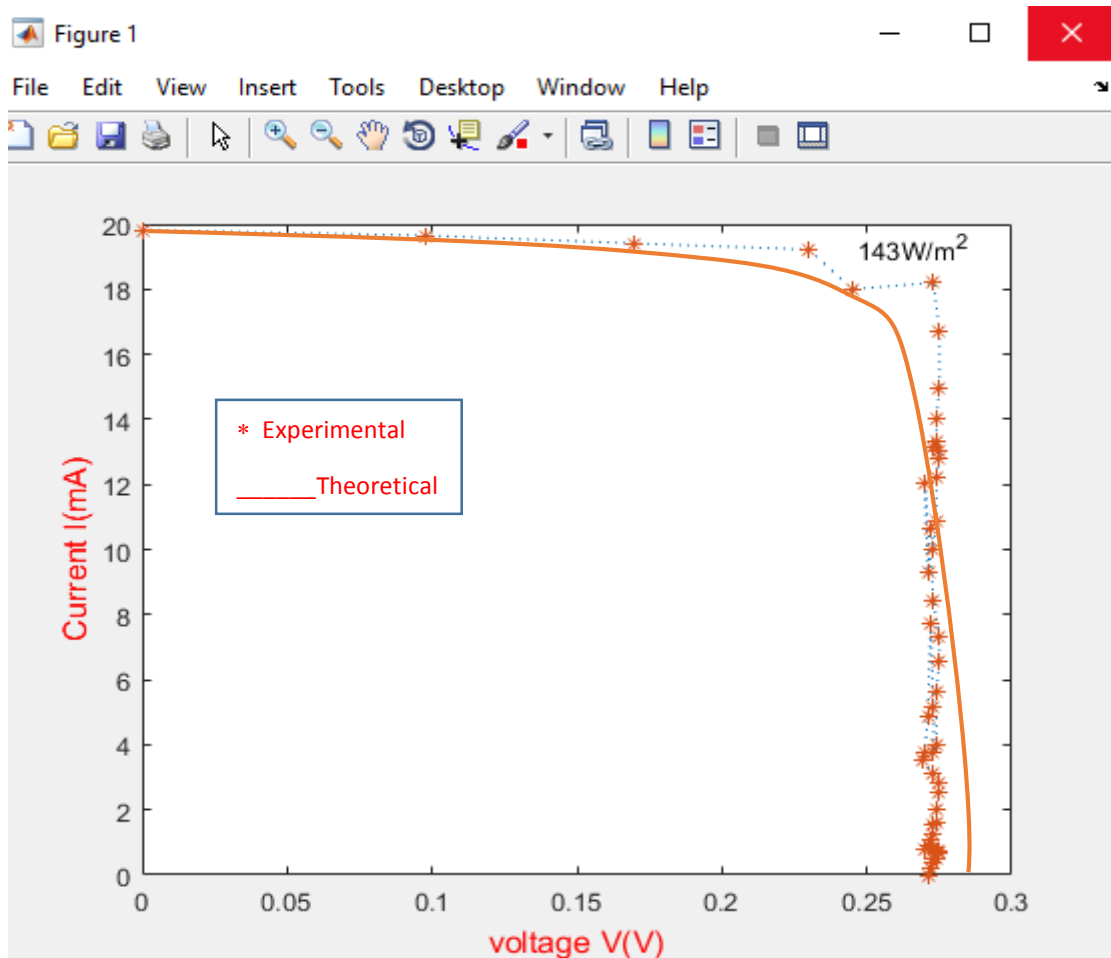


Figure.5.1: $V-I$ curve acquired during Test 1 under one sun.

Test 2

The principal characterization of the behavior of the solar cell is illustrated by the $V-I$ curve as shown in Figure.5.2, with an exposure duration of almost 3 hours, under light intensity of 89W/m^2 , where the ambient temperature is 35°C . The voltage is almost stable where the current decreases from 14.81mA , and the voltage takes a range between 0.260V and 0.269V . The cell temperature is increasing. The chart represents a correct behavior for a photovoltaic cell.

Comparing to test 1, the cell efficiency is lower proportionally to the irradiation and the temperature is a bit high.

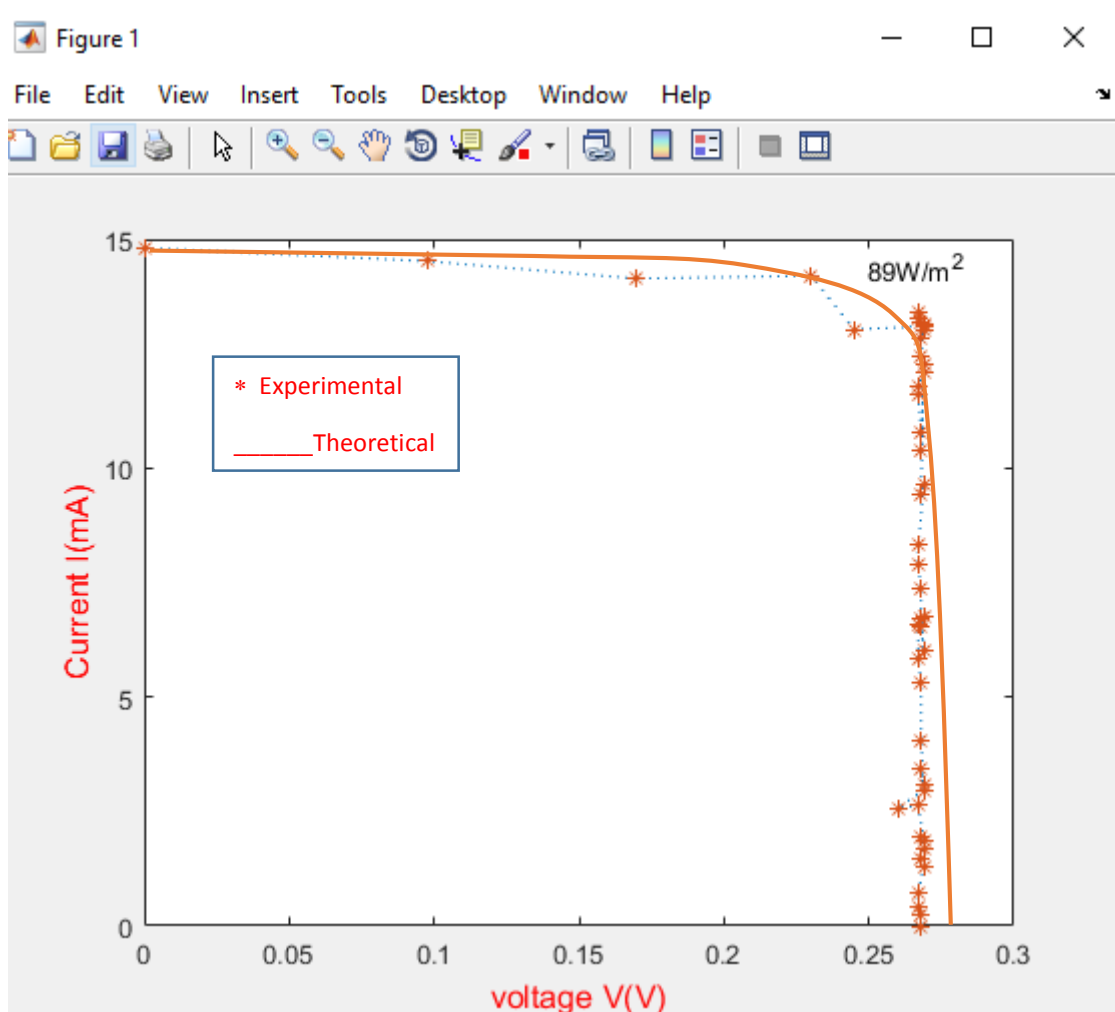


Figure.5.2: $V-I$ curve acquired during Test 2 under one sun.

Test 3

With almost the same exposure duration, under light intensity of 193W/m^2 , where the ambient temperature is 31°C , The principal characterization of the behavior of the solar cell is illustrated by the $V-I$ curve as shown in Figures.5.3, The voltage takes the range between 0.260V and 0.270V . The current decreases from 25.76mA . The cell temperature is increasing slowly and by the third hour it reaches 39°C . The chart represents a correct behavior for a PV cell.

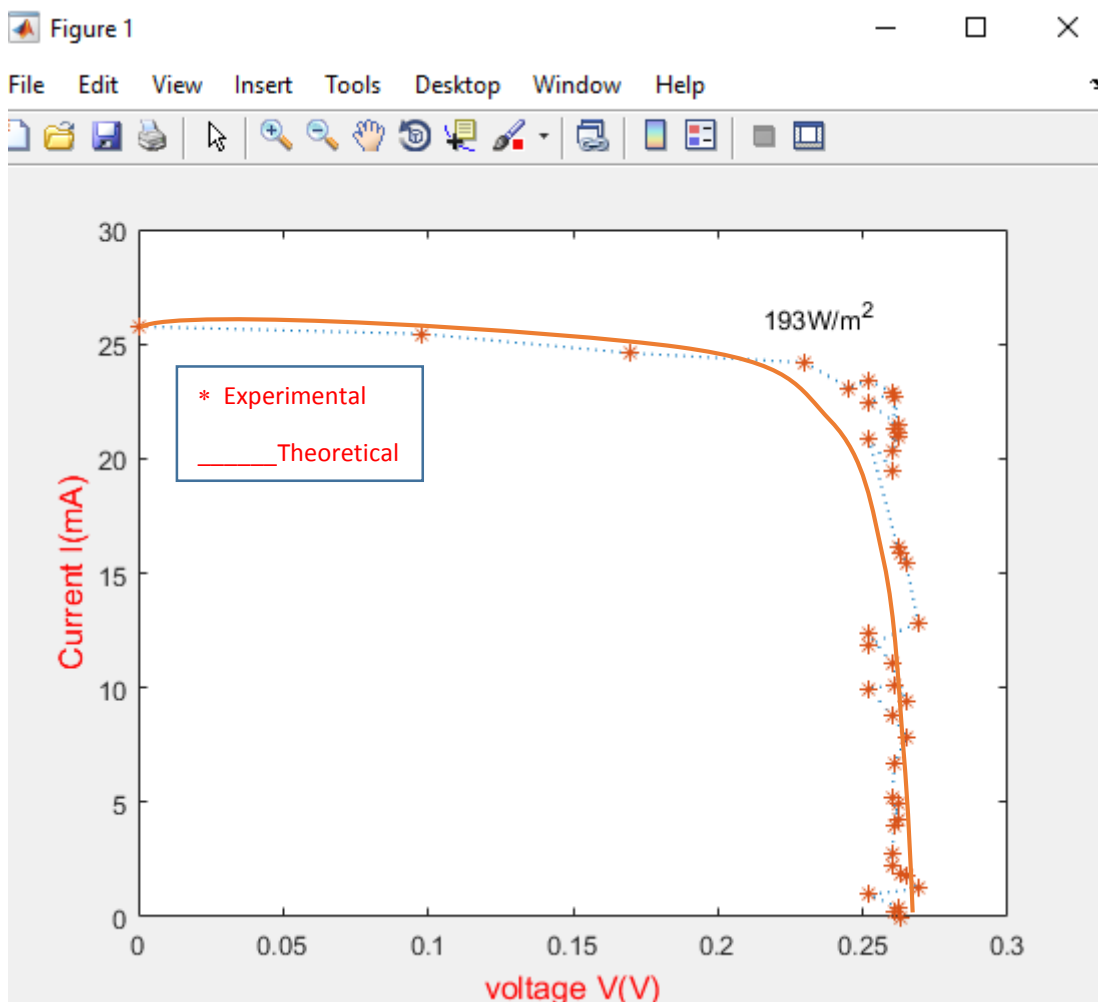


Figure.5.3: $V-I$ curve acquired during Test 3 under one sun.

Test 4

As can happen in outdoor tests, the conditions of solar illumination change, this modification of input power is visible corresponding to a lower $V-I$ curve in figure.5.4, where the exposure duration is 2hours.

When the irradiation change the for a specific temperature the court circuit current changes proportionally with the irradiation, in the same time the open circuit voltage changes a bit.

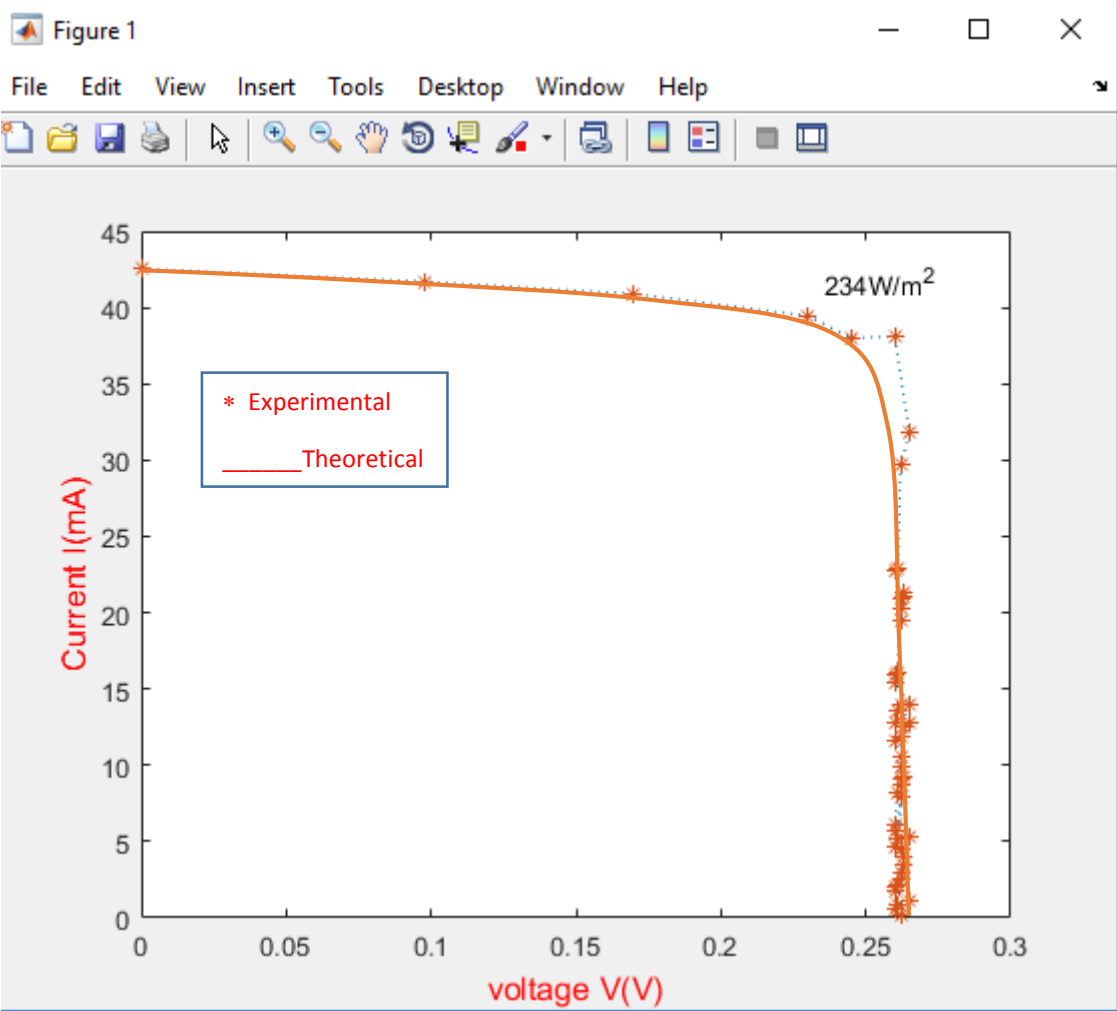


Figure.5.4: $V-I$ curve acquired during Test 4 under one sun.

Test 5

As can happen in outdoor tests, the conditions of solar illumination change, this modification of input power is visible corresponding to a lower $V-I$ curve in figure.5.5, where the exposure duration is 2hours.

When the irradiation change the for a specific temperature the court circuit current changes proportionally with the irradiation, in the same time the open circuit voltage changes a bit.

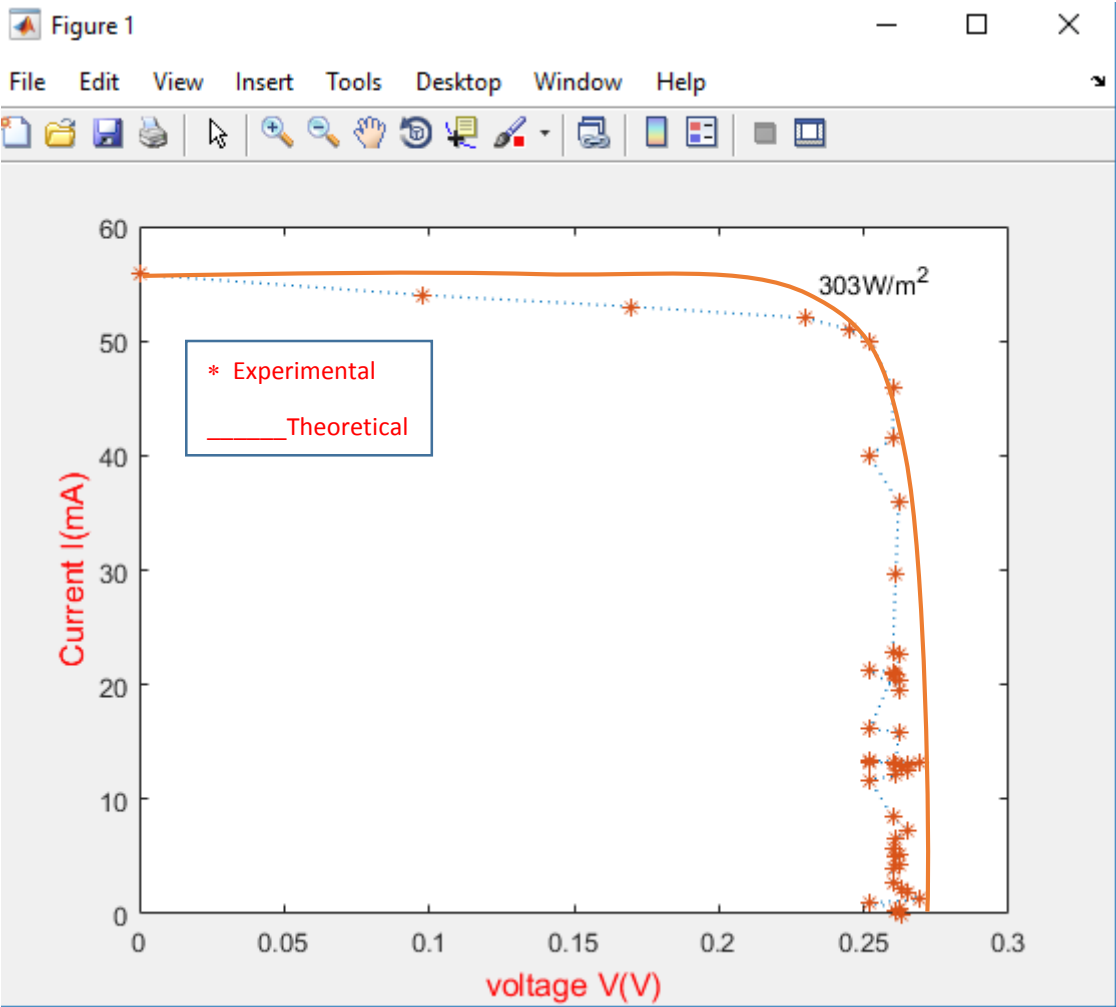


Figure.5.5: $V-I$ curve acquired during Test 5 under one sun.

Test 6

Under light intensity of 976W/m^2 . The principal characterization of the behavior of the solar cell is illustrated by the $V-I$ curve as shown in Figures.5.6
By varying the resistance we mention a variation in current and a fixed range of the voltage. The behavior is appropriate to the solar cell.

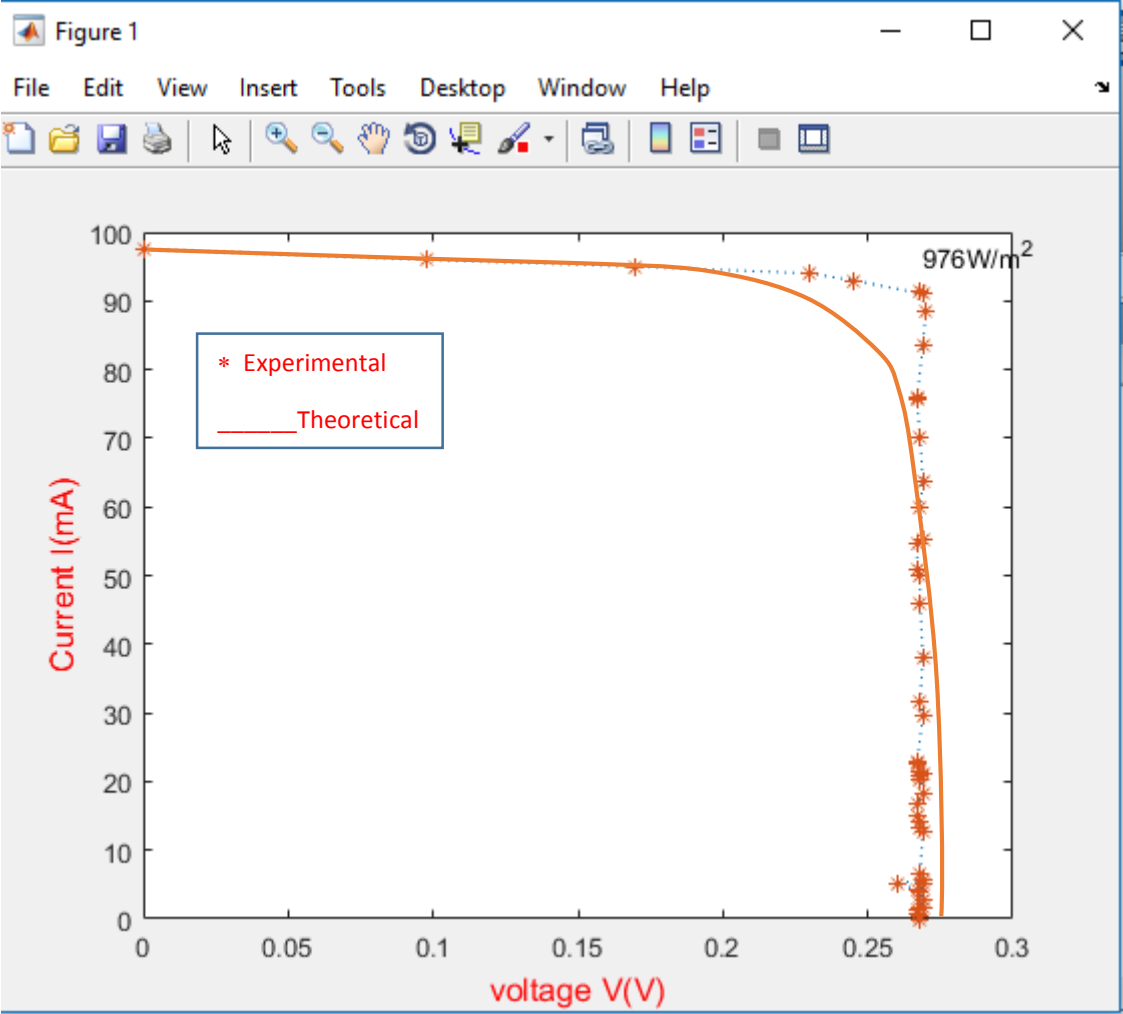


Figure.5.6: $V-I$ curve acquired during Test 6 under one sun.

Test 7

Results of this test are shown in figure.5.7, where the exposure duration is about 1.5hours. An important variation on the current where it decrease proportionally by time; in the last minutes the cell's temperature increases.

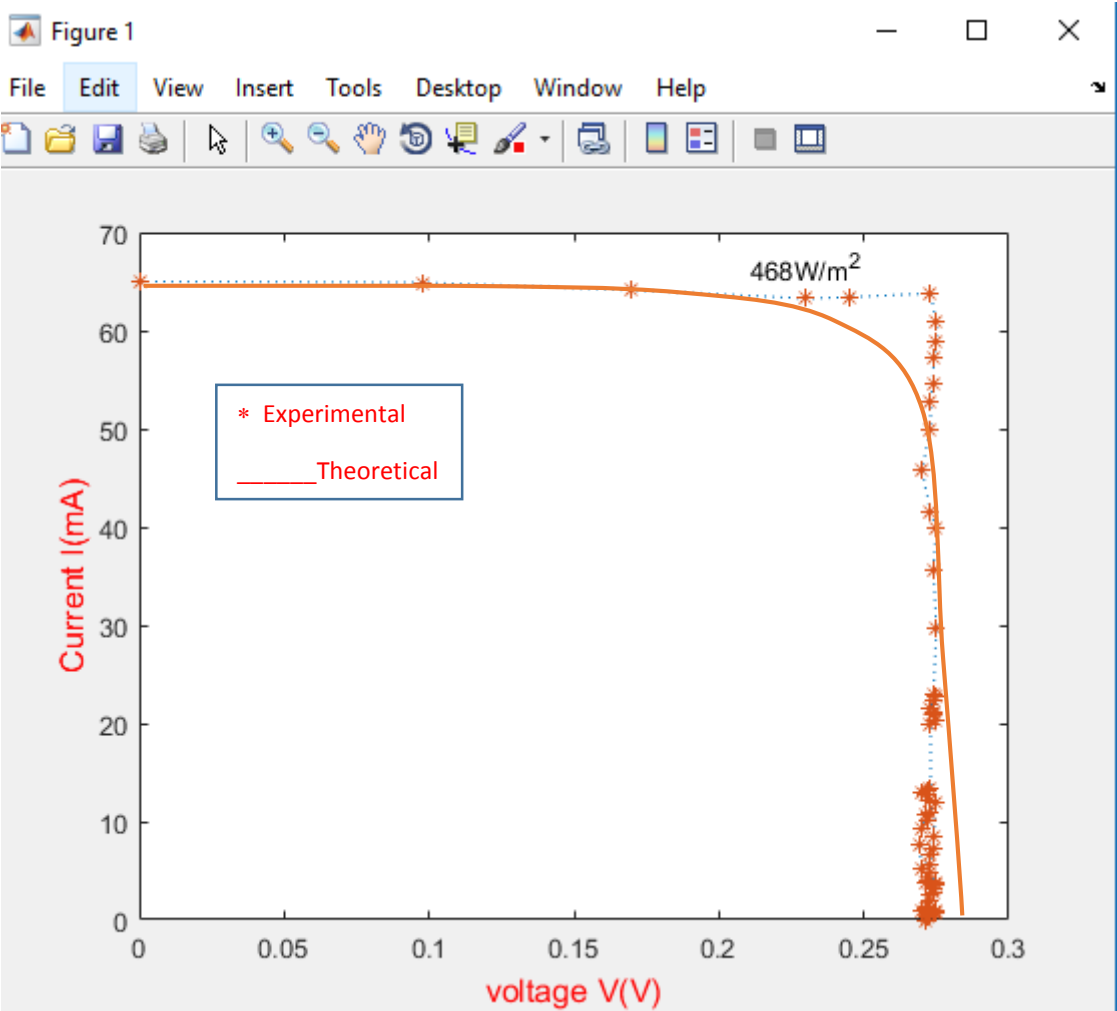


Figure.5.7: V-I curve acquired during Test 7 under one sun.

Test 8

The conditions of solar illumination change, this modification of input power is visible corresponding to a lower $V-I$ curve in figure.5.8, where the exposure duration is 1.5hours.

When the irradiation is important the cell reaches a very important value of current, by the end of the experiment work the cell's temperature increases.

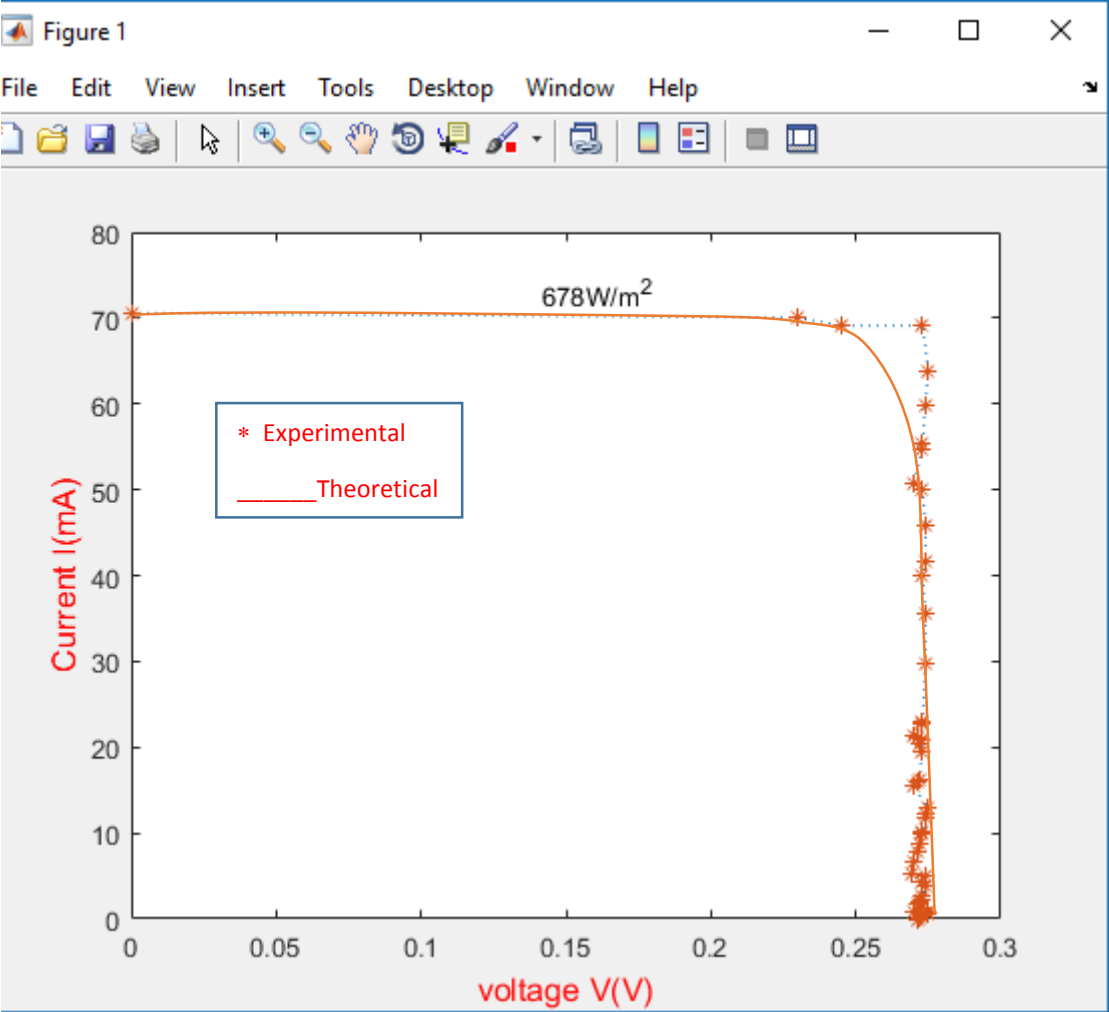


Figure.5.8: $V-I$ curve acquired during Test 8 under one sun.

According to the following Table.5.1, these results show clearly that both irradiation and temperature influence on the cell's behavior. And even if the irradiation is low the cell reaches an important efficiency as shown in Test2; where in Test6 the intensity is 976W/m^2 with 26% of efficiency.

These tests confirm a real behavior of a solar cell under one sun.

	Test 1	Test 2	Test 3	Test 4	Test 5	Test 6	Test 7	Test 8
Isc (mA)	19.82	14.81	25.76	42.54	55.82	97.54	65	70.6
Voc (V)	0.273	0.266	0.265	0.262	0.259	0.269	0.275	0.276
Ta (°C)	33	35	31	30	28	39	37	30
Tcell (°C)	41	42	39	38	45	43	44	38
I (W/m²)	143	89	193	234	303	976	468	678
Pmax (mW)	4.941	3.657	6.699	10.10	13.13	25.46	16.802	17.68
FF	0.91	0.93	0.95	0.90	0.90	0.97	0.93	0.91
η (%)	8.63	10.27	8.67	10.8	10.83	6.5	9	6.52

Table.5.1: Parameters characterizing of all Tests.

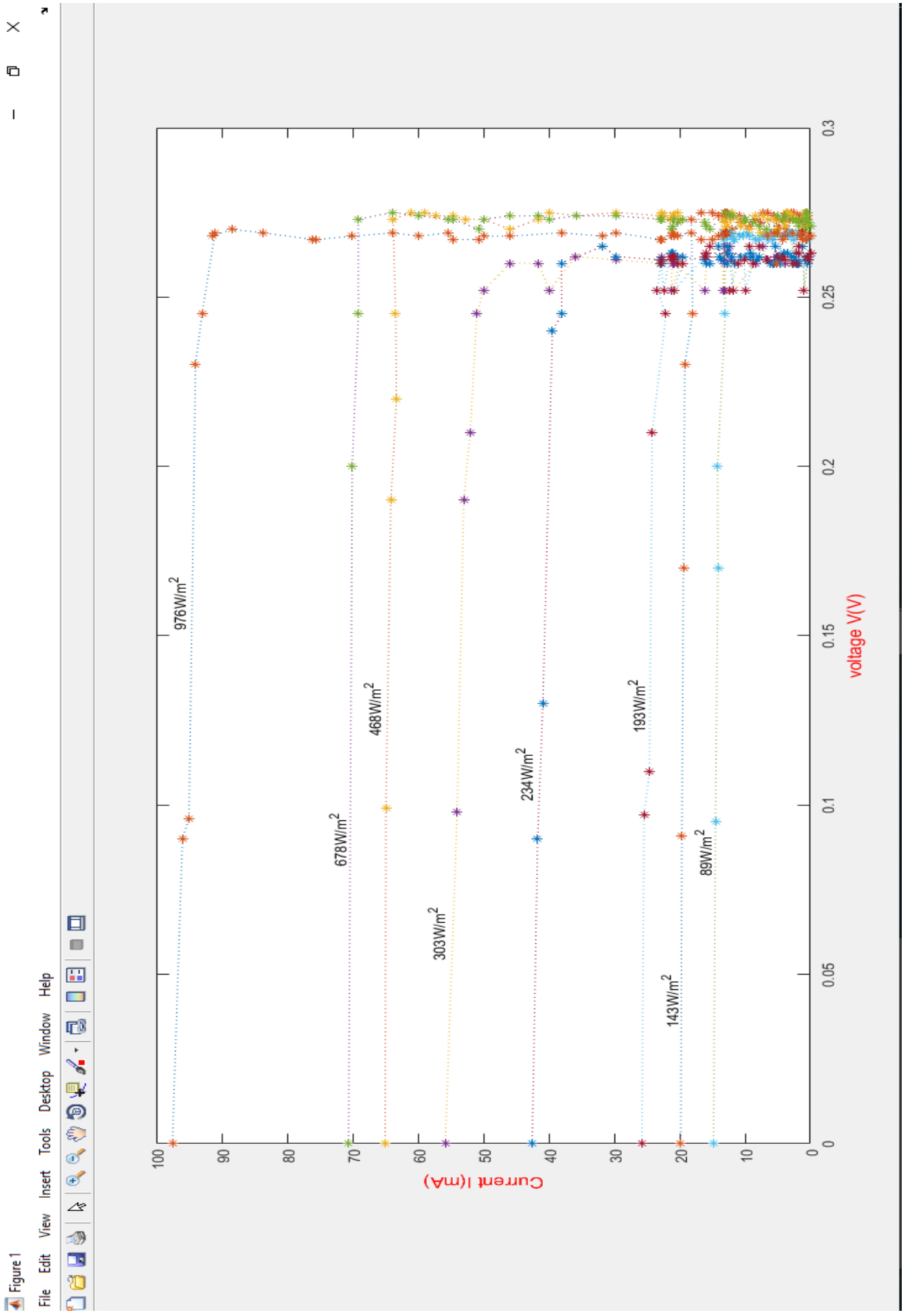


Figure.5.9: I-V characteristics for various conditions of solar radiation (considering series resistance) under one sun.

5.2 Results and analysis under concentration

Test 1

The temperature of the cell T_{Cell} is a very important quantity. During the basic exposure tests at $D = 7.4$ cm, where the whole area of the cell is covered with light just to have the homogeneity. At this distance higher temperatures are reached in the basic exposure tests, the range of T_{Cell} is 38–45°C

The power density incident on the cell remains constant during this test for almost 2 hours; the open-circuit voltage and the maximum electrical power extracted show only small fluctuations towards inferior values when T_{Cell} increases.

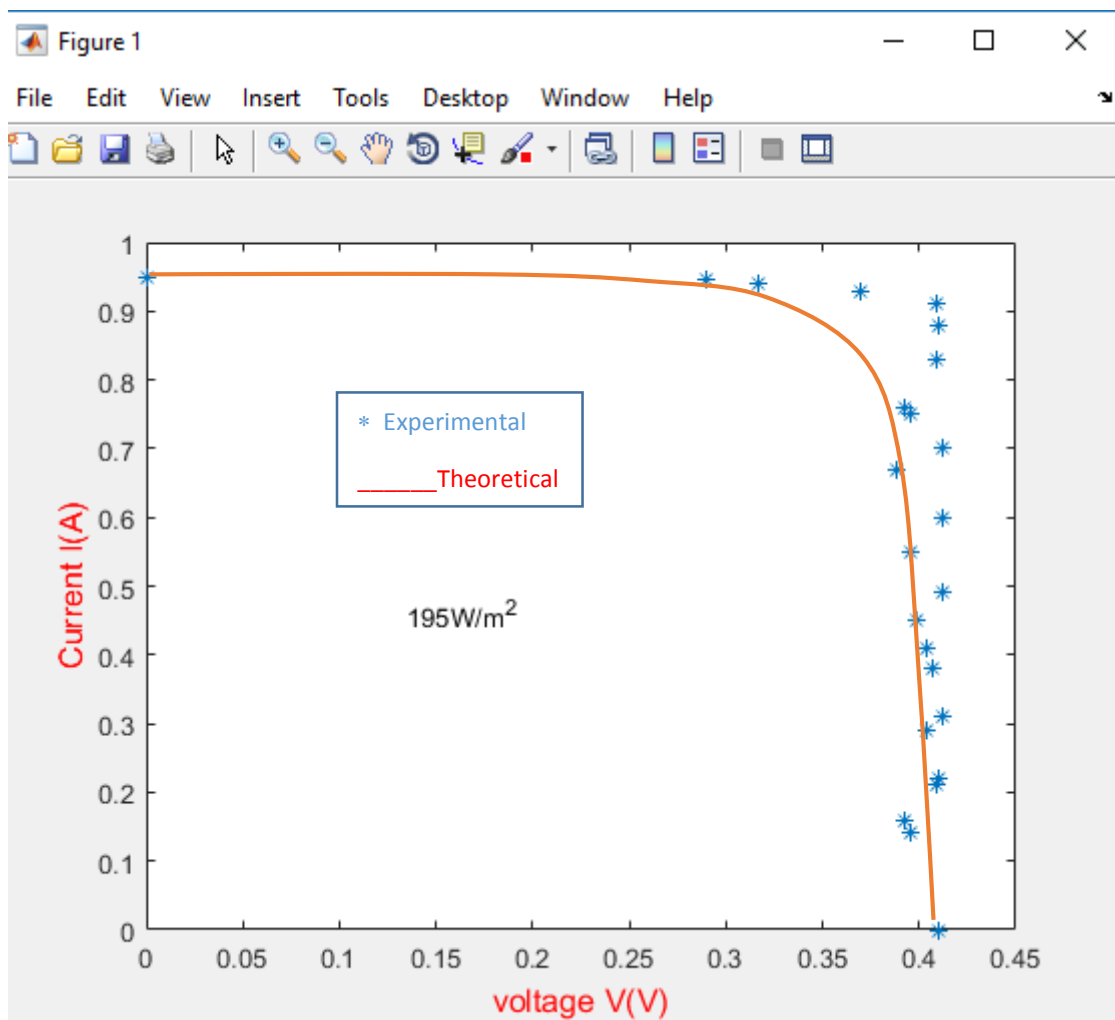


Figure.5.10: V - I curve acquired during Test 1 under concentration.

Test 2

The working conditions measured in correspondence with the V - I curve plotted in Figure.5.11; with an exposure duration of 1hour, under light intensity of 221W/m^2 ,

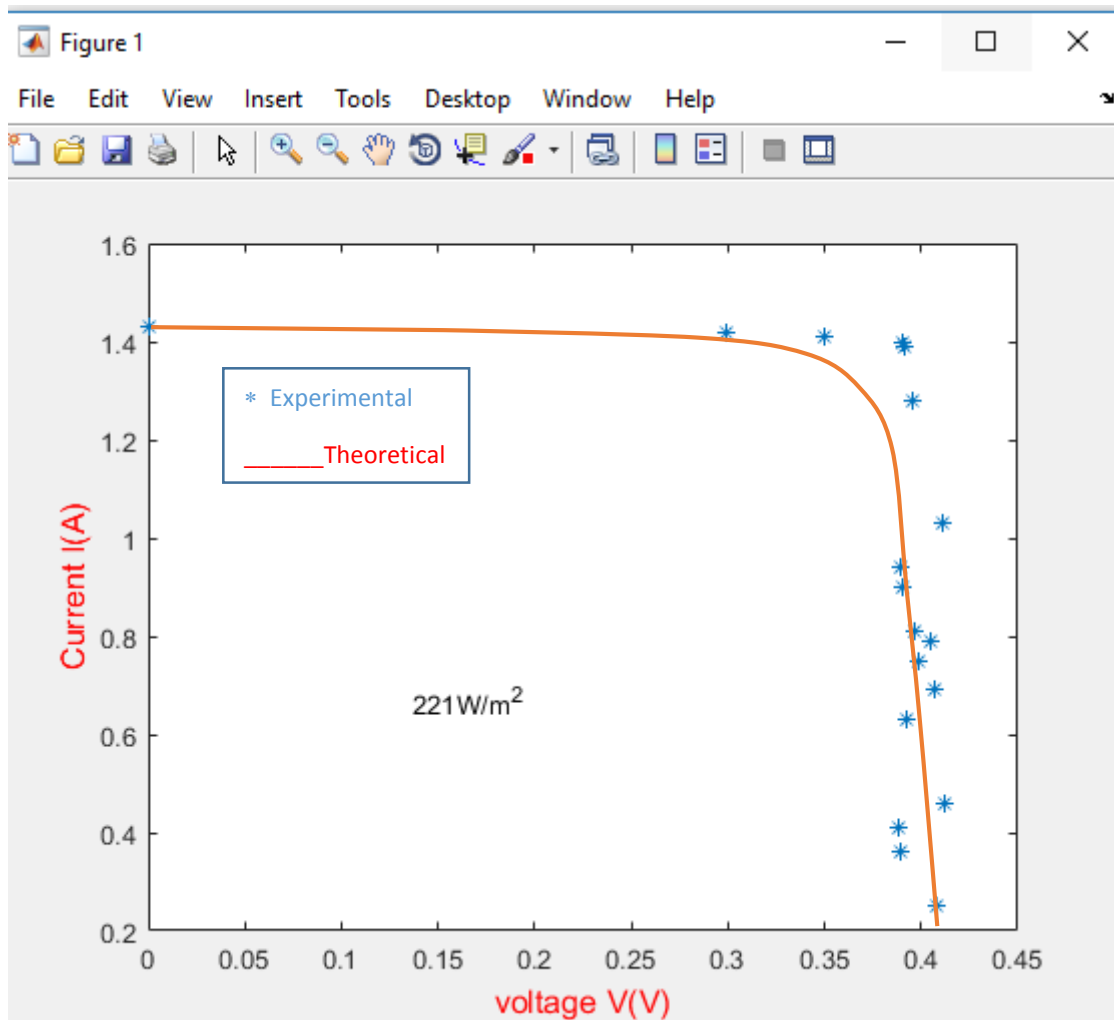


Figure.5.11: V - I curve acquired during Test 2 under concentration.

Test 3

Specifications are as follows: distance lens-cell: 7.5cm; duration of exposure: 2 hours; other parameters: variation of the cell temperature 33-60°C, in correspondence with the $V-I$ curve plotted in Figure.5.12.

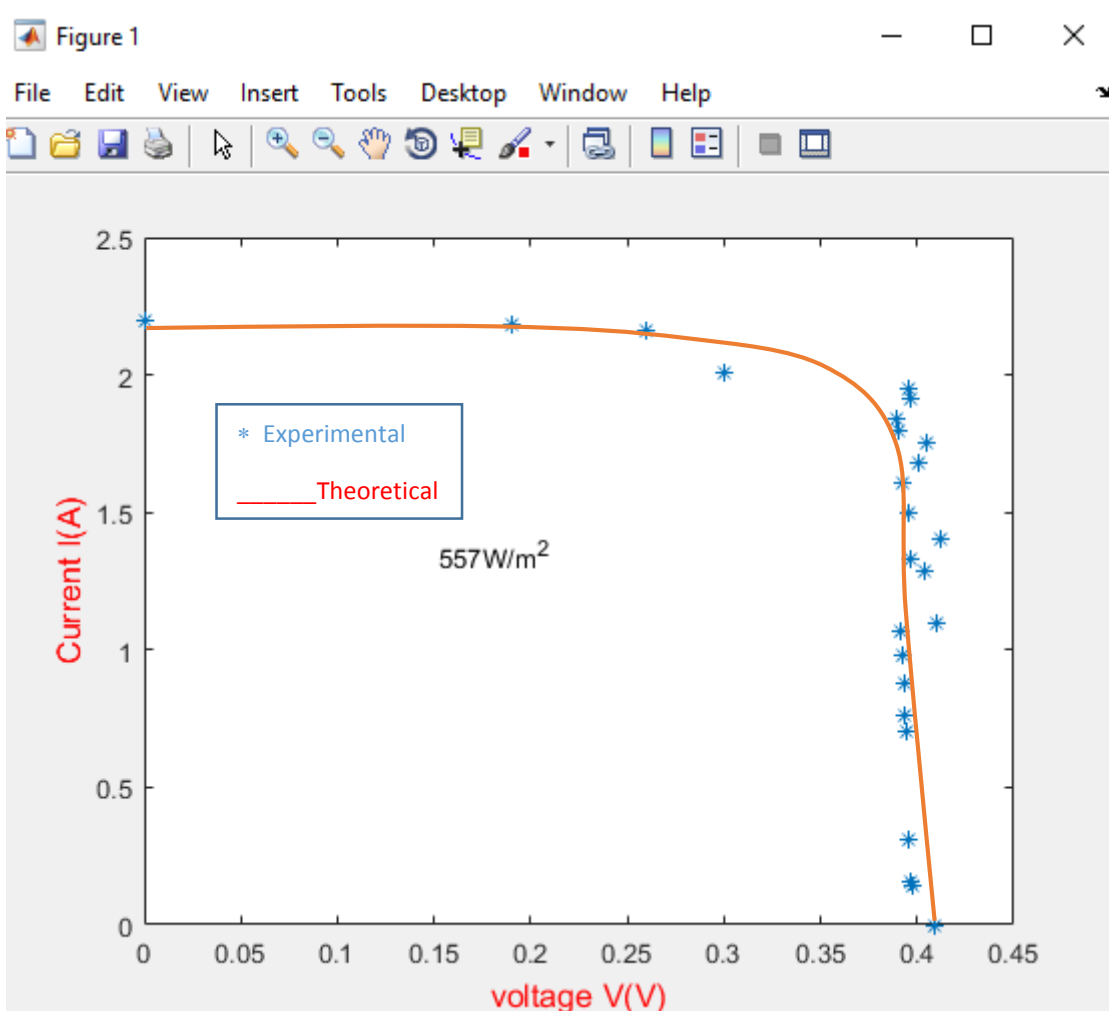


Figure.5.12: $V-I$ curve acquired during Test 3 under concentration.

Test 4

Specifications are as follows: distance lens-cell: 7.5cm; duration of exposure: 1.5hours; other parameters: variation of the cell temperature 40-52°C, in correspondence with the $V-I$ curve plotted in Figure.5.13.

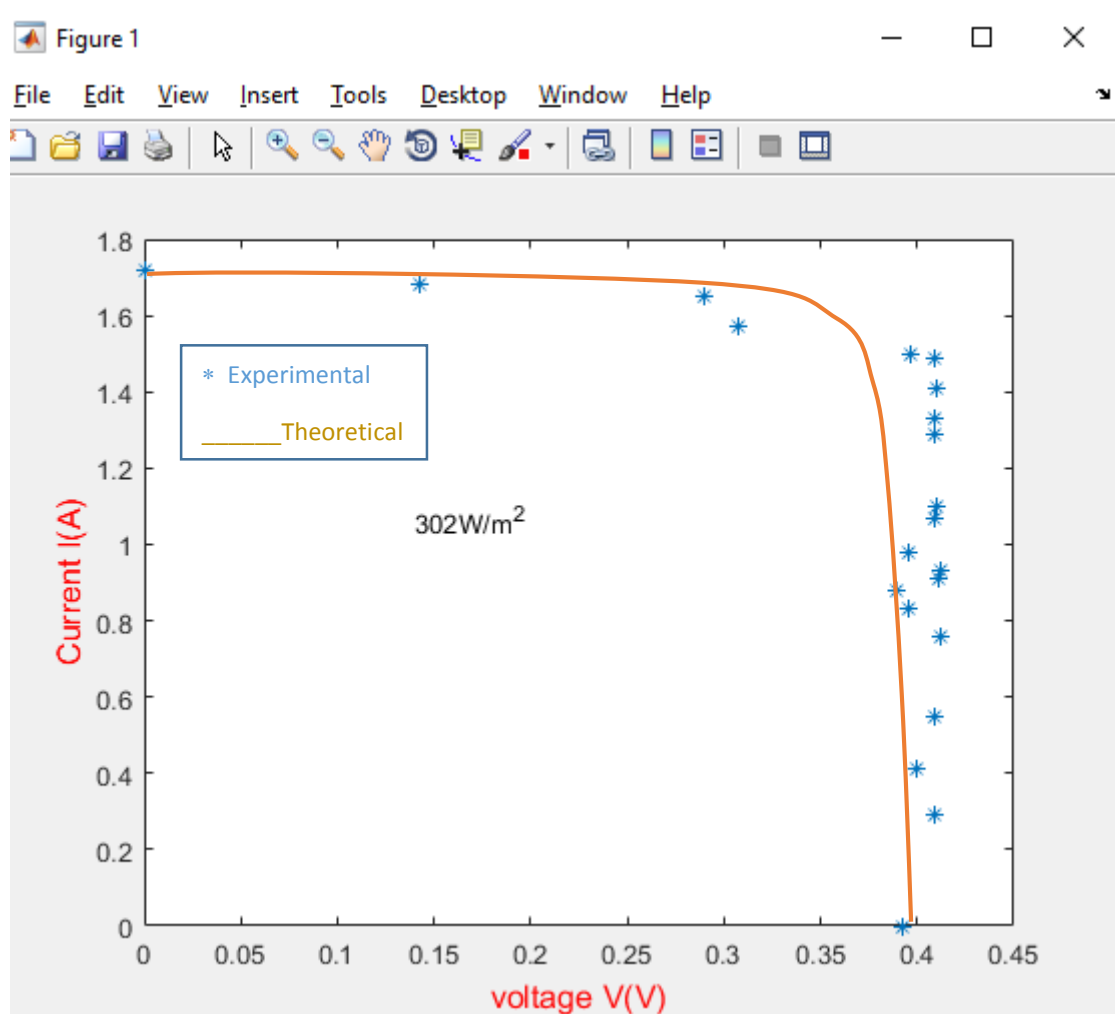


Figure.5.13: $V-I$ curve acquired during Test 4 under concentration.

Test 5

Specifications are as follows: distance lens-cell: 7.5cm; duration of exposure: 2 hours; other parameters: variation of the cell temperature 40-65°C, in correspondence with the $V-I$ curve plotted in Figure.5.14.

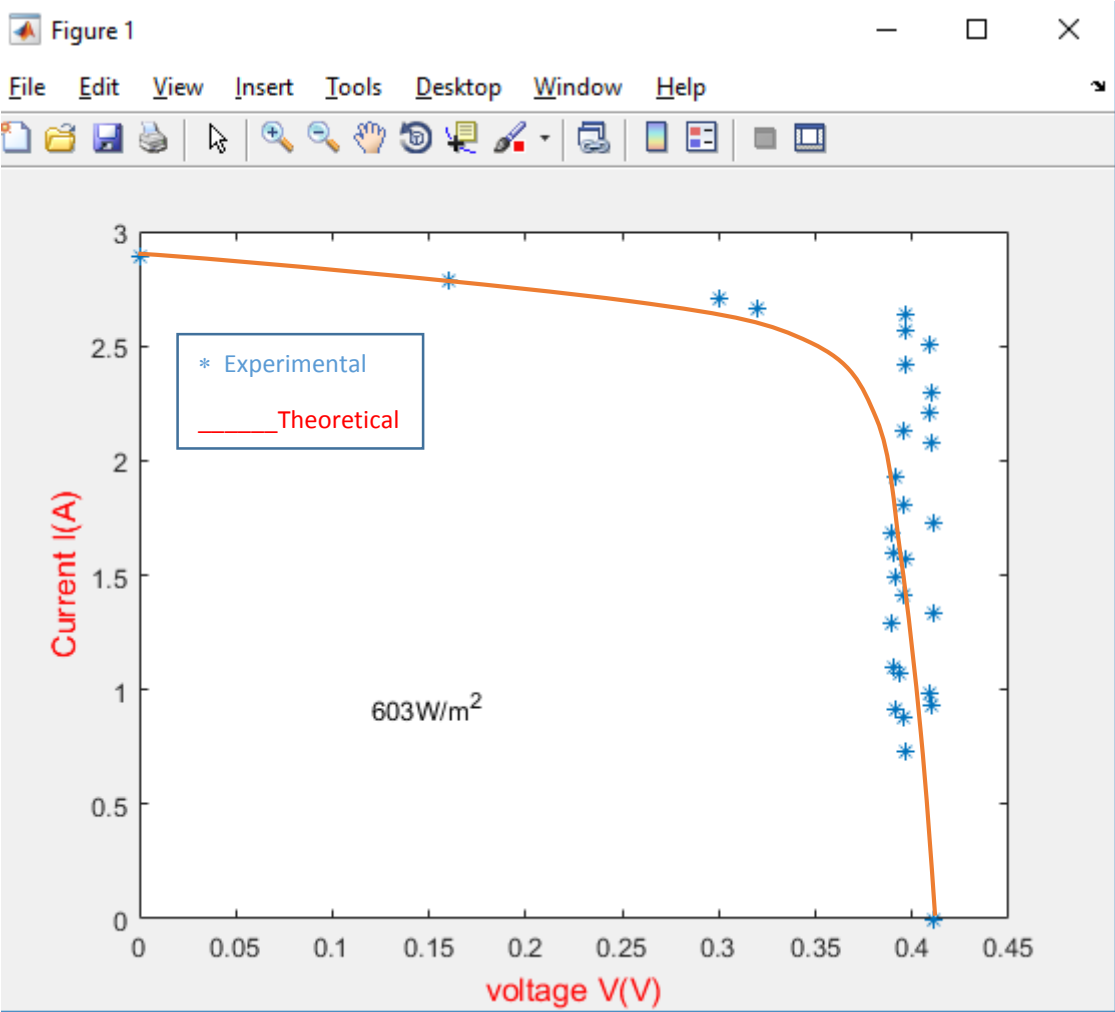


Figure.5.14: $V-I$ curves acquired during Test 5 under concentration.

Test 6

Higher temperatures are reached in the basic exposure tests specifications are as follows: distance lens-cell: 7.5cm; duration of exposure: 2 hours; other parameters: variation of the cell temperature 27-41°C, in correspondence with the *V-I* curve plotted in Figure.5.15.

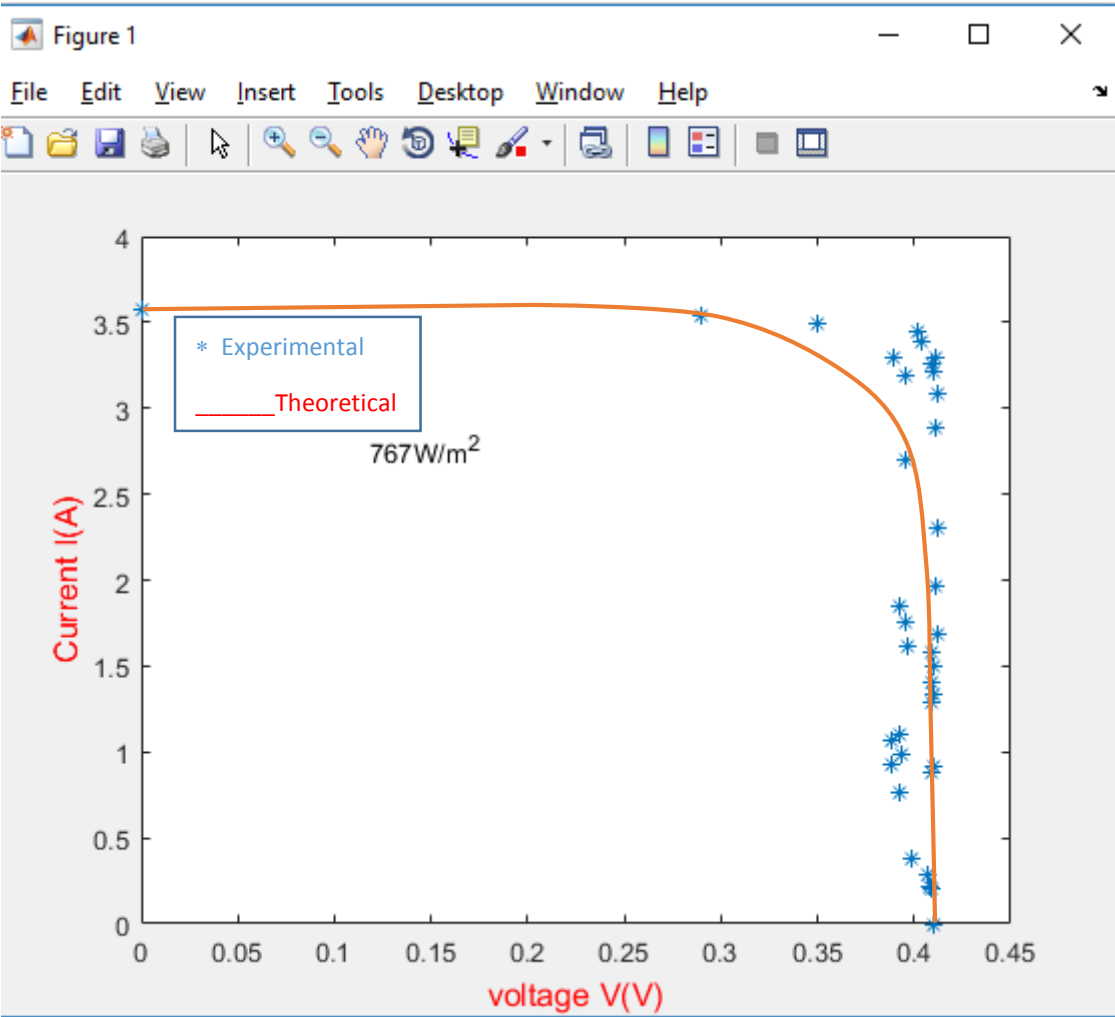


Figure.5.15: *V-I* curve acquired during Test 6 under concentration.

Test 7

Higher temperatures are reached in the basic exposure tests specifications are as follows: distance lens-cell: 7.5cm; duration of exposure: 2 hours; other parameters: variation of the cell temperature 33-67°C.

The open-circuit voltage and the maximum electrical power extracted show only small fluctuations towards inferior values when T_{cell} increases, in correspondence with the $V-I$ curve plotted in Figure.5.16.

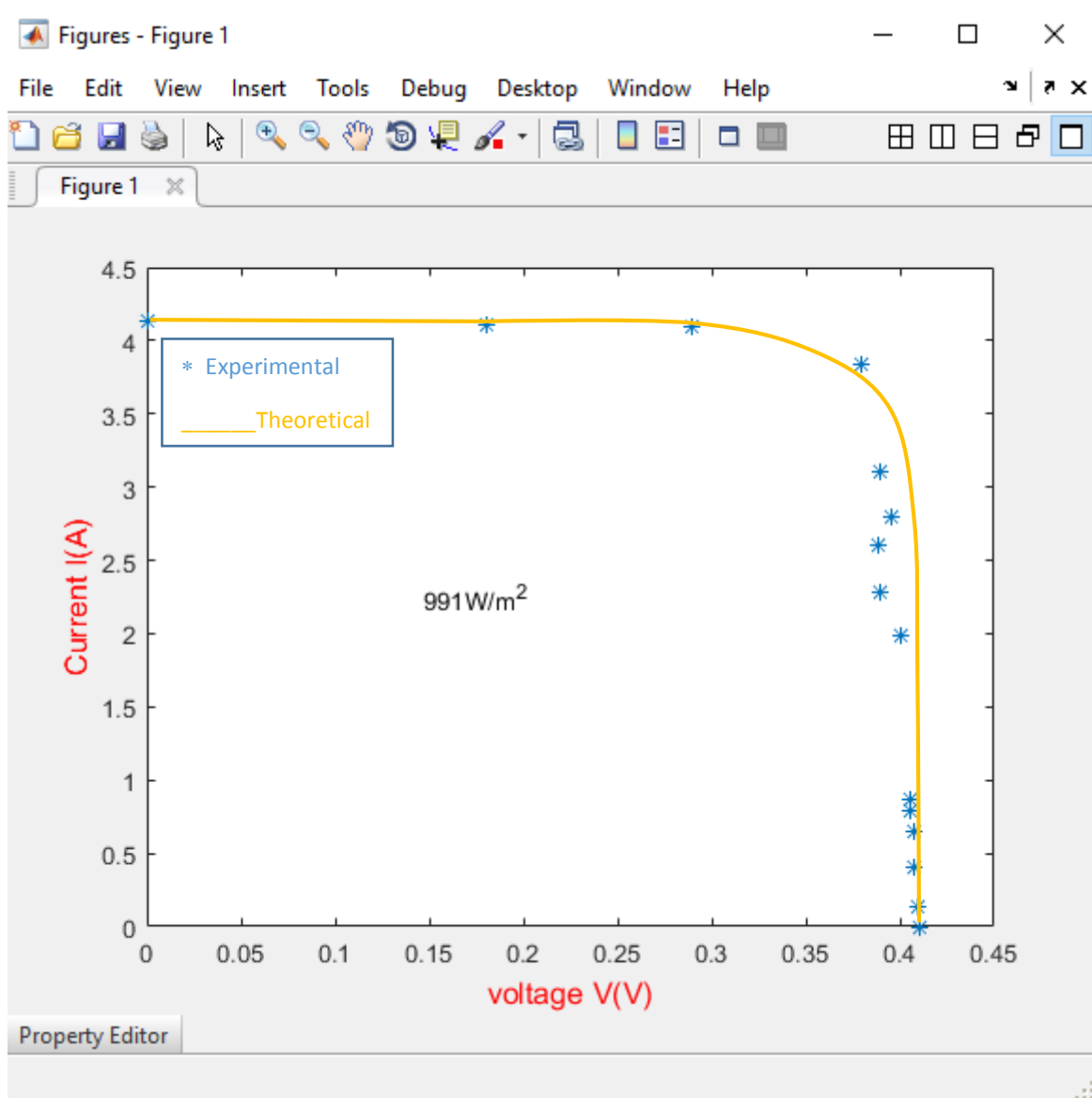


Figure.5.16: $V-I$ curve acquired during Test 7 under concentration.

According to the following Table.5.2, basing on the characterization of the solar cell, these results show clearly that both irradiation and temperature influence on the cell's behavior, under concentration with distance lens-cell: 7.5cm.

	Test 1	Test 2	Test 3	Test 4	Test 5	Test 6	Test 7
Isc (A)	0.95	1.43	2.02	1.72	2.89	3.57	4.13
Voc (V)	0.410	0.408	0.409	0.392	0.411	0.410	0.410
Ta (°C)	30	36	33	34	32	36	33
Tcell (°C)	45	41	60	52	65	41	67
I (W/m²)	195	221	557	302	603	767	991
Pmax (W)	0.37	0.57	0.80	0.66	1.14	1.43	2
FF	0.94	0.97	0.97	0.97	0.97	0.96	0.95
η (%)	11.24	15.28	8.51	13	11.22	11.04	11.98

Table.5.2: Parameters characterizing of all Tests under concentration.

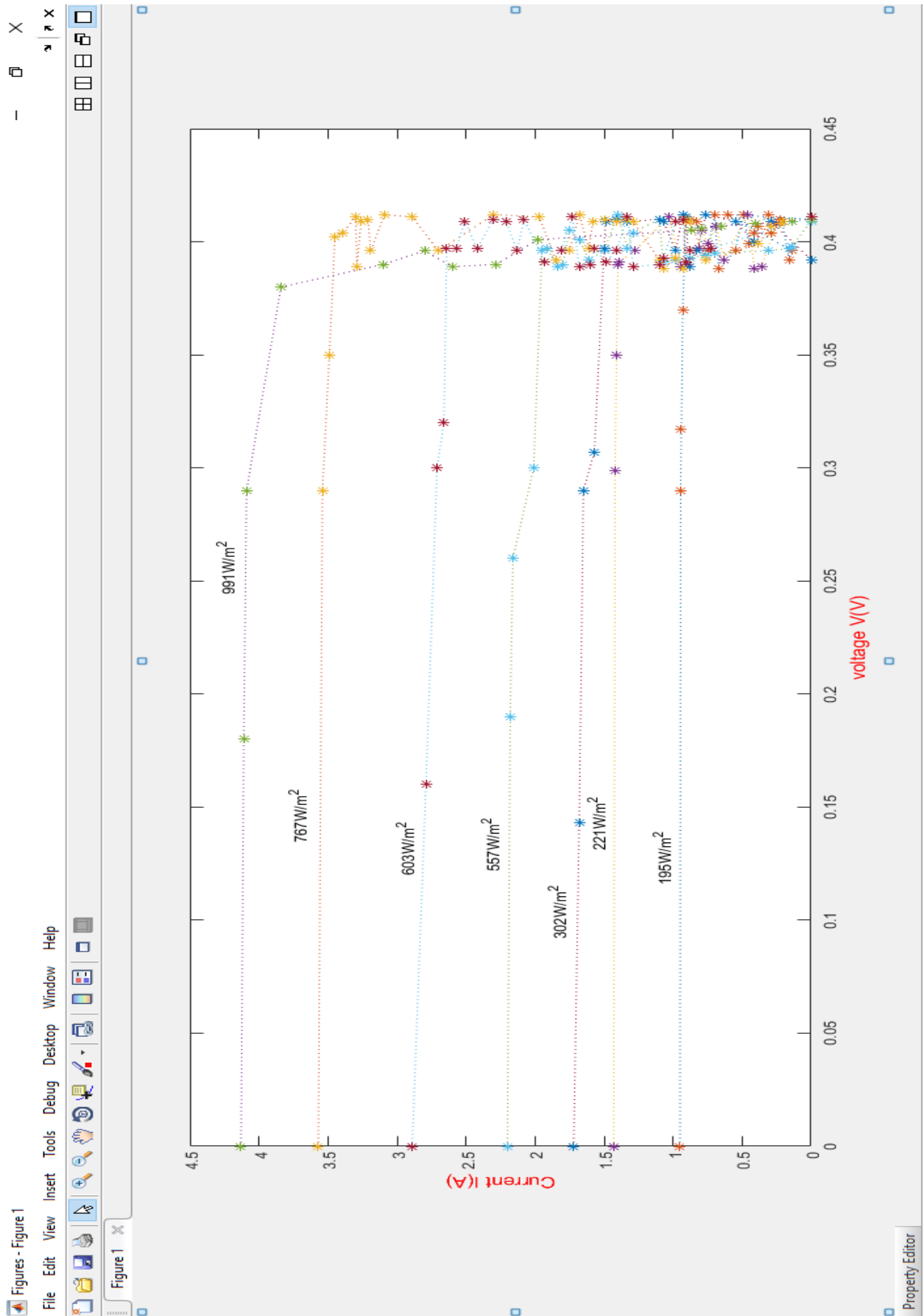


Figure.5.17: *V-I* curves acquired during all the Tests under concentration.

5.3 Comparative study

Comparing the results of the different exposure tests under one sun and concentration, it appears evident that Cell under one sun shows a correct behavior and an improved efficiency with respect to Cell under concentration.

The $V-I$ curves for Cell under one sun have a trend similar to the theoretical one for a photocell, while the $V-I$ curves for Cell deviate much from this trend; where the temperature does not influence that much on its behavior.

Also the performance of Cell under one sun and under concentration are definitely good, in terms of both open-circuit voltage and electrical power extracted with the different power density on the cell that change by changing the ambient conditions.

In all tests, the light intensity is varying and as much as it increases the current becomes important, the voltage rang is almost fixed.

The open-circuit voltage V_{OC} is around 0.265-0.277V for the cell under one sun, while the V_{OC} measured with cell under concentration is higher, 0.390-0.410V for lens cell.

For what concerns the behavior intime, the curves do not undergo significant changes for an exposure of 2 to 3 hours.

The temperature increase does not produce changes on the $V-I$ curves or alteration of the parameters, in the regime of temperatures examined (38–67°C) under concentration, and (38-45°C) under one sun.

According to the theoretical studies and the experimental results, as they are plotted in the previous curves, the measurements are approximatively in the same range. The average linear regression between the theoretical and the experimental curves is 97.7%.

To have more precision, the same solar cell is fixed at an altitude of 36°29'N, under one sun, where the ambient temperature is 29°C to have a daily average power and see if the fixed system or the tracking one is better. The curves plotted in Figure.5.18 show clearly that a fixed cell has a less daily average power because its position that does not change proportionally to the sun, so there is a loss in the absorption of sun light, however, thanks to the tracking system that follows the sun's path the curve is more important.

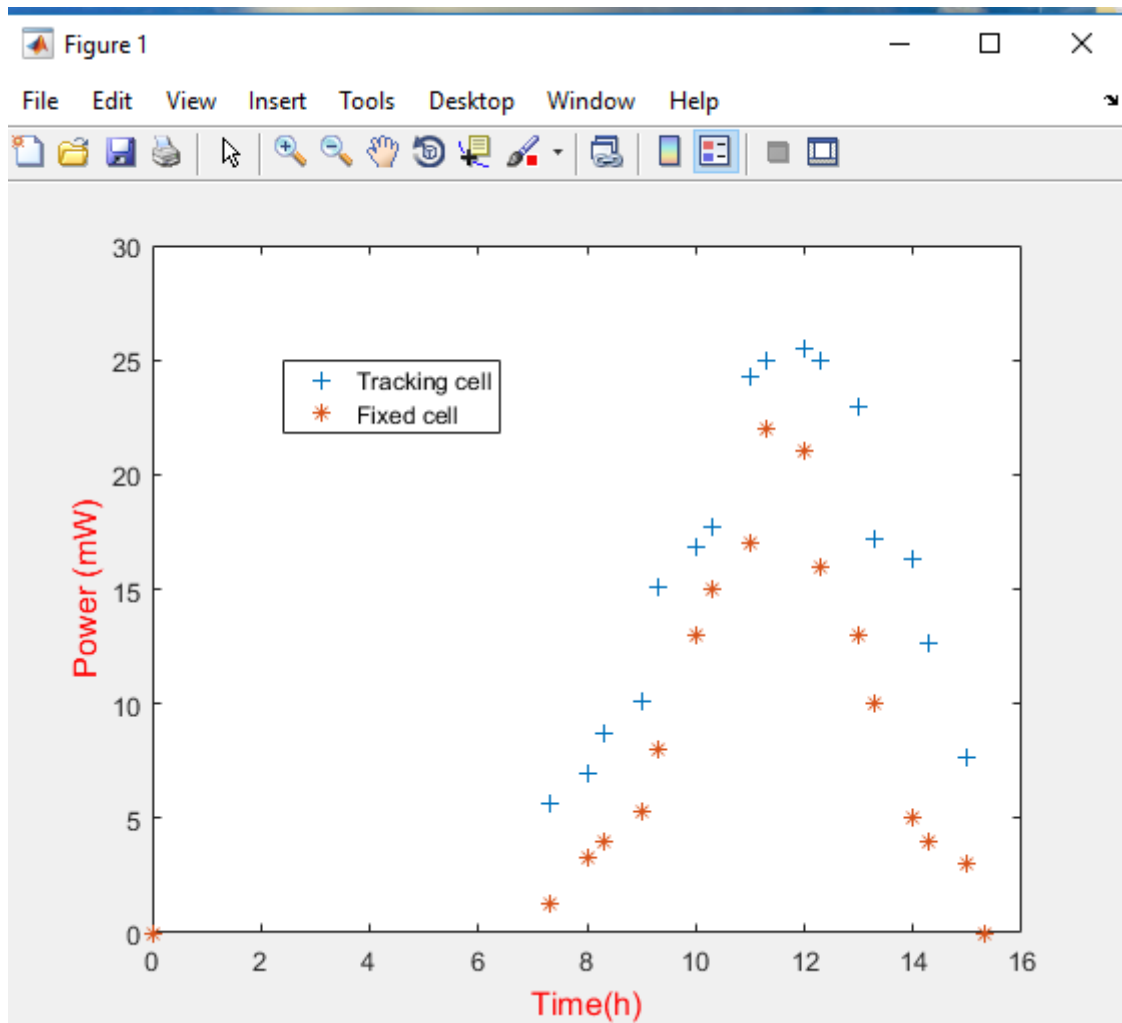


Figure.5.18: Daily Average Power on fixed and tracking cell.

According to the following Table.5.3, the average power under concentration with tracking is important comparing it to the cell under one sun with tracking system, and according to the experimental results in Table.5.1 and Table.5.2, the cell's power under concentration is more and more important than cell's under one cell, hence both concentration and tracking system are worth the work.

	A fixed cell	Cell under one sun (tracking)	Cell under concentration (tracking)
Average power $\langle P \rangle$ (mW)	7.81	12.31	995.71

Table.5.3: The average power of the solar cell.

Chapter 6

Conclusions and recommendations

6.1 Project conclusion

In practice, many systems are operated in different way, which can be considered a mixture or a combination of many technologies. In the thesis where clearly it is shown that the mechanism part of the tracker has many advantages on the work, it helps to find the perfect fit for the unique job site, installation size, local weather, degree of latitude, and electrical requirements are all important to have a good results and more precision. The cost of solar equipment is very high, especially solar cells or panels, which are the most expensive in the installation. Solar tracking is by far the easiest method to increase overall efficiency of a solar power system. By using this method, the solar tracker is successful in maintaining a solar array at a sufficiently perpendicular angle to the sun, especially in the use of Fresnel lens. The power increases gained over a fixed horizontal array was in excess of 30%.

When the solar cell is operating under the outdoor condition, the variation in the temperature for a given operating voltage will vary the cell operating condition.

Whatever the system consist on, under one sun or under concentration, both of irradiation and temperature influence on the cell's behaviour. Moreover, as the results confirm when the irradiation increase the current in short circuit increase proportionally to it. In addition, the voltage in open circuit varies a bit to the same temperature. Moreover, because the temperature is a very important parameter in the behaviour of a solar cell, when it increases the voltage in open circuit decreases, it is why in the previous figures of characterization, the cell is highly heated so some points were out of the main curve.

The average linear regression between the theoretical and the experimental curves is 97.7%.

The average efficiency of a cell of 2cm*2cm under one sun is about 8.9%, and about 11.75% for the cell under concentration, enough important for a cell with that tiny area and without forgetting the age factor; of the cell that it is more than 30 years and the lens that becomes having a yellowish layer. Moreover, the measurements error that influence a lot.

Cell's power under concentration is more and more important than cell's under one sun; as it is shown in this work. Hence, both concentration and tracking system are worth the combination.

For multiple reasons, the high cost of energy, the dropping cost of PV, and the existence of a reasonable solar resource, this report finds that a PV tracking system is a reasonable use.

6.2 Recommendations for future works

The goals of this project were purposely kept within what was believed to be attainable within the allowed time and resources. As such, many improvements can be made upon this initial work.

The following recommendations are provided as ideas for future expansion of this project:

Future solar project should use a programmer kit or a microcontroller which can be used as a stand alone, with a photo transistor.

According to this work, the combination of the solar tracker with CPV reaches an important efficiency, and then an economic study of this project must be done to see if it has a good economic prospect.

Using a paraboloid system in order to have a different level of concentration then reach the optimal concentration.

Summary

- ❖ The world is endeavoring to reach higher standards. My project focuses on Renewable Technologies that have become one of the most important things in human's lives. The history of human evolution and civilization is a history of energy consumption.

The photovoltaic are pivotal and have a huge influence on the industry because it can produce an immense quantity of electricity. To improve the efficiency of our solar cell we are using the solar concentration concept.

The main objectives of my study are:

- Outdoor experimentation of a solar cell, test with direct expose to the sun.
- Characterise a PV cell under one sun then under a high concentrated solar flux (using Fresnel lens).
- The IV curves production.
- The efficiency of the solar cell.

❖ العالم يسعى للوصول إلى مستويات أعلى. يركز مشروع على تقنيات الطاقة المتجددة التي أصبحت واحدة من أهم الأشياء في حياة الإنسان وفي تاريخ التطور البشري والحضارة وهو تاريخ استهلاك الطاقة الضوئية التي لها تأثير كبير على الصناعة لأنها تنتج كمية هائلة من الكهرباء. في هذا العمل قمنا بدراسة تركيز أشعة الشمس على خصائص خلية الضوئية.

وكانت الأهداف الرئيسية لهذا المشروع:

- عرض الخلية للشمس و تطبيق بعض الإختبارات عليها
- تحديد خصائص الخلية الشمسية تحت شمس واحدة ثم تحت تركيز الشمس.
- المنحنيات تيار توتر .
- مردودية الخلية الضوئية.

References

- [1] Conference paper, "State of art of solar PV technology'. April 2013, India.
- [2] A.F. Sherwani, State-of-the-Art of Solar Photovoltaic (SPV) Technology, Faculty of Engineering and Technology. Jamia Millia Islamia, New Delhi, 110025
- [3] "National Energy research Center(NERC)-Jordan," Feb 2012. [Online]. Available: www.nerc.gov.go.
- [4] e. a. D.L. King, "Photovoltaic array performance model," Sandia National Laboratory , New mexico, November, 2003.
- [5] D. M. Patrick Hearps, "Renewable Energy Technology Cost Review," no. Energy research institute, University of milborn, March 2011.
- [6] Venkat, "Go Green," July 2010. [Online]. Available: www.gogreen2020.blogspot.com.
- [7] Kurtz, S., A. Lewandowski, and H. Hayden, *Recent Progress and Future Potential for Concentrating Photovoltaic Power Systems*. 2004, NREL: Colorado, USA.
- [8] McConnell, R., *Concentrator photovoltaic technologies: Review and market prospects*. Refocus, 2005: p. 35-39.
- [9] NREL_ Laboratory. Efficiency solar cells chart; NREL: Colorado, USA.
- [10] A.F. Sherwani, State-of-the-Art of Solar Photovoltaic (SPV) Technology, Faculty of Engineering and Technology. Jamia Millia Islamia, New Delhi, 110025
- [11] Barret B., De Mazière M., Demoulin P. Retrieval and characterization of ozone profiles from solar infrared spectra at the Jungfraujoch. J. Geophys. Res. 2002:107. doi: 10.1029/2001JD001298.
- [12] Spinei E., Mount G.H. O₂-O₂ Absorption Cross Section Derived From Direct Sun Measurements at Different Locations. Presented at the OMI Science Team Meeting nr. 15; De Bilt, The Netherlands. 15-17 June 2010.

[13] Huster M. M.Sc. Thesis. Institut Für Meteorologie und Klimaforschung; Karlsruhe, Germany: 1998. Bau Eines Automatischen Sonnenverfolgers Für Bodengebundene Ir-Absorptionsmessungen.

[14] RSR2_Brochure, "Irradiance," Feb 2008. [Online]. Available: www.irradiance.com.

[15] P. Loutzenhiser and e. al., "Empirical validation of models to compute solar irradiance on inclined surfaces for building energy simulation," EL SEVIER, 2006.

[16] M. Zeman, "Solar Cells. Chapter 2:Solar Radiation," Delft University of Technology.

[17] Mokri, A., Emziane, M. Concentrator photovoltaic technologies and market: a Critical review. World Renewable Energy Congress 2011, 8-13 May, Linköping, Sweden, 2011.

[18] Development And Study Of A Dense Array Concentration Photovoltaic (Cpv) System, University of Trento, 2012/2013.

[19] Bernard Laurent. LES SYSTEMES A CONCENTRATION DANS LA CONVERSION PHOTOVOLTAIQUE : BILAN ET PERSPECTIVES. Micro and nanotechnologies/Microelectronics. Universit_e Paul Sabatier - Toulouse III, 1982. French. <tel-00181394>

[20] P. Roth, A. Georgiev and H. Boudinov "Design and construction of a system for suntracking, Renewable Energy », N 29, pages 393-402, June 2003.

[21] <http://www.gotronic.fr/art-carte-arduino-uno-12420.htm>.

[22] <http://shop.mchobby.be/cables-usb/68-cable-usb-type-a-b-arduino-uno-3232100000681.html>

[23] Jonathan Oxe, Hugh Blemings, 'Practical Arduino Cool Projects for Open Source Hardware'

[24] <https://www.arduino.cc/en/Main/Software>

[25] Atmel-42735-8-bit-AVR-Microcontroller-ATmega328-328P_Summary

[26] Arduino_-_Premiers_pas_en_informatique_embarquee.pdf

[27] <https://www.circuitspecialists.com/stepper-motor>

[28] <https://learn.adafruit.com/all-about-stepper-motors/what-is-a-stepper-motor>

[29] Akbarzadeh, A., and Wadowski, T., "Heat Pipe-Based Cooling Systems for Photovoltaic Cells Under Concentrated Solar Radiation," Applied Thermal Engineering, 16(1), pp.81-87, 1996.

[30] Royne, A., Dey, C. J., and Mills, D. R., "Cooling of Photovoltaic Cells Under Concentrated Illumination: A Critical Review," Solar Energy Materials and Solar Cells, 86(4), pp. 451-483, April 2005.

[31] M. G. Villalva, J. R. Gazoli, E. Ruppert F, "Comprehensive approach to modeling and simulation of photovoltaic arrays", IEEE Transactions on Power Electronics, 2009 vol. 25, no. 5, pp. 1198--1208, ISSN 0885-8993.

[32] Hairul Nissah Zainudin, Saad Mekhilef, "Comparison Study of Maximum Power Point Tracker Techniques for PV Systems", Cairo University, Egypt, December 19-21, 2010, Paper ID 278.

[33] Huan-Liang Tsai, Ci-Siang Tu, and Yi-Jie Su, "Development of Generalized Photovoltaic Model Using MATLAB/SIMULINK", Proceedings of the World Congress on Engineering and Computer Science 2008 WCECS 2008, October 22 - 24, 2008, San Francisco, USA.

[34] E.M.G. Rodrigues, R. Melício, V.M.F. Mendes and J.P.S. Catalão , Simulation of a Solar Cell considering Single-Diode Equivalent Circuit Model University of Beira Interior. R. Fonte do Lameiro, 6200-001 Covilhã (Portugal)

[35] L.Serra rio. Cillicon concentrator solar cell.phd thesis. March 2013. University of Trento.

Others

SOLAR CELLS TUTORIAL Part 2 _ Physics of Crystalline Solar Cells - YouTube (360p)

SOLAR CELLS TUTORIAL Part 3 _ Modeling and Simulation of Photovoltaic Devices and Systems - YouTube (360p)

SOLAR CELLS TUTORIAL Part 4 _ What is Different about Thin-Film Solar Cells_ - YouTube (360p)

Appendix

1. Plan of realisation of the solar tracker

R1= 5mm

16 cm

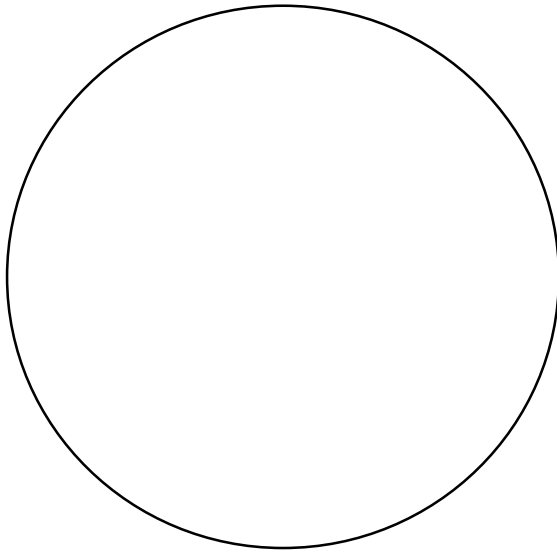


R1= 5mm

22 cm

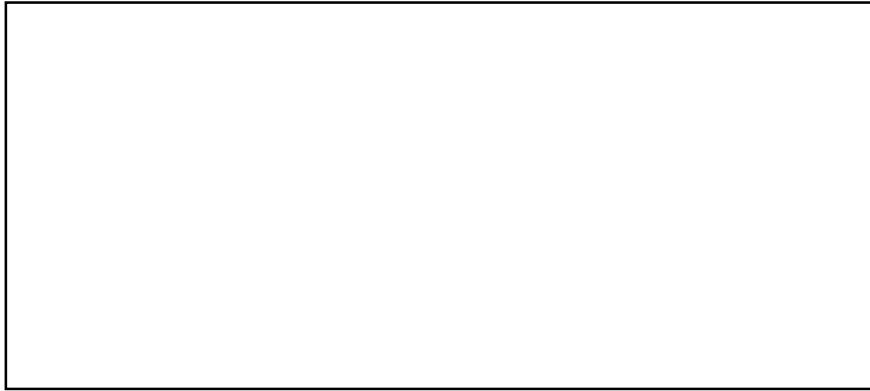


R2=13.5 cm



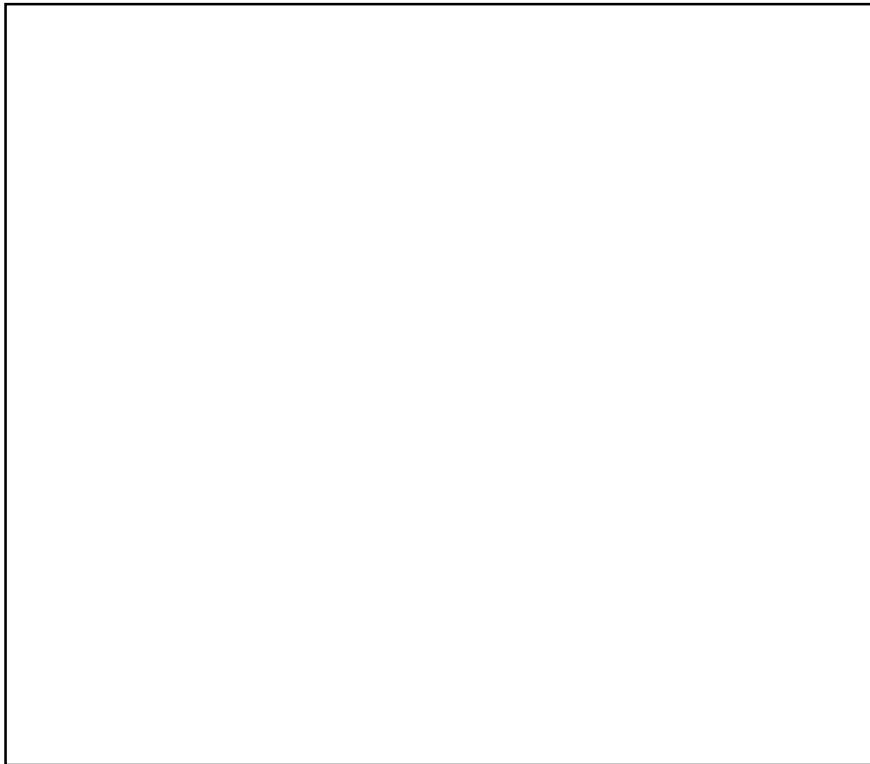
30cm

20cm

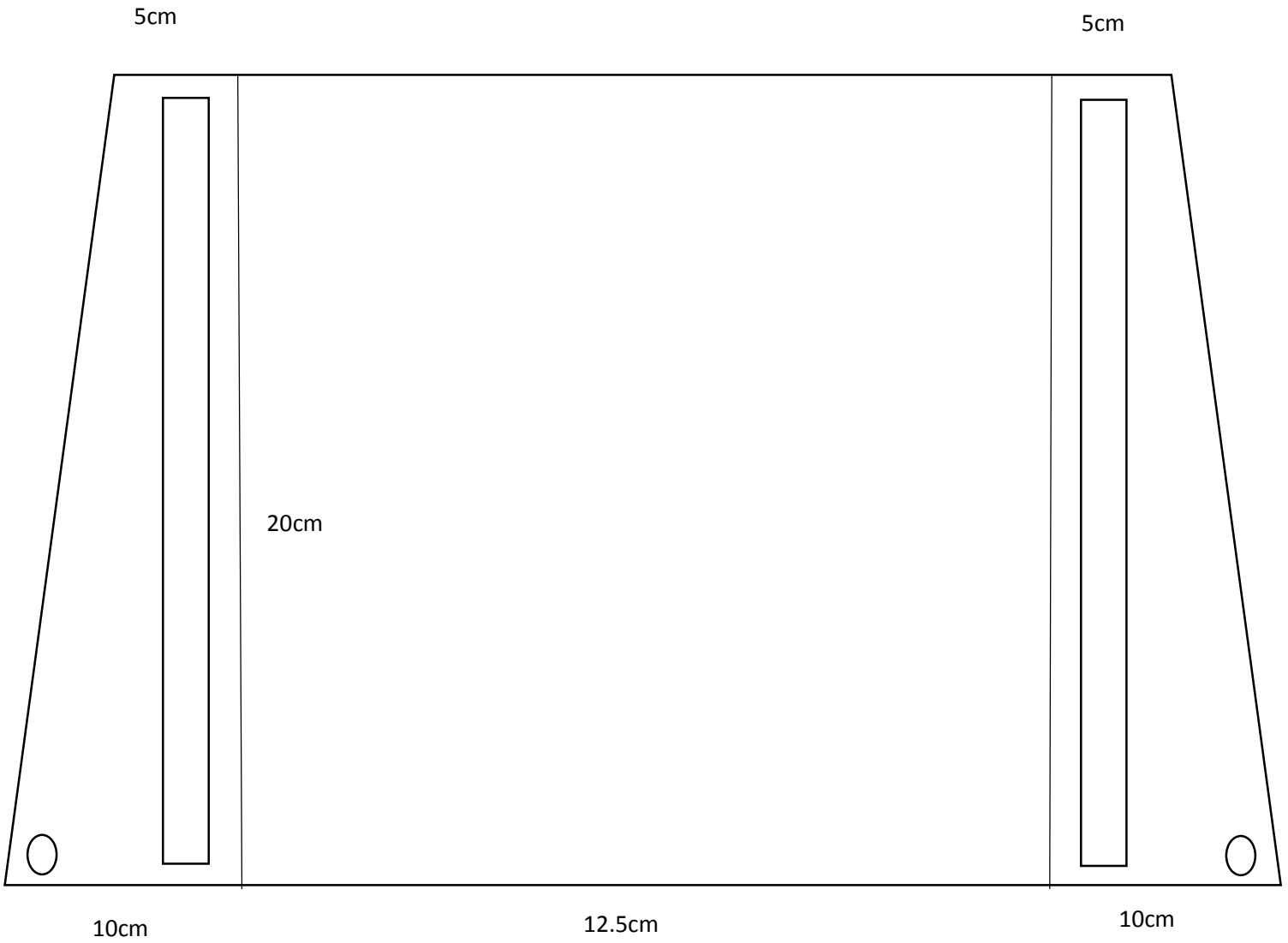


30cm

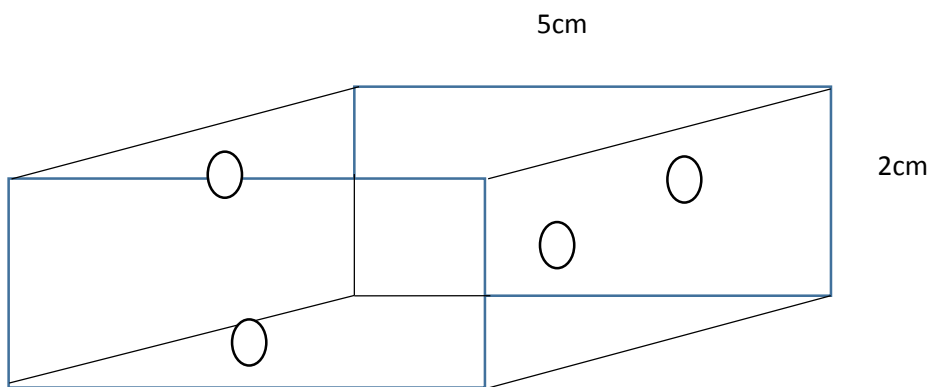
30cm



R1= 5cm



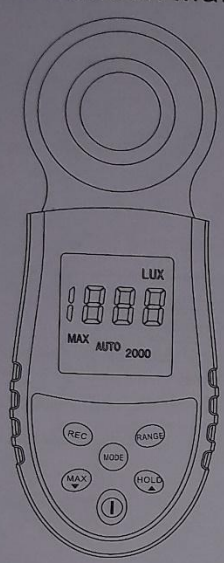
R1= 5mm





2. The lux meter datasheet HS 1010

The Digital Light Meter HS 1330 / HS 1332 / HS 1010 Instruction Manual



①

Thanks for choosing the product of our company, thank you very much. Before using our product, please read the instruction manual carefully, which will show you the correct way to operate. We wish that will help you experience the excellent performance of our product.

I. Features


- HS1330: Measuring range 0.01 lux-20000 lux
- HS1332: Measuring range 0.1 lux-200000 lux
- HS1010: Measuring range 1 lux-200000 lux
- Automatic measuring level selection
- max and min reading hold function
- LUX/FC unit selection
- Reading locked hold
- Automatic data recording

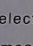
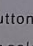
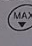
II. SPECIFICATIONS:

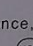
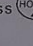
- Display: 3-1/2 digit LCD with a maximum reading of 1999
- Measuring range:
 - HS 1330: 20, 200, 2000, 20000 lux
(20000 lux range reading×10)
 - HS 1332: 200, 2000, 20000, 200000 lux
(20000 lux range reading×10)
(200000 lux range reading×100)
 - HS 1010: 2000, 20000, 200000
(20000 lux range reading×10)
(200000 lux range reading×100)
- P.S: 1 fc=10.76 lux

②


A --- illumination reading
 B --- Data hold sign
 C --- The battery low power sign
 D --- illumination unit FC
 E --- illumination unit LUX
 F --- Data record time unit second
 G --- Multiple of 20000, 200000 lux range
 H --- Measuring range (20, 200, 2000, 20000, 200000)
 I --- Automatic range selection sign
 J --- Data sign
 K --- Minimum measurement sign
 L --- Maximum measurement sign
 M --- Automatic data recording sign

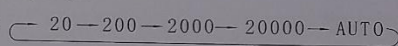
2. Power button  selection ON / OFF

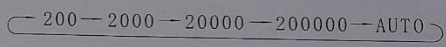
3. The maximum and minimum selection button: press  once, LCD displays MAX sign, starting Maximum measuring selection work, in the process of measuring with only the maximum. Press  twice, LCD displays Min sign, switching to the minimum measuring selection, in the process of measuring with only the minimum. And then press  a 3ed time, MIN sign will vanish, switching to real-time measuring data.

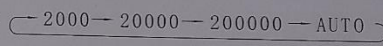
4. Reading data hold function: press  once, LCD displays sign, "H" and the measuring data locked and hold, press  twice, lock canceled, sign "H" will vanish, restarting to scan.

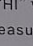
⑤

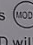
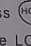
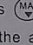
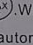
5. Measuring range selection button: Press  repeatedly to select the different measuring range.

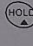
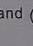
HS 1330 :  20 → 200 → 2000 → 20000 → AUTO

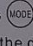
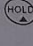
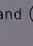
HS 1332 :  200 → 2000 → 20000 → 200000 → AUTO

HS 1010 :  2000 → 20000 → 200000 → AUTO

When displaying sign "AUTO", it means automatic range selection, which will select the proper range according to the light intensity automatically. When the sign "AUTO" vanished, it means manual range selection. When the measuring range is too low for the light intensity, sign "HI" will display, you need to press  manually to switch to the next measuring range.

6. Instrument function selection : long press  .5 secends later, starting the LUX/FC unit selection, sign "LUX" in LCD will start to flicker, if you want to switch to the FC selection, press , sign "FC" will start to flicker. If the sign "FC" is flickering in the LCD, but you want to switch to the LUX selection, just press . When the unit has been selected, press  one more time to start the automatic data recording parameter setting.

(1) To set the number of the times of data recording. The sign "REC" and sign "DATA" would both flicker in the LCD and the number of recording times displays. Press  and  to set the number from 1 to 50.

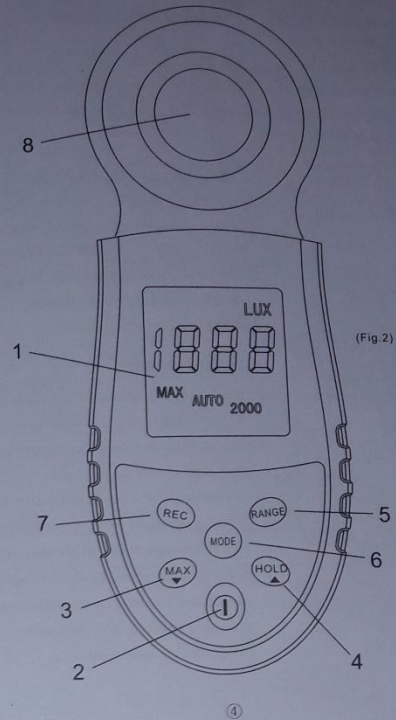
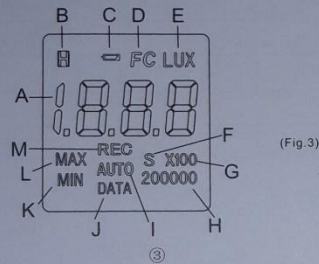
(2) To set the data sampling time interval. Press  again, the sign "REC" and "S" would both flickering (Fig.5) The number of the data sampling time interval displays in the LCD, unit for secends. Press  and  you can set the number from 1s to 60s.

⑥

- Spectral Response : CIE Photopic. (CIE human eye response curve)
- Spectral Accuracy: $f'_{\lambda} \leq 6\%$
- Cosine Response: $f'_{\theta} \leq 2\%$
- Accuracy:
(Calibrated to standard incandescent lamp at color temperature 2856K)
HS 1330, HS 1332 : $\pm 3\% \pm 10$ dgts (<10000 lux)
 $\pm 4\% \pm 10$ dgts (≥ 10000 lux)
HS 1010: $\pm 4\% \pm 10$ dgts (<10000 lux)
 $\pm 5\% \pm 10$ dgts (≥ 10000 lux)
- Repeatability : $\pm 2\%$
- Temperature Characteristic : $\pm 0.1\% / ^\circ\text{C}$.
- Measuring Rate : Approximately 2.0 time/sec
- Photo Detector: One silicon photo diode with filter
- Power Source: Two AAA batteries
- Dimensions: 162(L) \times 60(W) \times 32(H)mm.
- Weight: 130g.
- Accessories: Instruction manual, batteries.

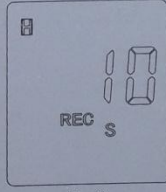
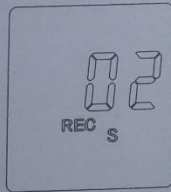
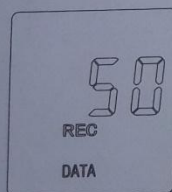
III. Specification (Fig.2)

1. Display: 3-1/2 digit LCD. Max reading 1999 (Fig.3)



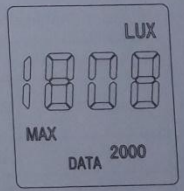
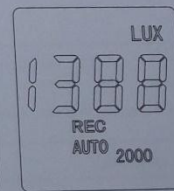
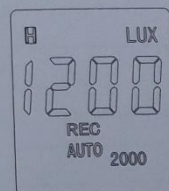
(3) To set the delay starting time of the data recording. Press the **MODE** again, the "REC" "S" and "H" will be flickering at the same time (Fig.6), the displaying number is the time of delay start of data recording. Press **HOLD** and **MAX** to set it, a maximum of 60 seconds, 1 second minimum. To set the delay time can make it easier to place the instrument in a suitable location, to avoid an unstable state of the object being measured, and reduce the factors which are bad for the accuracy to obtain accurate measuring results.

(4) Press **MODE** again, the Data automatic recording parameters setting will exit, back to the normal measuring mode. The parameters will be saved.



7. Data automatic recording. First press **REC**, then hold the first press and press **MODE** at the same time to start the automatic recording function. Sign "AUTO" will light to set the range automatically. Then the sign "REC" and "H" will both flicker in the LCD (Figure 7). It shows in the delay stage of the data recording, the delay time based on the time set before (1-60 seconds optional). When the sign "H" stops flickering but the sign "REC" flickering, indicating that the delay time has elapsed (Figure 8). Data automatic recording starting to work based on the pre-set number of times of data recording (1-50 optional), and pre-set time interval (1-60 seconds) to complete.

When the "REC" stops flickering, it means the automatic data recording has been completed. To check the recording data, please press **REC**, then hold press and press **HOLD** at the same time to view the data, the sign "DATA" will light with the sign "MAX" flickering (Fig.9), the displaying data refer to the maximum value in the measuring process. Press **HOLD**, the sign "MIN" will start flickering, the data displaying refer to the minimum value in the measuring process. Once again press the **HOLD**, you can turn to view the different individual data, each time you press **HOLD**, first display the data label, display would just maintain a few seconds then vanished, and the display sampled data of measuring values stability. Each time you press **MAX**, you can get back to view previous the data. When you finish checking the data, press **REC** to exit, the sign "DATA" would vanish, then turning into the normal measuring mode.



8. The photo detector: to detect the light intensity.

IV. OPERATION INSTRUCTIONS

1. Press **ON** button, turn it on.
2. press **RANGE** button, select the needed measuring range or select AUTO.

3. Remove the photo detector cap and face it to right side in horizontal position.
4. Read the data from the LCD display.
5. Refer to the guidance of every button, you can try different functions.
6. Measuring work done, replace the photo detector cap and press the Power button to turn it off.

V. BATTERY CHECK-UP & REPLACEMENT

1. As the battery power is not sufficient, there would be a sign in the LCD indicating that the batteries should be replaced.
2. Refer to the (Fig. 10), open the battery cover, replace the two AAA batteries.
3. Replace the battery cover.

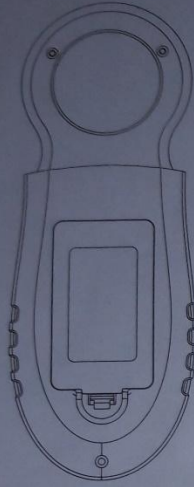


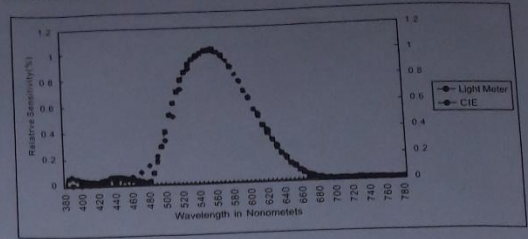
(Fig. 10)

VI. MAINTENANCE

1. Don't store or operate Where temperature or humidity is excessively high.
2. The white plastic disc on the top of the detector should be cleaned when necessary.
3. The reference level, as marker on the face plate, is the tip of the photo detector globe.
4. The calibration interval for the photo detector will vary according to operational conditions. In order to maintain the basic accuracy of the instrument, periodic calibration is recommended.

9

VII. THE SPECTRAL SENSITIVITY



VIII. Recommended illumination in different locations

1 fc = 10.76 lux

SCHOOL

illumination (lux)	Locations
1500~300	Laboratory, Computer room, Drafting room
750~200	Classroom, Conference room, Library
300~150	Hall, Rest room, Stairs, Big classroom
150~75	Corridor, Elevator, Toilet
75~30	Warehouse, Garage, Escape stairs

10

HOTEL, RESTAURANT, CLUB

illumination (lux)	Locations
1500~750	The front desk
750~300	The banquet hall, Meeting room, Park, Kitchen
300~150	Dining-room, Toilet
150~75	Playroom, Stairs, Bathroom, Changing room
75~30	Warehouse

HOME

illumination (lux)	Locations
2000~750	Handicraft, Tailor work
1000~500	Writing, Homework
750~300	Reading, Makeup, Desk, Telephone
300~150	Living room, Mirror, Wash sink
150~75	Chest, Bedroom, Toilet
75~30	Mailbox, Garage, Warehouse

MALL, SUPERMARKET

illumination (lux)	Locations
3000~750	Indoor display, Window, Counter, Packing desk
750~300	Hall, escalator
300~150	Conference room, Toilet
150~75	Lounge, General lighting

13

14

OFFICE BUILDING

illuminance (lux)	Locations
2000 ~ 1500	Design house
1500 ~ 750	Hall channels (day), Punch, Typing
750 ~ 300	Office, Computer room, Meeting room,
300 ~ 150	Stacks, Playroom, Lounge, Guard room, Toilet
150 ~ 75	Tea room, Dressing room
75 ~ 30	Escape stairs

FACTORY

illuminance (lux)	Locations
3000~1500	Ultra Precision Machining and inspection, Drawing
1500~750	Design, Analysis, Assembly,
750~300	Packaging, Surface work
300~150	Dyeing, Casting, Electrical room
150~75	Exit, Corridor, Channel, Stairs, Toilet
75~30	Warehouse, Garage, Escape stairs

11

HOSPITAL

illuminance (lux)	Locations
10000 ~ 5000	Special inspection
1500 ~ 750	Operating room
750 ~ 300	Anatomical room, Office, Conference room
300 ~ 150	Ward, Drug room, Corridor
150 ~ 76	Dressing room, X-ray room,
75 to 30	Dark room (photos), Escape stairs

BARBER SHOP

illuminance (lux)	Locations
1500~750	Perm, Hair dye, Makeup
750~300	Wash hair, Wash face, The front desk
300~150	Toilet
150~75	Corridor, Stairs

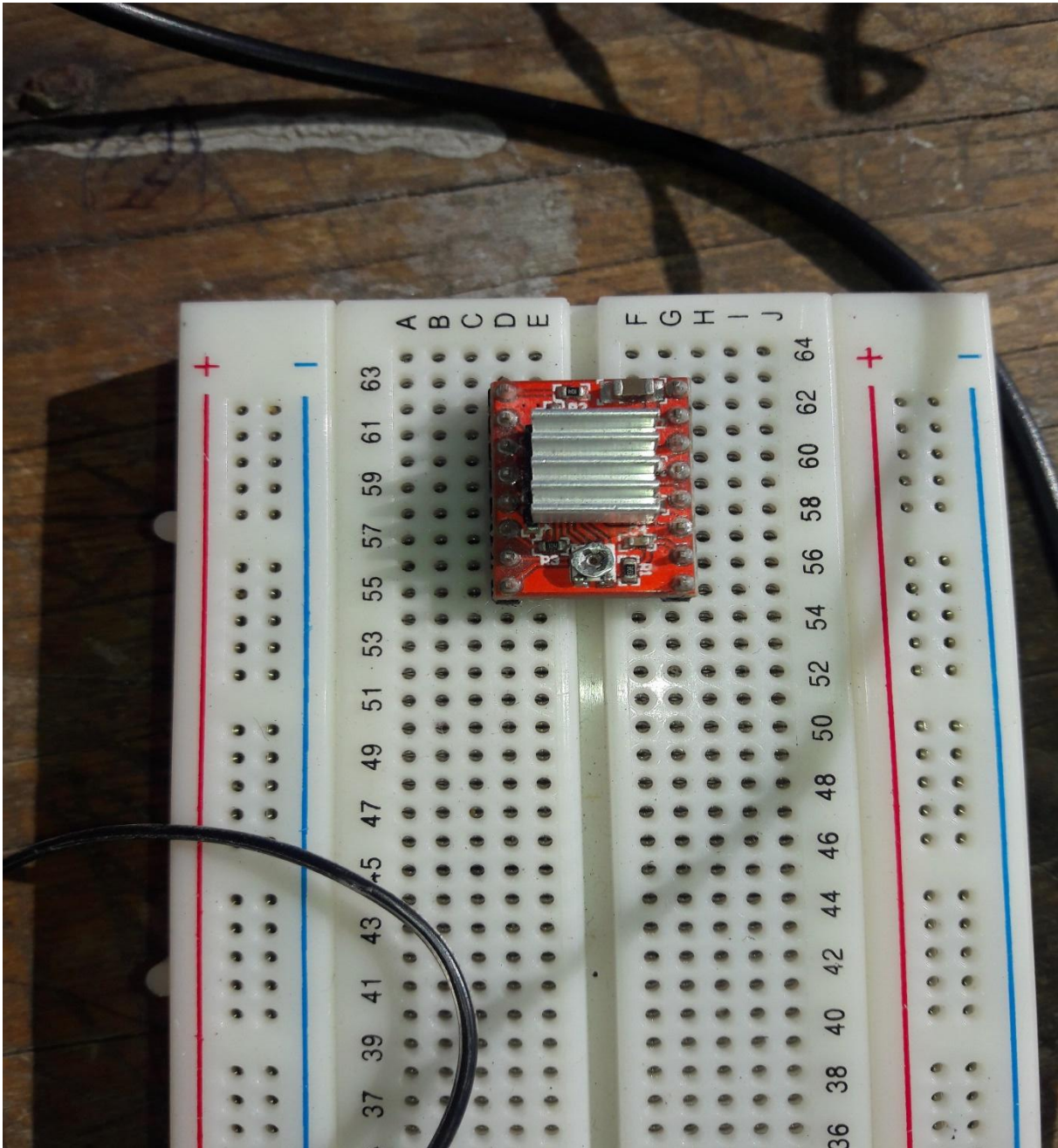
12

1w/m² = 683 lux (683 lumen/m²)

3. Step by step motor



4. Electrical circuit for step by step motor:



5. Arduino program

test_stepper_1 | Arduino 1.6.13

Fichier Édition Croquis Outils Aide



```
test_stepper_1

void setup() {
  // put your setup code here, to run once:
  pinMode(8, OUTPUT);
  pinMode(10, OUTPUT);
  pinMode(9, OUTPUT);
  digitalWrite(10, LOW);
  digitalWrite(8, LOW);
}

void loop() {

  digitalWrite(9, LOW);
  //analogWrite(9, 128);
  delay(3);
  digitalWrite(9, HIGH);
  delay( 3);

  // put your main code here, to run repeatedly:

1
```